Neurosurgery Research Group, Biomedicum Helsinki
Helsinki University Hospital
University of Helsinki
Helsinki, Finland

Atherosclerotic and inflammatory changes in saccular intracranial aneurysms

Eliisa Ollikainen

ACADEMIC DISSERTATION

To be presented,
with the permission of the Faculty of Medicine of the University of Helsinki
for public discussion in Lecture Hall 1 of Töölö Hospital
on August 24th, 2018, at noon.

Helsinki 2018

Supervisors

Riikka Tulamo
M.D., Ph.D.

Department of Vascular Surgery
Helsinki University Hospital
University of Helsinki
Helsinki, Finland

Juhana Frösen
M.D., Ph.D., Docent

Department of Neurosurgery
Kuopio University Hospital
Kuopio, Finland

Other contributing senior scientists

Petri Kovanen
M.D., Ph.D., Professor

Wihuri Research Institute
Biomedicum Helsinki
Helsinki, Finland

Mika Niemelä
M.D., Ph.D., Professor

Department of Neurosurgery
Helsinki University Hospital
University of Helsinki
Helsinki, Finland

Reviewers

Anne Räisänen-Sokolowski
M.D., Ph.D., Docent

Department of Pathology
Helsinki University Hospital
Helsinki, Finland

Sami Tetri
M.D., Ph.D., Docent

Department of Neurosurgery
Oulu University Hospital
University of Oulu
Oulu, Finland

Opponent

Tiit Mathiesen
M.D., Ph.D., Professor

Department of Neurosurgery
University of Copenhagen
Copenhagen, Denmark

Eliisa Ollikainen, M.D.

Neurosurgery Research Group, Biomedicum Helsinki
Haartmaninkatu 8
00290 Helsinki
Finland

e-mail: eliisa.ollikainen@helsinki.fi

ISBN 978-951-51-4399-0 (Paperback)
ISBN 978-951-51-4400-3 (PDF)
Helsinki University Print
Helsinki 2018

Cover, painted illustrations, and layout by Eveliina Netti

Contents


Lotti

Abbreviations

αSMA	α-Smooth Muscle cell Actin
AAA	Abdominal Aortic Aneurysm
ABCA-1	Adenosinetriphosphate-Binding Cassette A-1
AcomA	Anterior communicans Artery
ApoA-I	Apolipoprotein A-I
ApoB-100	Apolipoprotein B-100
ApoE	Apolipoprotein E
bFGF	Basic Fibroblast Growth Factor
BMI	Body Mass Index
CFD	Computational Fluid Dynamics
COX	Cyclo-oxygenase
CT	Computed Tomography imaging
CTA	Computed Tomography Angiography
DSA	Digital Subtraction Angiography
ECM	Extracellular Matrix
EEL	External Elastic Lamina
EP2	Prostaglandin E2 receptor
GPA	Glycophorin A
GWA	Genome-Wide Association
HDL	High-Density Lipoprotein
HIF-1A	Hypoxia-Inducible Factor-1A
HLA-DR	Human Leukocyte Antigen-DR
HNE	Hydroxynonenal (oxidized lipid)
HMG-CoA	Hydroxymethylglutaryl-Coenzyme A
HO-1	Hemioxygenase-1

IA	Intracranial Aneurysm (saccular)
ICA	Internal Carotid Artery
ICH	Intracerebral Hemorrhage
IDL	Intermediate-Density Lipoprotein
IEL	Internal Elastic Lamina
IF	Immunofluorescence
Ig	Immunoglobulins
IHC	Immunohistochemistry
ISAT	International Subarachnoid Aneurysm Trial
ISUIA	International Study of Unruptured Intracranial Aneurysms
LDL	Low-Density Lipoprotein
MC	Mast Cell
MCA	Middle Cerebral Artery
MCP-1	Monocyte Chemotactic Protein-1
MHC-II	Major Histocompability Complex type II
MMP	Matrix Metalloproteinase
MPO	Myeloperoxidase
MRA	Magnetic Resonance Angiography
MRI	Magnetic Resonance Imaging
NF-κB	Nuclear Factor-kappa B
SAH	Subarachnoid Hemorrhage (aneurysmal)
SMC	Smooth Muscle Cell
SNPs	Single Nucleotide Polymorphisms
SWI	Susceptibility Weighted Imaging
OA	Opthalmic Artery
ORO	Oil Red O, neutral lipid staining
PcomA	Posterior communicans Artery
PDGF	Platelet-Derived Growth Factor
PHASES	Population, Hypertension, Age, Size, Earlier SAH, and Site
PICA	Posterior Inferior Cerebellar Artery
TGF-b	Transforming Growth Factor-b
TNF-α	Tumor Necrosis Factor-α
USPIO	Ultrasmall Superparamagnetic Iron Oxide particles
ROS	Reactive Oxygen Species
VCAM-1	Vascular Cell Adhesion Molecule-1
VLDL	Very-Low-Density Lipoprotein
WSS	Wall Shear Stress

Original publications

The studies are referred to in the text by their Roman numerals.

This thesis is based on the following publications:

I **Mast Cells, Neovascularization, and Microhemorrhages are Associated with Saccular Intracranial Artery Aneurysm Wall Remodeling**.
Eliisa Ollikainen, Riikka Tulamo, Juhana Frösen, Satu Lehti, Petri Honkanen, Juha Hernesniemi, Mika Niemelä, and Petri T. Kovanen. J Neuropathol Exp Neurol 2014;73:855-864.

II **Smooth Muscle Cell Foam Cell Formation, Apolipoproteins, and ABCA1 in Intracranial Aneurysms: Implications for Lipid Accumulation as a Promoter of Aneurysm Wall Rupture**.
Eliisa Ollikainen, Riikka Tulamo, Satu Lehti, Miriam Lee-Rueckert, Juha Hernesniemi, Mika Niemelä, Seppo Ylä-Herttuala, Petri T. Kovanen, and Juhana Frösen. J Neuropathol Exp Neurol 2016;75:689-699.

III **Flow Conditions in the Intracranial Aneurysm Lumen Are Associated with Inflammation and Degenerative Changes of the Aneurysm Wall**.
Juan Cebral, Eliisa Ollikainen, Bong Jae Chung, Fernando Mut, Visa Sippola, Behnam Rezai Jahromi, Riikka Tulamo, Juha Hernesniemi, Mika Niemelä, Anne Robertson, and Juhana Frösen. AJNR Am J Neuroradiol 2017 Jan;38(1):119-126.

IV **Macrophage Infiltration in the Saccular Intracranial Aneurysm Wall as a Response to Locally Lysed Erythrocytes that Promote Wall Degeneration.**
Eliisa Ollikainen, Riikka Tulamo, Salla Kaitainen, Petri Honkanen, Satu Lehti, Timo Liimatainen, Juha Hernesniemi, Mika Niemelä, Petri T. Kovanen, and Juhana Frösen (accepted for publication in J Neuropathol Exp Neurol 2018).

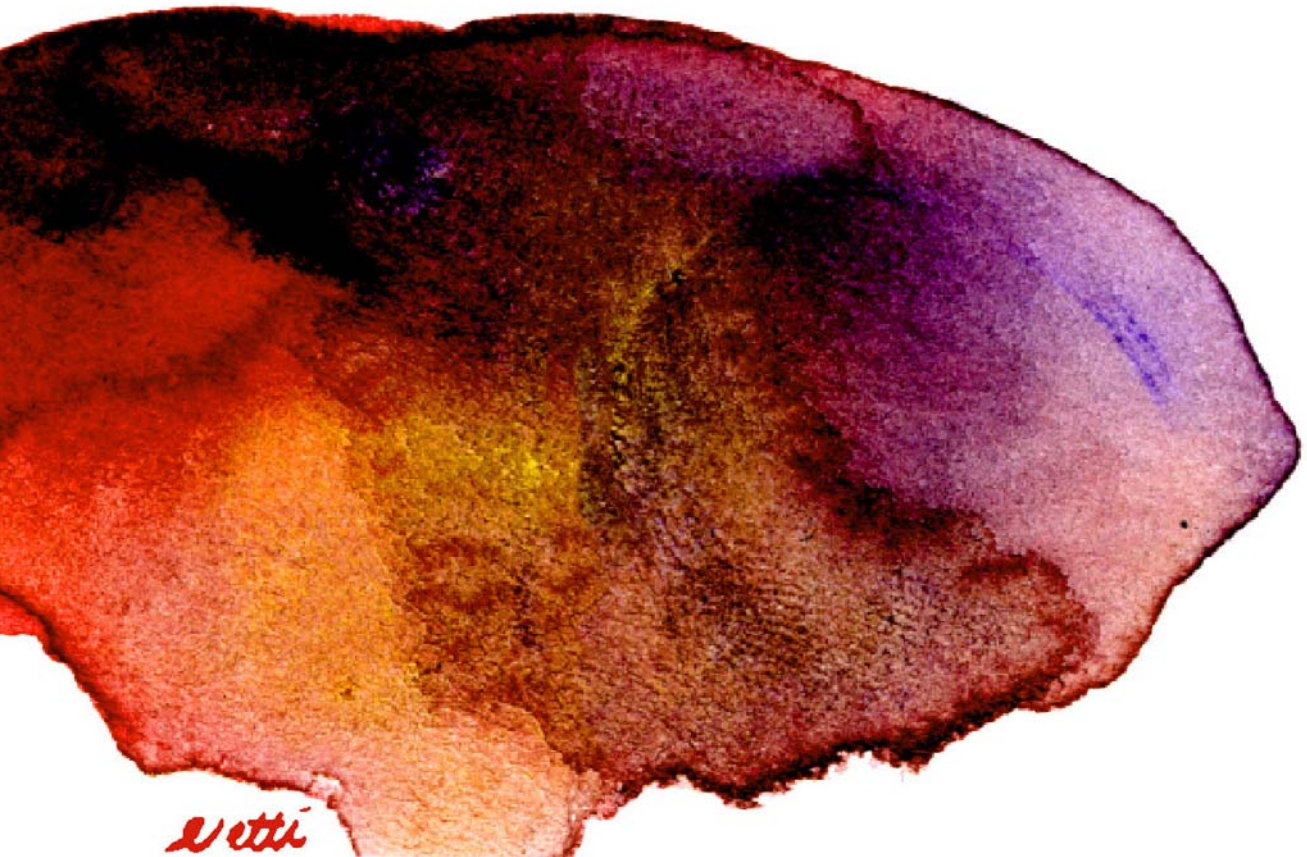

Abstract

Objective

A saccular intracranial aneurysm (IA) is a pathological pouch from an intracranial artery. Its rupture causes subarachnoid hemorrhage (SAH), an acute intracranial bleeding with high mortality (30-40%) and morbidity. Unruptured IAs are common in the population (2-3%), but their rupture rate escapes prediction. Clinical risk factors for IA formation and rupture are smoking, female sex, and hypertension. Hypercholesterolemia, a risk factor for atherosclerosis, plays an unknown role in IAs. IA walls show multiple histological changes that resemble those in atherosclerotic lesions. These include chronic inflammation, structural artery wall remodeling, mural cell proliferation and death, loss of endothelium, intraluminal thrombosis, and lipid accumulation. Non-physiological blood-flow conditions in the artery lumen can trigger arterial wall remodeling and are hypothesized to contribute to IA pathogenesis. The potential role of atherogenic mechanisms in IA pathobiology remains, however, unestablished. The aim of this thesis was thus to discover the role of atherosclerotic and flow-related inflammatory changes as a potential trigger of IA wall rupture and to discuss potential tools for imaging those changes.

Methods

In total, 55 (25 unruptured and 30 ruptured) intraoperatively resected IA fundus specimens were the focus. The role of atherosclerotic and other histopathological changes in the IA walls were evaluated by histological and immunohistochemical methods. Of the 55 IAs, 36 underwent analysis for wall degenerative remodeling, neovascularization, and proinflammatory and proatherogenic factors such as the presence of apolipoproteins, oxidized lipids, erythrocyte remnants, and infiltrations of $CD163^+$ and $CD68^+$ macrophages, $CD3^+$ T lymphocytes, and mast cells (MCs). Preoperative CT-angiography images provided the data source for hemodynamic simulations, which were then compared with histology in a subseries of 20 of the IAs. To correlate IA wall changes with MRI, 11 additional IAs underwent 4.7T MRI ex vivo, prior to their histological evaluation.

Results and Discussion

Aneurysm rupture status or degenerative wall changes did not associate in the series of 55 IAs with clinical parameters such as patient sex, age, hypertension or smoking status.

The 36 (16 unruptured and 20 ruptured) IAs studied for histology showed extensive degenerative remodeling changes, similarly to changes in earlier studies. All IAs showed accumulation of lipids, the apolipoproteins A-I and B-100 of high- and low-density lipoproteins (HDL and LDL), reflecting atherogenic processes in the IA walls. These changes occurred independent of plasma lipid levels. Extensive lipid accumulation correlated with the infiltration of all the inflammatory-cell subtypes, suggesting the proinflammatory potential in the IA wall of lipids. Foam cell formation in α-smooth muscle cells and macrophages and their expression of adenosine triphosphate-binding cassette A1 (ABCA-1) indicated lipid clearance by these cells and via the ABCA-1 – apoA-I pathway. The extracellular load of neutral lipids and adipophilin, a marker of lipid intake, reflected potential insufficient cellular lipid clearance and subsequent foam-cell death from their excess lipid-load in degenerated and ruptured IAs.

In addition to their extensive, potentially LDL-derived lipid load, another source of lipids in the IA wall appeared to be cholesterol-rich erythrocytes, because their membrane-protein glycophorin

A (GPA) massively accumulated in degenerated and ruptured IAs. Importantly, the presence of GPA in all layers of the IA walls and in the organized (old) intraluminal thrombus suggested that erythrocytes in the IA wall do not originate from the rupture, but rather represent a chronic accumulation. Subjected to lysis, erythrocytes release hemoglobin, a potent oxidant because of its iron-containing heme. The presence of oxidized lipids in the IA wall reflected the existence of this oxidative stress.

Infiltration of $CD163^{+}$/$HLA\text{-}DR^{-}$ (human leukocyte antigen-DR) phagocytes in the IA wall suggests the presence of a hemorrhage-associated macrophage phenotype previously described in coronary atherosclerotic lesions and abdominal aortic aneurysms. This finding thus suggests the role of a similar atheroprotective macrophage population in the IA wall, potentially specialized in hemoglobin clearance. Hemosiderin, a lysosomally generated product of hemoglobin, was deposited adjacent to adventitial neovessels, interpreted as sources of intramural microhemorrhages. Pro-oxidative hemoglobin may play a role in the regulation of inflammatory response in IA wall degeneration, pushing towards the wall's eventual rupture.

Ex vivo MRI provided signal-intensity changes associated with GPA and hemosiderin in histology. However, an iron-associated signal void, once spatially demonstrated in giant human IAs, was not visible in the present series of small IAs. Flow models of IAs showed the association of low and high wall shear-stress levels with IA wall inflammation and remodeling, suggesting that hemodynamic simulations, as well, could serve as a tool in detection of rupture-prone human IA walls.

Conclusion

Aneurysm walls show a variety of degenerative remodeling changes similar to those in extracranial atherosclerosis, changes which may predispose to IA wall rupture. Experimental models are warranted to verify the suggested mechanisms. Nevertheless, the present study provides important clarification of IA-wall pathogenesis which may prove useful in development of preventive treatment for low-risk IAs and better diagnostic methods to reveal high-risk IAs.

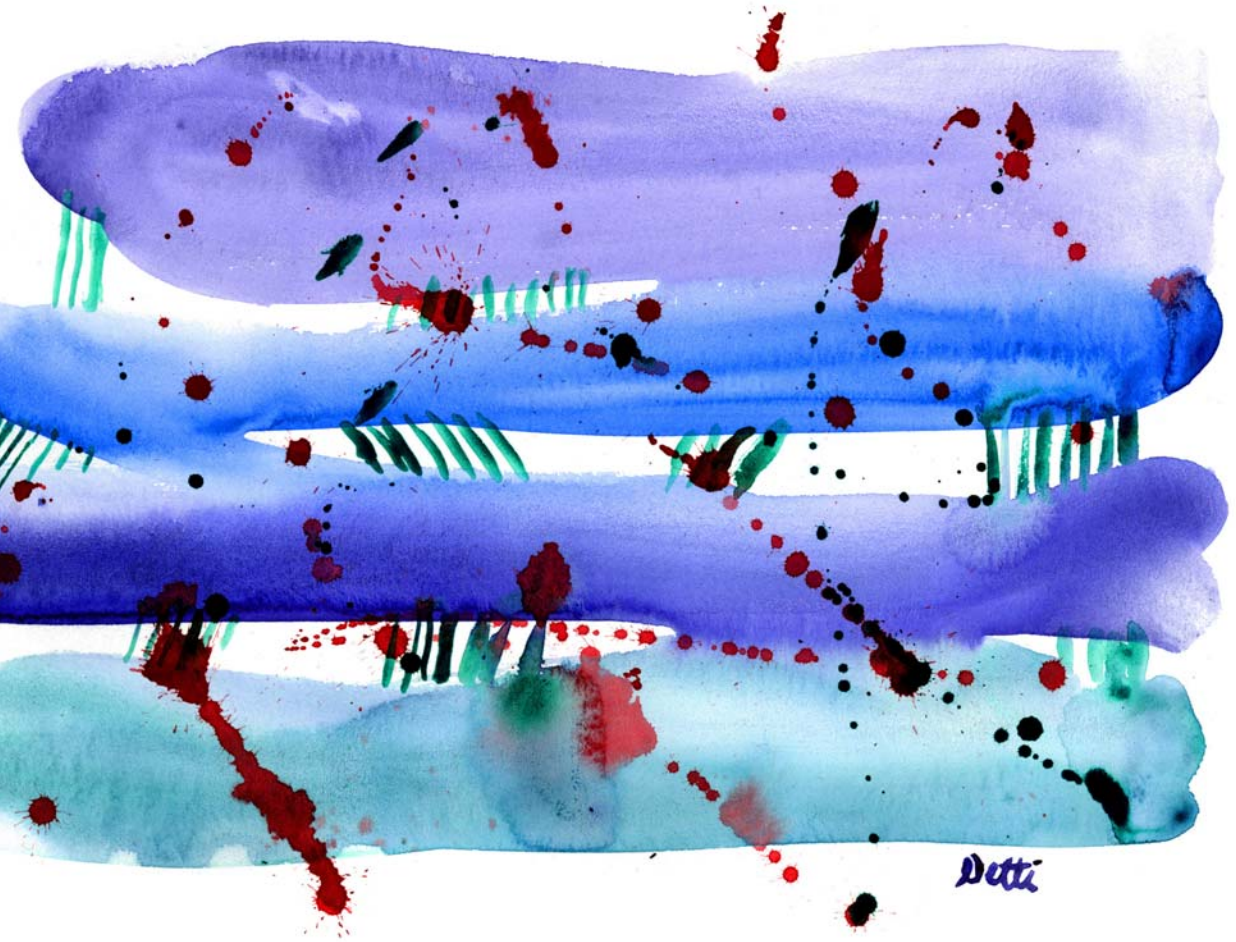

Cross-section of a rupture-prone IA wall, an abstract illustration by artist Eveliina Netti.

Tiivistelmä

Tausta

Aivovaltimoaneurysma (AA) on kallonpohjan valtimon sairaus, jossa tyypillisesti lähelle valtimon haarautumiskohtaa verisuonen seinämästä muodostuu pussimainen uloke, aneurysma. AA on sekä Suomessa että maailmalla yleinen: sen kantajia arvioidaan olevan väestöstä 2-3%. Tunnettuja riskitekijöitä ovat tupakointi, naissukupuoli ja korkea verenpaine. Puhkeamaton AA ei yleensä aiheuta kantajalleen oireita, mutta AA:n puhkeaminen johtaa vaaralliseen lukinkalvonalaiseen aivoverenvuotoon (subaraknoidaalivuoto). Vuodon saaneista lähes puolet kuolee (30-40%), ja hengissä selvinneistä moni vammautuu. AA voidaan eristää verenkierrosta sulkemalla AA:n tyvi joko avoleikkauksessa (klipsaus) tai verisuonen sisältä käsin (koilaus ja/tai stenttaus). AA:n hoitovaihtoehdot sisältävät riskejä, eikä kaikkia AA:a tarvitse hoitaa toimenpiteillä - kaikki AA:t eivät puhkea ihmiselämän aikana. Puhkeamisvaarassa olevaa AA:a ei kuitenkaan osata tunnistaa riittävällä varmuudella. Oikea-aikaisen hoidon kohdentamiseksi olisi ymmärrettävä, miksi AA puhkeaa.

Tiedetään, että puhjenneen AA:n seinämä on yleensä pitkälle rappeutunut. Rappeutuneissa AA:ssa jyllää krooninen tulehdus ja seinämän rakenne on muuntunut. Normaalin valtimon

seinämästä pääosan muodostaa yhtenäinen sileälihaskerros; AA:ssa todetaan sekä sileälihassolujen katoa että näiden lisääntymistä ja yleistä epäjärjestystä. Merkkinä valtimon sisäpintaa verhoavan endoteelin vauriosta AA-pussin sisäpinnalle on usein muodostunut verihyytymää, joka on ajan kuluessa voinut sulautua osaksi itse AA:n seinämää. Sairaaseen AA:n seinämään kertyy lisäksi rasvaa. AA:n seinämämuutokset muistuttavatkin kudostasolla valtimotaudin (ateroskleroosin) vaurioittamaa verisuonen seinämää. Näiden muutosten yhteyttä AA:n seinämän rappeutumiseen ei tunneta. Sekä ateroskleroosin että AA:n tyyppisijainti valtimon haarautumiskohdassa on osaltaan aiheuttanut epäilyä paikallisten veren virtausolosuhteiden kuluttavasta vaikutuksesta valtimon seinämään. Näitä vaikutuksia AA:n kudostason rappeutumiseen ei kuitenkaan tunneta. Myös ateroskleroottisten verisuonen seinämämuutosten vaikutus AA:n rappeutumiseen on tuntematon.

Tässä tutkimuksessa selvitettiin AA:n seinämän ateroskleroottisten muutosten sekä veren virtausolosuhteiden vaikutusta AA:n seinämän tulehdukseen, rappeutumiseen ja puhkeamiseen. Lisäksi selvitettiin muutosten kuvannettavuutta kokeellisella magneettikuvaustekniikalla.

Menetelmät

Työssä tutkittiin AA-leikkauksessa klipsattuja ja irroitettuja AA:n seinämänäytteitä: yhteensä 55 AA:aa, 25 puhkeamatonta ja 30 puhjennutta. AA:n seinämän kudosta tutkittiin ohutleikkeiltä immunohistokemiallisin ja histologisin värjäyksin. AA:n seinämien rakenteellista rappeutumista kuvattiin aiemmin käytetyllä seinämätyyppiluokittelulla (ABCD). 36 AA:n seinämästä (16 puhkeamatonta ja 20 puhjennutta) etsittiin uudisverisuonitusta ja erilaisia tulehdussoluja sekä rasva- ja punasolujätettä. 20 AA:sta tehtiin matemaattinen mallinnus verenvirtausolosuhteista ennen leikkausta otettujen tietokonetomografiakuvien perusteella, ja virtausolosuhteita verrattiin AA:n kudostason muutoksiin. 11 AA:aa kuvannettiin koeputkessa magneettikuvauslaitteella, ja magneettikuvia verrattiin AA:n seinämien kudostason näkymiin.

Tulokset ja Pohdinta

Tässä näytesarjassa AA-potilaan ikä, sukupuoli, ajankohtainen tupakointi, tiedossa oleva verenpainetauti tai kolesteroliarvot eivät liittyneet AA:n puhkeamiseen tai seinämämuutoksiin. Tutkitussa 36 AA:n sarjassa AA:n seinämistä 9 olivat sileälihassolukerrokseltaan järjestyneitä ja endoteeliltaan hyvin säilyneitä muistuttaen normaalia valtimonseinämää (tyyppi A), 12:ssa seinämä oli paksuuntunut ja sileälihassolut olivat epäjärjestyksessä (tyyppi B), 11:ssa rappeutunut seinämä sisälsi alueittaista solupuutosta ja runsaasti vanhaa verihyytymää (tyyppi C), ja 2:ssa AA:n seinämä oli äärimmäisen ohut (tyyppi D). Uudisverisuonitusta ($CD34^+$) oli 28:ssa (78%) näytteistä, eniten tyypin C seinämissä.

Jokainen tutkittu AA sisälsi rasvaa. Veressä kolesterolia kuljettavien lipoproteiinien HDL ja LDL (high- ja low-density lipoprotein) osasia, apolipoproteiineja A-I (HDL) ja B-100 (LDL), oli kertynyt kaikkiin AA:n seinämiin; laaja kertyminen liittyi AA-seinämän rappeumaan ja tulehdukseen. Rasvalla voidaankin olettaa olevan tulehdusta lisäävä vaikutus AA:n seinämässä. Osa AA:n tulehdussoluista ($CD68^+$ ja $CD163^+$ makrofagit) oli täynnä rasvaa, viitaten solujen pyrkimykseen poistaa rasvaa seinämästä syömällä sitä. Rasvaa oli joutunut myös seinämän sileälihassolujen ($aSMA^+$) sisään. Normaalisti rasva poistuu valtimon seinämän soluista solukalvon tietyn porttiproteiinin (ABCA-1) ja HDL-kuljetuksen avulla. Vaikka näitä rasvan poistoon tarvittavia tekijöitä oli AA:n seinämässä runsaasti, solujen syömä rasva (adipofiliini$^+$) näytti loppusijoittuneen solunulkoiseen tilaan. Ilmiö viittaa rasvaa sisältäneiden solujen kuolemaan ja rasvan vapautumiseen solun hajotessa. Koska tällainen rasvakertymä liittyi vahvasti AA:n seinämän rappeutumiseen ja puhkeamiseen, oletettavasti rasva aiheuttaa AA:ssa solukuolemaa ja heikentää seinämää, lisäten sen puhkeamisriskiä.

Rasvan lisäksi AA-seinämissä todettiin runsaasti punasoluperäistä jätettä. Punasolun solukalvoja (glykoforiini A^+) oli laajalti kertyneenä iältään vanhoissa seinämän verihyytymissä sekä rappeutuneissa ja puhjenneissa AA:n seinämissä. Huomattavaa oli punasolujätteen runsas määrä myös vuotamattomissa AA:n seinämissä. Näin ollen punasoluja kertyy AA:n seinämään jo ennen sen puhkeamista,

millä voi olla hiljattaista AA:aa rappeuttavaa vaikutusta. Seinämään kertynyt punasolu vapauttaa hajotessaan solukalvojensa kolesterolia ja sisältämäänsä hemoglobiinia, jossa on voimakkaan hapettavaa rautaa. Punasolujen kertyminen liittyikin AA:n seinämässä hapettuneen rasvan kertymiseen sekä tulehdukseen, mikä tukee käsitystä punasolujen hajoamistuotteiden haitallisesta vaikutuksesta. Hemoglobiinia syöviä makrofageja ($CD163^+$) esiintyi AA:ssa erityisen paljon. Mielenkiintoinen yksityiskohta oli makrofagien tuottaman hemoglobiinin hajoamistutteen, hemosideriinin kertyminen seinämän uudisverisuonten ympärille, viitaten seinämänsisäisiin mikroverenvuotoihin uudisverisuonten tihkumseen seurauksena.

Punasolujätteen kertyminen liittyi myös signaalimuutoksiin AA:n seinämästä kuvatuissa magneettikuvissa, joissa hemosideriinin kertyminen liittyi tummaan kontrastiin ja glykoforiini A:n kertyminen liittyi kirkkaaseen kontrastiin. Näin ollen nämä AA:n rappeutumiseen liittyvät muutokset voisivat olla kuvannettavissa magneetilla myös potilailta. Vaikka löydös on lupaava, vaatii se vielä tarkempia tutkimuksia, sillä nyt tutkitussa pienessä, pienien aneurysmien sarjassa todettu yhteys jäi tilastollisen vertailun tasolle. AA:n sisäisten verenvirtausolosuhteiden mallinnukset osoittivat, että AA:n seinämää kuluttava verenvirtaus liittyy lisääntyneeseen tulehdukseen ($CD45^+$ solujen runsaus) seinämässä sekä seinämän rakenteelliseen rappeutumiseen. Näin ollen myös virtausmallit voisivat tulevaisuudessa olla avuksi korkean vuotoriskin AA:ien tunnistamisessa.

Johtopäätökset

AA:n seinämässä on paljon ateroskleroosia muistuttavia rappeutumismuutoksia, kuten rasvan ja punasolujen sekä näiden hajoamistuotteiden kertymistä. Todennäköisesti näiden jätteiden kertyminen AA:n seinämään aiheuttaa seinämässä tulehdusta, hapettumista ja edelleen seinämän heikkenemistä, lisäten AA:n puhkeamisriskiä. Tutkimuksessa tarkennettiin tämänhetkistä käsitystä AA-seinämän tautitilasta ja sen mekanismeista; oletettujen patologisten mekanismien varmentamiseksi tarvitaan tulevaisuudessa kokeellisia malleja. Uutta tietoa voidaan hyödyntää AA:n puhkeamista ehkäisevien lääkkeellisten hoitomuotojen kehittelyssä sekä korkeariskisten AA-seinämien tunnistamisessa potilailta.

1. Introduction

Subarachnoid hemorrhage (SAH) is a sudden manifestation of the often fatal (30-40%) intracranial bleeding that may occur without warning in anyone afflicted with an intracranial aneurysm (IA). In SAH, circulating blood breaks through the intracranial artery wall into the subarachnoidal space lining the brain, leading to severe headache, nausea, and often loss of conciousness. Even among those who survive, this injurious bleeding may cause disability and dependence upon others for the rest of the patient's life. Worldwide, approximately 2-3% carry a saccular intracranial aneurysm (IA), whose rupture is the origin of non-traumatic SAH (85%). IA prevalence is highest in the working-age and elderly population, other risk factors being female sex, smoking, and hypertension. The role of other risk factors common for cardiovascular diseases in general, such as diabetes and hypercholesterolemia, is unclear.

An unruptured IA is silent and rarely causes any symptoms. To prevent rupture, IAs can be treated by closure of the IA from the circulation by clipping the IA neck or filling the IA sack with a platinum coil. Modern neurosurgical and endovascular treatment techniques are, however, associated with risks for complications and even with a small but non-negligble risk of death. Pharmacological treatment for IA and SAH prevention does not yet exist. Since not all IAs will ever rupture even if untreated, invasive treatment should be targeted selectively to IAs of high risk for rupture, leaving low-risk

and stabile IAs untouched. However, identifying the rupture-prone IAs among all IAs has remained a challenge. Accomplishment of novel methods for diagnostics and preventive treatment requires complete knowledge of IA pathogenesis.

IA is a frequent disease of a large cerebral artery wall, manifested by a focal outpuching lesion in the bifurcation area of the artery. Typical IA locations in the Circle of Willis arteries are in the middle cerebral artery and the anterior and posterior communicating arteries. Some IAs may evolve from the branches of the internal carotid artery, ophthalmic artery, posterior inferior cerebellar artery, or the basilar tip. Along with its bulging, the IA lesion has undergone a dynamic pathological wall remodeling process under the burden of chronic inflammation, one that may have evolved for years or even decades. Although family- and genetic background may play some role in IA pathogenesis, IAs are mainly considered to be sporadic lesions, influenced mainly by lifestyle- or environment-related factors.

Similar to IA, atherosclerosis is a well-known chronic inflammatory disease of the arterial wall. Atherosclerosis, besides affecting all extracranial arteries, is present also in intracranial arteries which show lipid accumulation. Imbalanced function of the circulatory lipoproteins: high-density lipoprotein (HDL) and low-, intermediate-, and very low-density lipoproteins (LDL, IDL, VLDL) plays a role in systemic atherogenic processes. Lipid accumulation is associated with intraluminal injury and atherothrombotic complications of the arterial wall. Similar changes in the IA walls such as inflammation, lipid accumulation, and intraluminal thrombosis are associated with IA rupture. However, the role of these changes in IA wall degeneration and rupture remain unknown.

The IA wall ruptures when mechanical stress resulting from the blood pressure exceeds wall strength. Understanding the pathobiological mechanisms that lead to IA wall weakening and rupture is highly important for the development of specific imaging techiques and pharmacological treatment methods to prevent fatal SAH. This thesis deepens the knowledge of IA pathogenesis particularly from the perspective of atherosclerotic, inflammatory changes that may contribute to IA wall degeneration and rupture. Through the correlation of IA wall histopathology with hemodynamic flow models and MRI presentations of IAs, this thesis also discusses potential diagnostic tools which might improve detection of high-risk IAs.


Vatti

2. Review of the Literature

2.1 Saccular intracranial aneurysm (IA) and subarachnoid hemorrhage (SAH)

This section reviews the macroscopic features of saccular intracranial aneurysms (IAs), their epidemiology, clinical manifestations, and treatment.

2.1.1 Rupture of an IA causes SAH

An IA is a pathological saccular lesion of a large intracranial artery at the base of the brain. IAs are typically located at bifurcation sites of arteries of the Circle of Willis [27,248] (Figure 1), where focal weakening of the arterial wall causes its outpouching. A majority of unruptured IAs are small (<5-7 mm) [146], but their diameters may range from a few millimetres to several centimeters for giant IAs. Whereas an intact IA rarely causes its carrier any harm, rupture of an IA is devastating.

A ruptured IA bleeds into the subarachnoidal space that surrounds the brain, causing a subarachnoid hemorrhage (SAH, Figure 2). An IA may also bleed into brain tissue, into the ventricular system, or into the subdural space of the brain [248]. Although SAH can also originate from head trauma or arise spontaneously without any predisposing aneurysmal formation, IA rupture may account for 85% of all SAH incidents, making it the most notable cause for SAH.

2.1.1.1. Other aneurysm types in the brain vasculature

This thesis focuses on the saccular pouching type of IA, which accounts for the majority of all aneurysms arising in large intracranial arteries. However, an intracranial aneurysm can also be of fusiform type (Figure 3). A review of 329 surgically treated intracranial aneurysms reported the proportion of fusiform type aneurysms as 5%, the rest being of saccular type [196]. There are also microaneurysms of saccular morphology, known as Charcot-Bouchard aneurysms, which occur in the smallest branches of intracranial arteries (arterioles) in proximity to the basal ganglia of the brain [233]. Due to their subcortical location, ruptured microaneurysms are a common primary cause of intracerebral hemorrhages, whereas IAs may cause intracerebral hemorrhages secondary to SAH.

2.1.2 Epidemiology of IAs and SAH

2.1.2.1. Prevalence of IAs

Unruptured IAs are common worldwide. International systematic reviews including imaging- and autopsy studies from 1955-2011 estimate that in a population without specific comorbidities, 2.3 to 3.2% (95% confidence interval, CI, 1.7-3.1 and 1.9-5.2) are IA carriers [209,252] (Figure 4). One-third of them may harbor multiple, i.e. two or more IAs. An autopsy study of 289 SAH patients found multiple IAs in 31% of them [51]. Epidemiological studies show similar proportions. A prospective study from a single medical center based in the USA reported in 1277 consecutive patients with aneurysmal SAH two or more IAs in 387 (30%) [162]. Among 114 unselected IA carriers in eastern Finland, the prevalence of multiple IAs was similar, 34% [210].

2.1.2.2 Worldwide incidence of SAH

Although prevalences of IAs appear similar in the USA, China, Japan, and several European countries, including Finland [252], the reported incidence of aneurysmal SAH (referred to simply as SAH) varies among populations. According to large international studies, the incidence of SAH has been estimated as 9 to 10 cases per 100 000 population per year

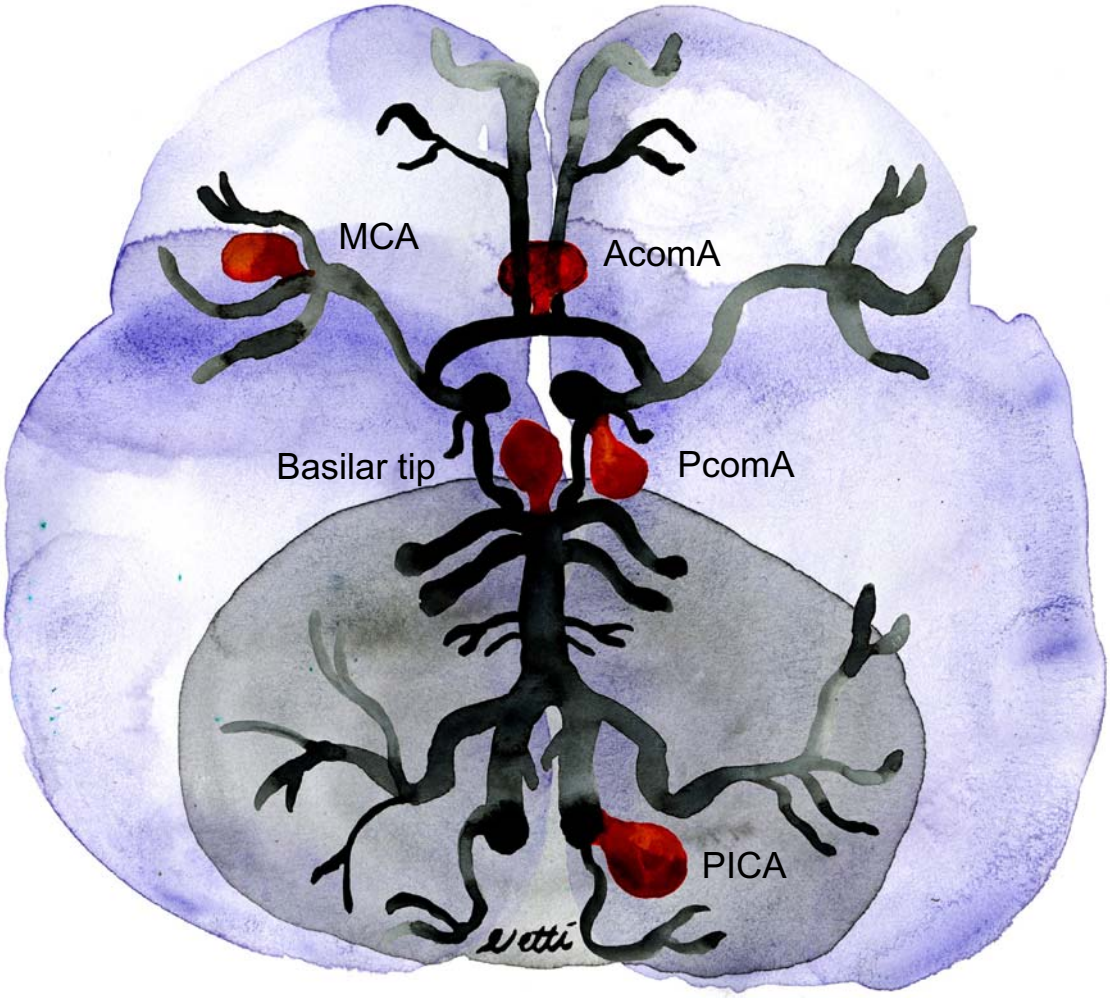

Figure 1. Schematic presentation of common IA locations: anterior and posterior communicating arteries (AcomA, 30%; PcomA 12-13%), middle cerebral (MCA, 30-40%), basilar (5%), and posterior inferior cerebellar (PICA, 1-2%). An IA may also occur in internal carotid, ophthalmic, and pericallosal arteries (not visible in the illustration). Site percentages are from an unselected Finnish population [94,146].

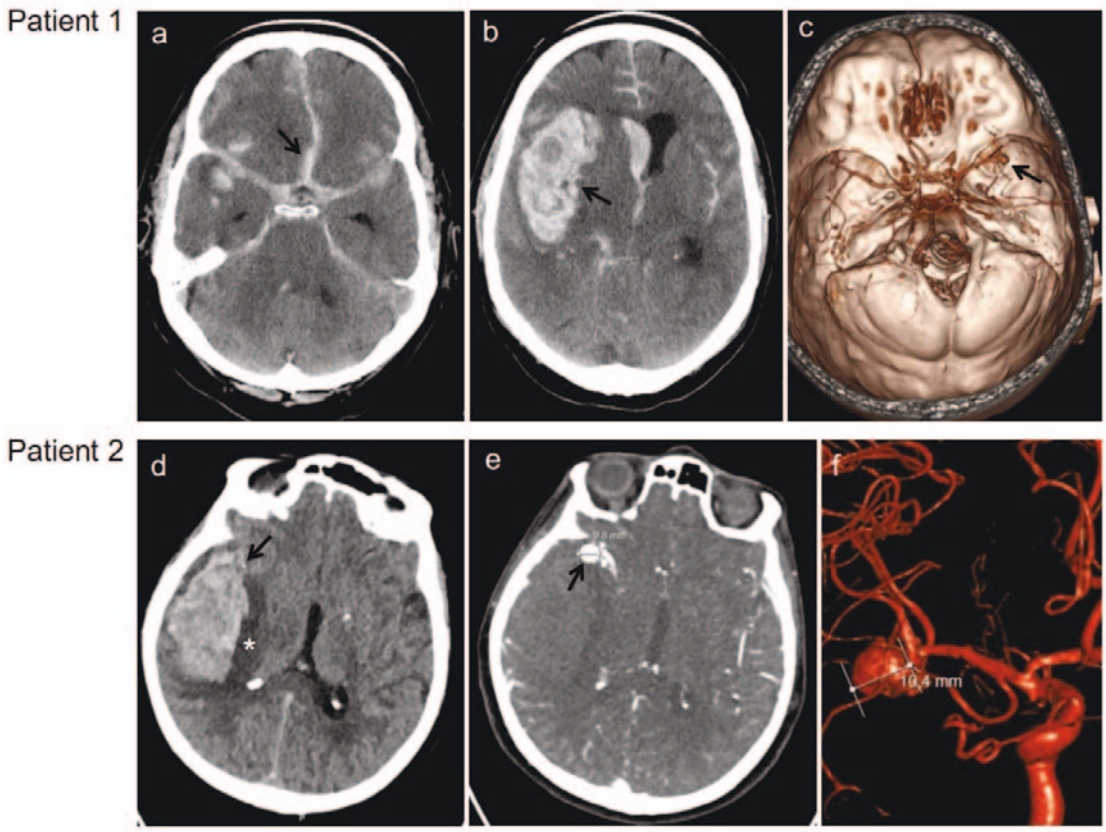

Figure 2. Computed tomography (CT) images of two patients with ruptured middle cerebral artery (MCA) bifurcation IAs. **a** Patient 1: subarachnoid hemorrhage (SAH, white, arrow) and **b** intracerebral hemorrhage (ICH, white, arrow), **c** CT-angiography (CTA) reconstruction, same patient, showing the aneurysm (arrow) in MCA. Patient 2: **d** ICH (arrow) is surrounded by edema (star). **e** shows the IA in CT-angiography CTA and **f** in 3D digital subtraction angiography (DSA) images. (Images from Dr. Juhana Frösen, Department of Neurosurgery, Kuopio University Hospital, Kuopio, Finland.

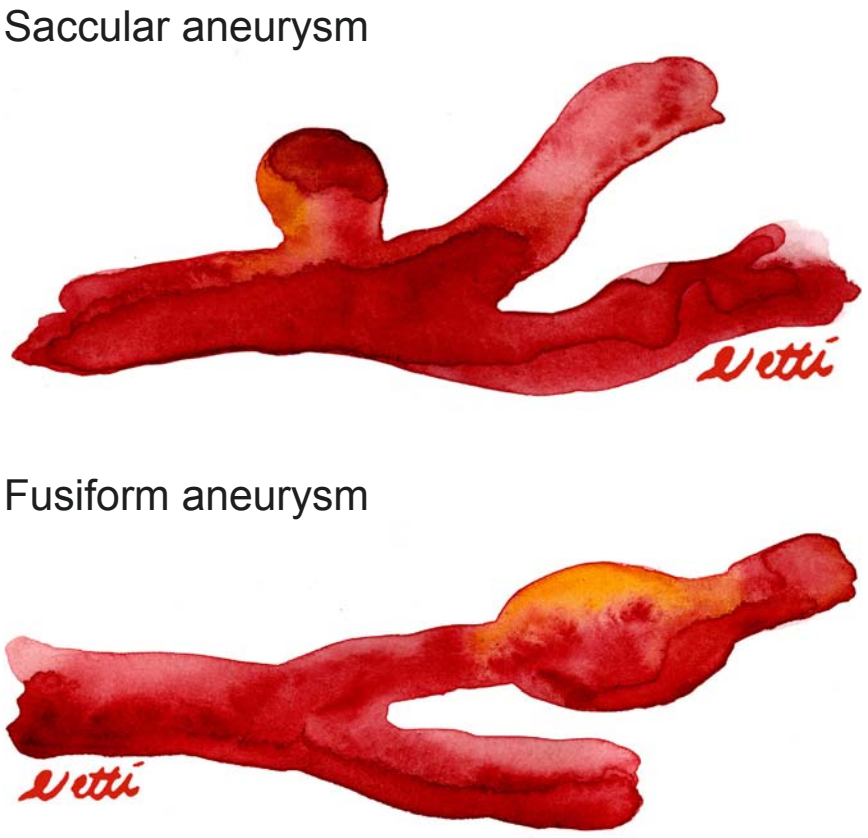

Figure 3. Saccular vs. fusiform aneurysm types. Unlike a saccular intracranial aneurysm, a fusiform aneurysm represents segmental dilatation of the entire blood vessel wall. Although also occurring intracranially, fusiform-type aneurysms are more common extracranially, particularly as abdominal aortic aneurysms.

in most European countries and in North America (9.1; 8.8-9.5), but significantly fewer in South and Central America (4.2; 3.1-5.7), and in China (2.0; 1.6-2.4). In Japan, SAH has shown exceptionally high rates (22.7 and 21.9-23.5) [55], and Finland has shown similarly high rates of SAH in the same studies: 19.7 and 18.1-21.3 [55] to 22.5 and 20.9-24.1 [96], however, current epidemiological data have revealed a much lower Finnish incidence of SAH.

2.1.2.3 Incidence of SAH in Finland

Recent Finnish studies show a SAH incidence lower than earlier estimated: approximately 7 to 9 cases per 100 000 per year [102,123]. This would account for 400 to 500 cases per year, significantly fewer than the earlier estimate of 1000 SAH cases annually in Finland. A study of 1965 hospital-admitted SAH patients from the catchment area of Tampere University Hospital between 1990 and 2014 reported SAH incidence as annually 7.41 per 100 000, without a clear trend upwards or downwards. However, in comparison with other hospital regions, marked regional differences emerged, with Jalava et al. reporting a 64% higher SAH incidence in eastern Finland than in the Tampere region [102].

One Finnish nationwide study, based on the register of the National Institute for Health and Welfare, found a 24% decrease (11.7 vs. 8.9 per 100 000) in average annual SAH incidence when comparing 1998-2000 and 2010-2012 [123]. The incidence of SAH decreased together with smoking, an important risk factor for SAH, which may explain in part this decrease. Of other cardiovascular disease risk factors, serum cholesterol and blood pressure values have also decreased among the Finnish population, according to wide surveys of risk factors performed in several geographical regions during 1972-2007 [249]. Still, no evidence exists of causal relations between the changes observed in SAH incidence and Finnish smoking habits or cardiovascular health.

It is notable that different studies of the incidence of SAH may prove controversial due to exclusion of cases in which sudden death occurred without confirmation of the diagnosis through an autopsy [121]. Of all deaths from SAH, approximately 10 to 20% are sudden [96,121,180]. In Finland, the autopsy rate for sudden deaths is high in any international comparison, which may have affected

earlier data showing Finland's comparably high SAH rate on an international scale [121]. Results of epidemiological research may also vary widely between research centers due to differing study time-periods, as well as differences in population age, if not adjusted for. Thus, exact SAH incidence rates remain unknown.

2.1.2.4 Outcome of SAH

The outcome of IA rupture is catastrophic: nearly half (40-50%) of SAH patients die during the first month after SAH, including those 10 to 20% who die immediately, before receiving any medical attention [96,180]. Age-adjusted fatality rates of SAH also show regional dependency. Risk of death after SAH has been two-fold higher in Eastern than in Western Europe (62% in Yugoslavia-Novi Sad's population vs. 32% in Sweden-Göteborg) [96], and around 12% lower in Japan (27%) than on average in Europe, the USA, Australia, and New Zealand [180]. A large international meta-analysis shows also a slight 17% decrease in fatality from SAH during the period 1973-2002, possibly explained by improved treatment strategies [180].

Patients who survive may suffer from systemic complications of SAH, IA rebleedings, and long-term neuropsychological disabilities [248]. SAH patients are typically women (63%) of working-age, mean age around 60 [180]. In women, SAH occurs at a later mean age than in men (63 vs. 55 years) [180]. The overall mean age of SAH patients has been increasing during recent decades [55,111]: age 52 to 53 years in 1973 to 1992 to 62 years in 1993 to 2002, according to one meta-analysis [180]. Despite such an increase in mean age, loss of productive life-years due to disability or death from SAH is a burden on both individuals and society.

2.1.2.5 IA rupture risk

Not all IAs rupture. In a lifelong follow-up of a cohort of 118 Finnish working-aged IA carriers, 34 (29%) experienced SAH [122]. Risk for IA rupture accumulates over time, with average annual rupture risk of an IA estimated as 1.6% (range 0-6.5%) in a group of patients with life-long follow-up [122]; as 1.1% in another Finnish long-term (median 21 years) follow-up cohort of 181 IAs (142 patients)

[111]; and 0.76% (95% CI 0.58-0.98) in a Japanese cohort of 1960 patients during 10 years of follow-up [173].

IA rupture risk most likely does not, however, increase linearly year by year. Rather, it may stay low for a long time, until rising before IA rupture [208]. Interestingly, the Finnish long-term follow-up study revealed no IA ruptures after 25 years, suggesting a decrease in rupture risk over very long periods [111]. Importantly, rupture risk of an IA is dependent on risk-factor burden [77,122], which may cause a risk increase up to many-folds higher [149].

2.1.3 Clinical risk factors for IA and SAH

IAs are not congenital, as they develop during one's lifetime [231]. Their etiology is complex. Multiple independent, mainly environmental but also some inherited factors, are involved in IA formation. Currently IA rupture defies prediction, but several risk factors elevate rupture risk. Major patient- and aneurysm-related risk factors are in Table 1.

2.1.3.1 Patient-related risk factors

Fortunately, the most important risk factors, such as smoking and hypertension, can be influenced by lifestyle choices. However, some patient characteristics, including family history, genetics, sex, and age, are non-modifiable.

Non-modifiable risk factors

Family history and genetic backround

Familial and genetic background may be one risk factor for IA and SAH [29,213,214,252]. Having IA carriers or SAH patients in first-degree relatives is associated with 3- to 4-fold risk for IA in a large meta-analysis by Vlak et al. (prevalence ratio, PR 3.4; 95% CI 1.9-5.9) [252], and with 4- to 7-fold risk for SAH in series of 146 [214] and 163 [29] SAH patients. Approximately 10% of SAH patients belong to families of SAH aggregation [29,214]. Familial IAs have been reported to rupture 6 to 7 years younger than do sporadic ones (median ages of SAH 46.6 vs. 53.4 years) [29], they grow large more often prior to rupture (>10 mm; risk ratio, RR 2.1; 1.2-3.6)

Figure 4. IA carriers. Those harboring IAs are 2-3% of the worldwide population, often unaware of their condition.

Table 1. *Risk factors for intracranial aneurysm (IA) prevalence and rupture.*

	Effect	
Risk factor	IA prevalence	SAH incidence
Patient characteristics		
Family history of IA	Increase 3-4 x [252]	Increase 4-7 x [29,214]
Genetic background	Potential increase [3,213,241]	Potential increase [3]
Female sex	Increase 1-2 x [252]	Increase 1-2 x [209]
Old age	Increase [25,208]	Increase [111]
Specific comorbidities		
Polycystic kidneys	Increase [25]	Increase [248]
Ehlers-Danlos type IV	Increase [25]	Increase [25]
Aortic coarctation	Increase [25]	
Earlier SAH	Increase [208]	Increase [25]
Modifiable risk factors		
Hypertension	Increase [147]	Increase 2-3 x [62]
Hypercholesterolemia	Decrease <1 x [251]	Decrease <1 x [62,95]
Atherosclerosis	Increase 1-2 x [252]	
Diabetes mellitus		Decrease <1 x [62,147]
Current smoking	Increase 2-3 x [252]	Increase 2-3 x [62]
Alcohol consumption		Increase 1-2 x [62,111]
Use of narcotics		Increase [28,64,215]
Coffee consumption		Increase [28] [98]
Aneurysm characteristics		
Large size		
Diameter 7 mm or more		Increase [110,111]
Diameter 10 mm or more		Increase [97]
Large volume		Increase [110]
Growth		Increase [25,110]
Irregular shape		Increase 4-7 x [118,146]
Location		
AcomA*		Increase [110,111]
Posterior circulation		Increase [25]

*AcomA: anterior communicans artery

[214], they show multiplicity [214], and they favor a location in the middle cerebral artery [29] 2 to 3 times more often than do sporadic ones.

Genome-wide linkage studies analyzing whether specific DNA markers linked with disease genes occur in IA families have, however, revealed only a limited number of gene loci showing replication in various populations [213]. A comprehensive review of 10 genome-wide linkage studies identified four such loci [213], including perlecan- and elastin genes involved in the maintenance of structural components of the extracellular matrix (ECM), i.e. vascular-wall-supporting tissue [213]. As a limitation, definitions of an IA family varied in the genome-wide linkage studies reviewed: differences appeared in the number of affected family members (2, 3, or more) and in the relationship between them [213].

The loci detected through a linkage study, however, do not necessarily apply to sporadic IAs. Thus, the genetic basis for sporadic IAs has been studied by genotyping single nucleotide polymorphisms (SNPs) to mark specific disease-associated gene alleles and further performing genome-wide association (GWA) studies to define genetic markers for increased IA risk [3,241]. A meta-analysis of genetic association- and GWA studies identified 19 SNPs, suggesting the association of various genes and multiple pathophysiologic pathways with sporadic IA formation and rupture [3].

However, the contribution of gene variants to SAH risk appears relatively small. According to a large Nordic twin study of 79,644 twin pairs identified from Finland, Sweden, and Denmark, SAH had occurred for 498 pairs (152 monozygotes and 346 dizygotes), of whom only 6 were concordant (1.2%, 5 monozygotes, 1 dizygote) [124]. Thus, Korja et al. concluded that environmental and lifestyle factors seem more significant contributors to familial SAH risk than is clustering of disease genes.

Female sex and age

IAs are more common in women than in men at all ages (PR 1.61; 1.02-2.54 for a population of mean age < 50; and PR 2.2; 1.3-3.6 for a population of mean age > 50), and the risk for developing an IA increases with age especially in women [252]. Systematic reviews report that compared to male IA carriers, female carriers also show greater risk for IA rupture (RR 2.1; CI 1.1-3.9) [48,209].

More specifically, SAH incidence is higher in women than in men after age 55 (RR 1.24; CI 1.09-1.42) [55], close to the mean age of menopause: 52 to 53 years [235]. The preponderance of women has thus been hypothesized to relate to changes in female hormone levels. Studies investigating hormone replacement therapy in postmenopausal women or oral contraceptives at their fertile age have shown no clear change in SAH risk, although some associations have appeared (see the separate section).

Specific comorbidities

A few congenital abnormalities are risk factors both for IA formation and for rupture. Aortic coarctation, vascular Ehlers-Danlos syndrome (type IV EDS), and autosomal dominant polycystic kidney disease (ADPKD; prevalence ratio 6.9; 3.5-14 [252]), are associated with several factors which contribute also to IA disease [25,231,248,252]. Secondary hypertension is associated with aortic coarctation and may trigger the onset of IA in those patients. Connective tissue disorder due to mutation in the type III procollagen gene COL3A1 [254] is associated with type IV EDS and may also contribute to IA formation through structural fragility of the vascular wall. Altered hemodynamic-flow sensing (SMC and the endothelium –derived ADPKD gene products polycystin-1 and -2 responsible for mechanotransduction [193]), IAs are also associated with other cerebrovascular malformations such as cerebral dural arteriovenous fistulas, potentially due to formation mechanisms related to altered blood flow [78,86].

Modifiable risk factors

Hypertension

Together with smoking, the main risk factor for IA formation and rupture is chronically elevated blood pressure. An eastern Finnish single-center study of all hospital-admitted IA cases 1995-2007 suggested the contribution of high blood pressure to IA formation [147]. Lindgren et al. observed a high prevalence of hypertension in IA patients, as 73% of those 467 patients with unruptured IAs and 62% of those 1053 patients with ruptured IAs used antihypertensive medication. Untreated hypertension was more prevalent in patients with ruptured IAs (29% vs. 23%) [147].

IA rupture risk increased in patients with hypertension. In a worldwide meta-analysis of case-control- and longitudinal studies of 3936 SAH-patients, Feigin et al. showed that hypertension elevates SAH risk 2- to 3-fold (RR, 2.5; 2.0-3.1) [62]. Their other study, focusing on the population of the Asia-Pacific region (30,6620 participants), specified the cutpoint level of systolic blood pressure as 140 mmHg, above which SAH risk was markedly increased (hazard ratio, HR, 2.0; 95% CI, 1.5-2.7) [61]. Moreover, every 10-mmHg increase in systolic blood pressure was associated with a SAH risk 31% (95% CI, 23-38%) higher [61].

Atherosclerosis and hypercholesterolemia

Atherosclerosis is a common systemic disease of the arterial wall, characterized by lipid accumulation, chronic inflammation, and gradual occlusion of arteries. IAs have been more common in patients with atherosclerosis than in patients without the disease (PR 1.7; 0.9-3.0), although not to a statistically significant level [252]. That large meta-analysis of unruptured IAs did not, however, clearly specify how atherosclerosis was defined there [252]. Since the diagnosis of atherosclerosis can be based on findings in several different examinations, such as stenoses and calcifications of arteries in angiography, clinical observations in surgery or autopsy, or typical symptoms of affected organs, assessing atherosclerosis in a large number of patients is not straightforward from merely a database. In the meta-analysis, the atherosclerotic patients showed a wide range, including those with a history of transient ischemic attack or ischemic stroke. Besides from an atherosclerotic etiology, ischemic strokes often also arise from cardiac embolism. However, these potential confounders were not reported in detail in that study. Based on the heterogeneity of patients with atherosclerosis, epidemiologic connections between atherosclerotic diseases and IAs are challenging by meta-analysis, and it remains unknown whether there are more among atherosclerosis patients with IA than suspected.

The main risk factor for atherosclerosis is hypercholesterolemia [15]. Interestingly, in a case-control study of 206 IA carriers and 574 controls, Vlak et al. found hypercholesterolemia to be an independent factor reducing the risk for IA occurrence (OR 0.5; 95% CI 0.3-0.9) [251]. According to a meta-analysis by Feigin et al.,

hypercholesterolemia has also been consistently associated with decreased SAH risk (RR, 0.8; 0.6-1.2) [62]. A Japanese case-control study showed that 285 patients of all age-groups with unruptured IAs had hypercholesterolemia more often than did those 858 with ruptured IAs (OR 0.24-0.53; 95% CI 0.12-0.76). Interestingly, IA rupture risk was particularly reduced in patients under 60 with hypercholesterolemia (OR 0.38; 0.22-0.68) [95]. Here, the threshold for total cholesterol level was at 220 mg/dL, i.e. 5.7 mmol/l [95], whereas in the large study of the Asia-Pacific population, it was 4.5 mmol/l for a trend of lower SAH risk at higher cholesterol levels (HR 0.9; 0.7-1.3) [61]. In contrast, a recent systematic review found that elevated total cholesterol elevated SAH risk in men [145]. The mechanism by which cholesterol level affects SAH risk is, indeed, unknown. The potential hypercholesterolemia-associated statin use mediating some protective effect on the artery wall has been discussed (see the separate section), although not defined.

Diabetes mellitus and body weight

Diabetes mellitus (DM) has been associated with a decreased risk for SAH in the meta-analysis by Feigin et al. (RR 0.3; 0-2.2) [62], and recently in a large study of over 2 million participants, 4327 of them with SAH (RR 0.4, 95% CI: 0.29-0.56 [258]. Both reports left DM type undefined. An eastern Finnish study assessed the use of DMII medication in 484 IA carriers and 1058 SAH patients, finding no association between the prevalence of medically treated DMII and SAH [148]. Further, neither body weight nor body mass index (BMI) has shown any clear association with SAH risk, since the data have been inconsistent in systematic reviews [48,61,62]. However, vigorous physical exercise (> 3x per week) has been an independent risk reducer for IA (OR 0.6; 95% CI 0.3-0.9) [251], suggesting a role for regular exercise in IA prevention.

Tobacco

Current smoking is an independent risk factor for IA (OR 2.9; 95% CI 1.9-4.6) according to the case-control study by Vlak et al. [251]. When combined with hypertension, the effect of smoking on IA occurrence appears synergistic (OR 8.3; 95% CI 4.5-15.2) [251]. In the Finnish long-term follow-up of patients with unruptured IAs,

smoking raised IA rupture risk, as well, up to 2- to 3-fold (HR, 2.44; 1.02-5.88) [111]. Similar SAH risk ratios have been demonstrable in the meta-analysis of case-control studies by Feigin et al. (RR 2.2; 1.3 to 3.6) [62]. A Finnish population-based cohort of 613 young (<40 years) IA patients with 105 unruptured and 508 ruptured IAs demonstrated that smoking is a particular risk factor for SAH in younger individuals (hazard ratio, HR, 2.8, 95% CI 1.2-7.0) [200]. That study showed that even former smoking doubles risk for SAH when compared to never-smoking [62], suggesting that smoking has a long-term effect on increased SAH risk. What has not been established, however, is the mechanism of how smoking influences IA prevalence and rupture.

The use of snus, a smokeless tobacco product of high nicotine content, has been investigated in one group of 120 northern-Swedish SAH patients [126]. Of these participants, 10.8% were active snus users and 77.1% previous or current smokers. Similar to findings by others, also in that study smoking was associated with approximately 2.5-fold higher risk for SAH (RR, 2.63, 1.20–5.72 for men and 2.26, 1.69–3.01 for women), whereas snus consumption did not affect their SAH risk (RR, 0.48, 0.17–1.30 for men and 1.30 0.33–5.18 for women). The authors suggest that nicotine is unlikely to be responsible for the smoking-related increased SAH risk [126].

Alcohol

Heavy drinking is a potential risk factor for SAH. In the meta-analysis by Feigin et al. and the Finnish follow-up study by Juvela et al., consumption of up to 12 doses or standard drinks (100-150 g) of alcohol per week was associated with up to two-fold risk for SAH when compared to that for non-drinkers (RR 2.1; 1.5-2.8 [62] and HR, 1.27; 1.05-1.53 [111]). A retrospective case-control study of 4701 IA patients (28% with ruptured IAs) reported increased IA rupture risk in current drinkers (43%, OR 1.36, 1.17-1.58), a risk increase that did not persist in former drinkers (6.5%, OR 1.23, 0.92-1.63) [35].

Narcotics

Cocaine, amphetamins, and ecstasy have all been related to hypertension-associated intracerebral hemorrhages (ICH) and vascular malformations [163]. One British retrospective study

identified 13 patients using those substances prior to ICH. Ten of them underwent angiography, revealing six IA carriers and three carriers of arteriovenous malformations [163]. Other studies have also shown an association between cocaine and neurovascular complications, including ICH, ischemic stroke, and IA rupture [64]. Fessler et al. showed that of 77 SAH patients, those 33 using cocaine were younger (32.8 vs. 52.2 years) and had smaller IAs (4.9 vs. 11.0 mm) at rupture, than did the control group of 44 non-cocaine users [64]. A case-control study of 312 SAH patients and 618 matched controls showed that 3% of SAH patients had used cocaine within the previous 3-day period prior to SAH, whereas none of the controls had done the same (OR 24.97; 95% CI 3.95-adjusted estimate not calculable) [28]. Cerebral vasospasm has been suggested to be the cause of cocaine-related SAH, through direct smoothmuscle constriction, catecholamine secretion, and the subsequent acute elevation of blood pressure [28,163]. Marijuana has also been reported as an independent risk factor for SAH in a US Kansas-based nationwide study of 118.7 million people, of whom 2.1% were cannabis users (OR: 1.18; 1.12-1.24). The mechanism of any link between cannabis and aneurysmal SAH was lacking. However, the authors stated that the effect of cannabis could be related to reversible cerebral vasoconstriction syndrome (RCVS) [215].

Coffee and caffeine

A prospective single-center study from Tromso, Norway, reported that drinking more than five cups of coffee per day is associated with SAH (OR 3.86; 1.01-14.73) [98]. However, their 27 161 subjects included only 26 SAH cases, of whom 85% (vs. 59% of controls) were high coffee-consumers. Later, Broderick et al. also reported that such caffeine consumption within the previous 3 days prior to SAH was associated with SAH (OR 2.48; 95% CI 1.19-5.20) [28]. A possible mechanism for coffee consumption's contribution to SAH lies in its hemodynamic effect. Caffeine causes vasoconstriction through antagonizing endogenous adenosine, acutely elevating blood pressure level (5-15 mmHg for systolic and 5-10 mmHg diastolic value) [103]. With its half-life of approximately 5 hours, caffeine's effect may persist for several hours after consumption of coffee beverages. Habitual coffee drinking may thus associate with IA formation through its effects on vascular stress, but causalities remain unstudied.

A randomized trial investigating the effect of coffee consumption on blood-pressure values in 107 young normotensive adults showed that 9 week's abstinence from coffee reduced only slightly blood pressure level (systolic -3.4 mmHg; 95% CI -7.1-0.3) compared to levels in those who consumed 4 to 6 cups per day [17]; a minor, non-significant depression in heart rate occurred [17]. Therefore, considering SAH-preventive intervention, coffee abstinence may not be the most effective method for reducing blood-pressure level. Nor was coffee consumption associated with development of coronary and carotid atherosclerosis in a multicenter cohort of 5115 young adults during 20 years follow-up [203].

Hormone replacement therapy and oral contraceptives in females

Risk for SAH in postmenopausal is higher than in pre-menopausal women, according to a systematic review of 3580 SAH patients (odds ratio, OR 1.29; 1.03-1.61) [4]. In that review of a population of 1671 post-menopausal women, use of hormone replacement therapy (HRT) associated with decreased risk for SAH (OR 0.86; 0.69-1.08 for current use and OR 0.74; 0.54-1.00 for ever use) [4]. However, a large prospective study of 93 676 postmenopausal women (44% HRT users) showed contradictory results: during 11 to 13 years of follow-up, SAH occurred in 114 patients and showed higher rates in those actively using HRT than in those not using the therapy (0.14% vs. 0.11%, OR 1.5; 95% CI 1.0-2.2) [199]. The potential effect of HRT on SAH risk may, according to these authors, be explained by estrogen-receptor-mediated pro-inflammatory mechanisms in the vascular walls. However, they reached no conclusions as to the potential contribution of HRT to SAH risk.

Treatment with combined oral contraceptives (OC; including estrogen and progestogen), has also elevated SAH risk. One meta-analysis showed increased SAH risk in OC users (RR 1.42; 1.12-1.80), but the increase was not significantly dependent on estrogen dose (RR 1.94; 1.06-3.56 for high dose vs. RR 1.51; 1.18-1.92 for low dose) [108]. The more recent systematic review of SAH patients found that current use of OC raised (OR 1.31; 1.05-1.64) and everuse of OC lowered (OR 0.90; 0.75-1.09) the risk for SAH [4]. A physiological explanation for this also contradictory result remains, however,

unclear. The phases of hormonal changes in the female life-cycle, such as parity, menarche age, pregnancy, labor, or puerperium, have shown no association with SAH risk [4]. In short, how female sex affects IA formation and rupture, and whether the altered estrogen levels after menopause play a role in IA occurrence and their rupture-tendency, remains unknown.

2.1.3.2 Aneurysm-related risk factors

Known IA-related risk factors for IA rupture include large size or irregular shape, as well as tendency for growth or development of daughter-sacks. Additionally, some IA locations associate with higher IA rupture risk. Among other clinically relevant risk factors, particularly those possible to examine by molecular imaging or other methods, are hemodynamic stress, macrophages, and myeloperoxidase (MPO) expression manifesting high inflammation, and IA-wall remodeling – all are associated with IA rupture.

Macroscopic features of an IA

The International Study of Unruptured Intracranial Aneurysms (ISUIA) [97] assessed the outcomes of IAs, showing that IA rupture risk is higher for larger (>10 mm) than smaller IAs. In a prospective 10-year follow-up cohort of 2252 Japanese IAs, ones larger than 5 mm were associated with a significant increase in rupture risk (hazard ratio 12.24, 95% CI 7.15-20.93 [173]). A meta-analysis showed that larger size is also a risk factor for IA growth, which increases in larger IAs; RR for >5 mm IAs being 2.56 (95% CI 1.93-3.39), and for >10 mm IAs 5.38 (95% CI 3.76-7.70), when compared to 4 mm IAs [16]. Accordingly, the growth rate of an IA is associated with its rupture risk. In a Finnish series of 181 IAs (142 patients), IA diameter over 7 mm increased risk for SAH during decades of follow-up (HR, 2.60; 1.13-5.98) [110]. However, a significant proportion of IAs rupture at under 7 mm [146], so size alone is insufficient for detection of rupture-prone IAs that require treatment.

Irregularly shaped IA morphology and elongated IAs with high aspect ratios (fundus length: neck diameter) are at higher risk for rupture than are wider IAs, according to a recent systematic review (OR 4.8 95% CI 2.7-8.7) [118]. A Finnish single-center registry-based study of 5814 IAs (48% ruptured) in 4074 patients also noted that the irregular or multilobular shape of an IA associates strongly with

rupture, irrespective of IA size (OR 7.1 95% CI 6.0-8.3), and such IAs should be considered as high-risk, even in patients without other risk factors for rupture [146].

Location in the posterior cerebral circulation, such as in the basilar artery, vertebrobasilar, or posterior cerebral artery (PCA) or posterior communicating artery (PcomA), has, in a multi-center study, been another independent predictor of rupture [97], whereas in the Finnish population, IA in the anterior communicating artery (AcomA) has been an independent risk factor for SAH (HR, 3.73; 1.23-11.36) [111]. A recent United Kingdom (UK) -based multicenter case-control study of 2334 IA-patients (74% with ruptured IAs) showed the predominance of both anterior (ACA or AcomA; OR 3.21, 2.34-4.40) and posterior (PcomA or other; 3.92, 2.67-5.74 and 3.12, 2.08-4.70) locations in ruptured IAs, over location in the middle cerebral artery (MCA) [92].

2.1.4 Diagnostics of IA and SAH

Unruptured IAs are mostly asymptomatic and not commonly screened. Thus, their detection is mainly incidental. If located near cranial nerves, an IA may sometimes cause palsies by nerve compression. However, any warnings preceeding rupture are rare [27]. SAH due to rupture of an IA is an emergency condition, manifested by typical symptoms (see Figure 5).

2.1.4.1 Imaging of IA and SAH

Routine examinations

Non-invasive angiography identifies an IA. The imaging can be performed by contrast-enhanced computed tomography (CT) or magnetic resonance imaging (MRI) or invasively with catheter angiography. Since angiography can specify the size, morphology, and location of an IA, it is required for planning operative treatment. To identify SAH, non-invasive, non-contrast CT-scanning of the brain is the primary method to detect the acute bleeding [27,248]. CT is sensitive for SAH within 6 hours from onset of symptoms [22]. Signs of older bleeding can be detectable from cerebrospinal fluid examination via lumbar puncture [27], which should be performed in CT-negative patients with symptoms strongly suggesting SAH.

Experimental and molecular imaging

Simulation of hemodynamics within the IA lumen can be reconstructed from three-dimensional rotational CT and MR-angiography (MRA) images providing further information as to flow conditions in the IA. Computational fluid dynamic (CFD) simulations for 210 IAs showed that ruptured aneurysms are associated with concentrated inflows, concentrated wall-shear stress distributions, high maximal wall-shear stress, and small viscous dissipation ratios [177]. It is likely that altered hemodynamic forces and increased wall-shear stress play roles in the pathogenesis of an IA, probably similar to that in atherosclerotic arteries [221].

Contrast-enhanced MRI can serve for molecular imaging of the IA wall structure and inflammation [20]. Ferumoxytol- or other ultrasmall superparamagnetic iron oxide nanoparticles (USPIOs) may be able to act as a marker of IA wall instability, due to their potential uptake by macrophages of the wall [84,264]. Gadolinium is another contrast material which can visualize inflammation in the vascular wall [34]. Gounis et al. have demonstrated in an experimental rabbit elastase-aneurysm model that enhanced gadolinium (di-5-hydroxytryptamide of gadopentate dimeglumine) can serve as a specific biomarker for myeloperoxidase [75], a neutrophil- or macrophage-derived enzyme present also in human IAs [76].

MRI can detect histopathological changes in the IA wall even without any use of contrast material. Honkanen et al. demonstrated that Perl's-positive iron visualized in 4.7 T ex vivo MRI-scannings of three giant IAs [91]. Hence, iron may prove a promising marker of IA pathogenesis. A hybrid of opposite-contrast 3T MRA has been introduced to detect atherosclerotic plaques with high sensitivity (88%) and specificity (100%) in a small series (n=16) of unruptured IAs [156]. Collectively, these imaging methods allow a closer evaluation of the IA wall and may serve as a potential tool predicting risk for IA rupture in the future.

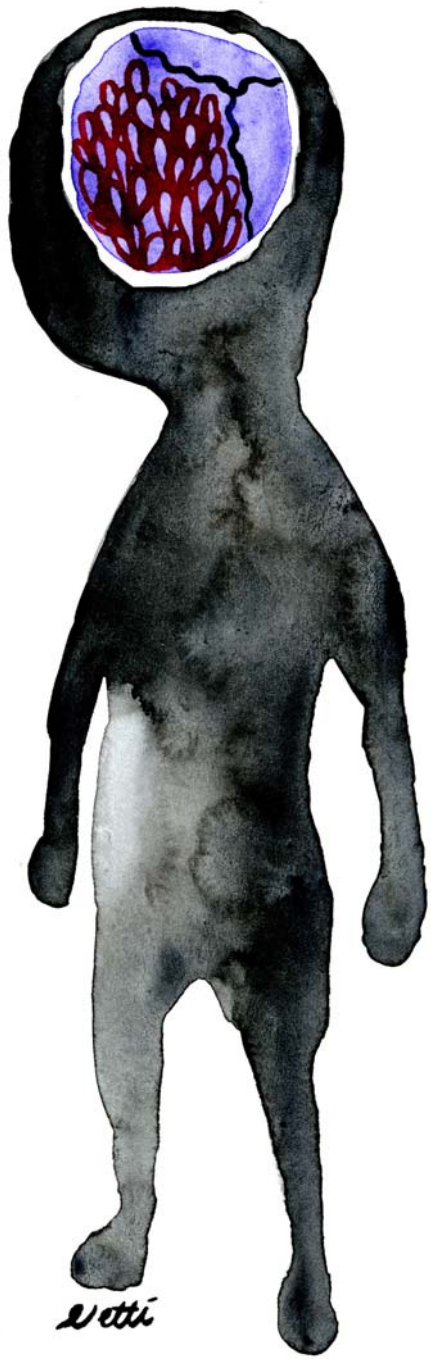

Figure 5. Illustration of a sudden SAH. Rupture of an IA is classically manifested as sudden, global headache, which the patient may describe as “worst headache ever”. Additional symptoms may be nuchal rigidity, nausea, drowsiness, hemiparesis, and coma [27].

2.1.5 Treatment Options for IA

IAs are currently managed via operative occlusion of the IA fundus, or are followed up. To date, pharmacological preventive methods have not yet been taken into wide clinical use. However, aspirin, a widely known standard treatment for prevention of atherothrombotic incidents in patients with atherosclerotic diseases, seems to be potentially protective also in IAs.

2.1.5.1 Operative procedures

To prevent the rupture of an intact IA or after rupture to prevent further bleeding, the main goal of operative treatment is the IA's permanent occlusion. Methods for isolating an IA from the circulation are clip ligation of the IA neck by open neurosurgery (clipping), endovascular occlusion of the IA sack by filling it with coils (coiling), or placement of a flow-reducing stent (a flow diverter) over the IA neck [149] (Figure 6). After any such treatment, the IA becomes thrombosed, with the neck-area endothelialized.

However, both open and endovascular techniques are associated with significant risks [168]. Surgical clipping of unruptured IAs has been estimated to associate with 5 to 7% morbidity and 1 to 2% mortality [127]. The International Subarachnoid Aneurysm Trial (ISAT) suggests that coiling is associated with lower risk of disability or death by one year, whereas clipping appeared a more permanent treatment in the long term [168,169]. Since not all IAs rupture during a patient's lifetime, what is still under discussion is whether and whose incidental IAs require a surgical or endovascular approach, and by which treatment method [25,149].

2.1.5.2 Potential pharmacotherapy

Aspirin, an inhibitor of platelet function and inflammatory response through acetylation of cyclo-oxygenase (COX) [33], has been protective against IA rupture. For a conservatively managed subgroup from the ISUIA cohort of 1,691 patients [97], frequent aspirin users showed a lower IA rupture risk than did non-users (OR 0.4, 0.18-0.87) [85]. Similarly, a UK-based case-control study of 2,334 IA patients (74% with ruptured IAs) revealed a lower SAH risk (OR 0.22, 0.17-0.28) [92]. In one mouse model of an aneurysm, aspirin reduced aneurysm formation and rupture, whereas selective inhibition of COX-1 did not [228]. Thus, the potential beneficial

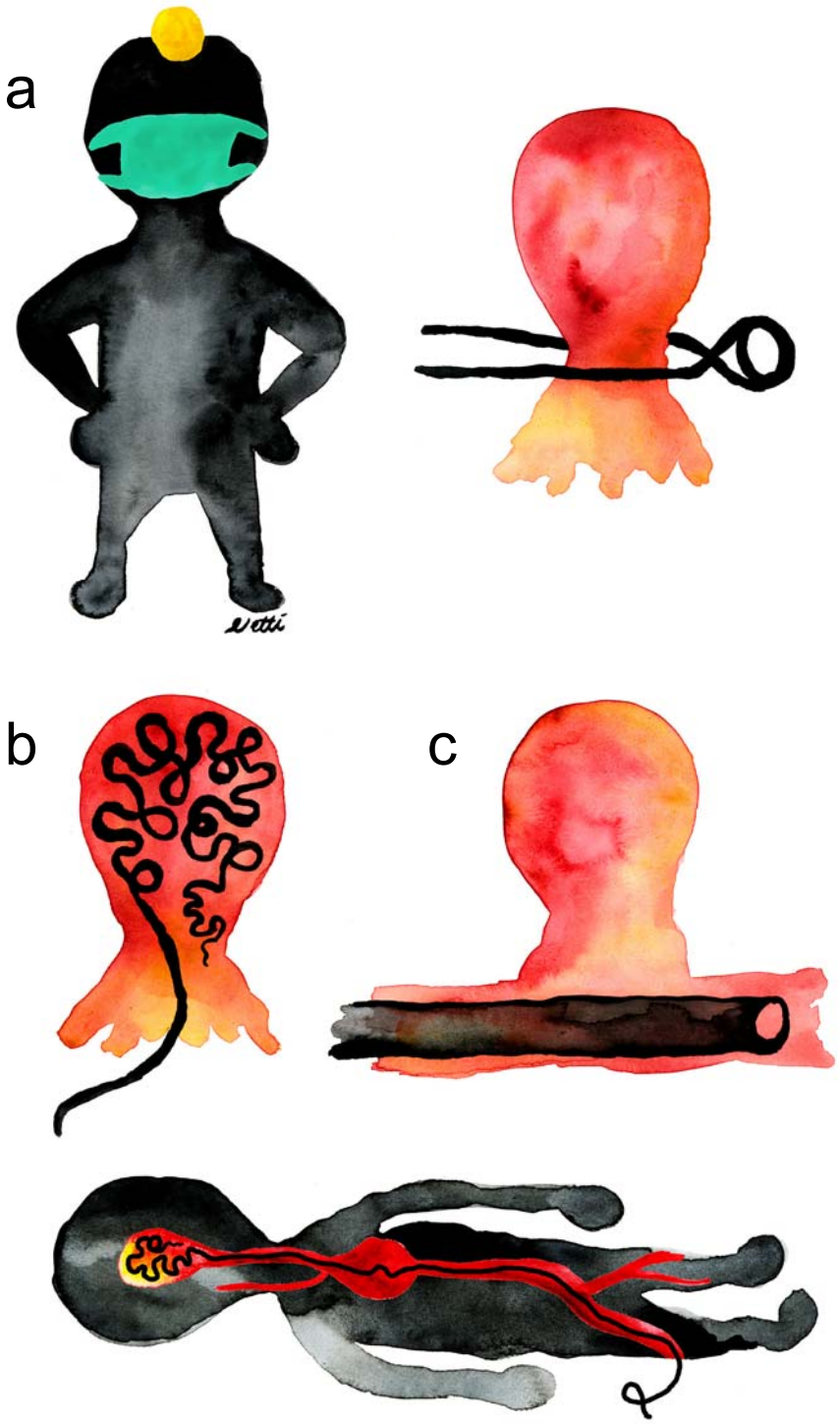

Figure 6. Surgical and endovascular treatment options for isolating an IA from the circulation include: a placing a clip to close the IA neck via craniotomy, b filling the IA sack with densely packing coils via femoral artery, or c placement of an intraluminal stent (a flow diverter) to divert blood flow to pass the IA sack.

effect of aspirin in the IA wall may be mediated through its COX-2 inhibition. Despite the effect of primary thrombosis inhibition by aspirin, its use did not associate with poor outcome in 274 SAH patients [79], suggesting that aspirin would not cause additional complications if the IA ruptures. Clinical trials to investigate whether aspirin therapy could reduce IA formation and rupture, especially in patients carrying small (3-7 mm) unruptured IAs, are currently underway.

Statins, hydroxymethylglutaryl-coenzyme A (HMG-CoA) reductase inhibitors, are in wide use to lower cholesterol levels. Their effect on the aneurysmal artery wall in ex vivo cultured, unruptured human AAAs show that statin treatment is beneficial by inhibiting proinflammatory effects of the nuclear factor-kappa B (NF-κB) signaling pathway, matrix metalloproteinases (MMPs) 2 and 9, and monocyte chemotactic protein-1 (MCP-1) [260]. The anti-inflammatory effect of statins was independent of their lipid-lowering effects in an elastase-induced rat AAA model, in which atorvastatin also increased collagen and elastin synthesis in the aneurysm wall [223]. Similarly, in experimental rat cerebral aneurysms, simvastatin [8] and pitavastatin [11] suppressed inflammation and inhibited medial thinning and enlargement of the aneurysm wall. In an epidemiological study statin was associated with lower IA rupture risk (OR 0.40, 0.33-0.50) [92].

It therefore appears that the anti-inflammatory functions of statins could prove useful in treatment of IAs. However, a large retrospective cohort of 28,931 carriers of unruptured IAs showed no difference in their risk for SAH in a mean follow-up time of 30 months, when comparing risk in current or recent statin users (41.3%) to the risk in those without treatment [19]. Whether statins have any beneficial effect on human IA in vivo, and whether their potential effect would be mediated via their anti-inflammatory or cholesterol-lowering functions, thus remains unknown.

2.1.6 Prediction of IA rupture

No comprehensive methods for IA rupture prediction exist. PHASES scoring is one tool to evaluate an individual's SAH risk based on selected risk factors for IA rupture: Population, i.e. ethnic background, Hypertension, Age, Size, Earlier SAH, and Site [77].

The total score corresponds to annual IA-rupture risk (range 0.4-17.8 [77]). Notably, the PHASES score does not include the effect of smoking; moreover, hypertension in the score refers only to hypertension history, not taking into account any blood-pressure interventions after IA detection. Currently, risk for IA rupture is estimated individually for each IA patient, based on the risk characteristics of both the IA and the patient.

2.1.7 Challenges in IA Management

Rupture of an IA is unpredictable and often fatal, and the operative methods for preventing of the IA rupture are invasive and risky. Many IAs would remain silent for a lifetime [122], even if left alone. The largest multicenter study of unruptured IAs, the ISUIA, suggests that risk from surgery is greater than rupture risk for small, less than 10 mm, IAs during 7.5 years of follow-up [97]. However, that time-frame is relatively short when applied to the average working-aged population of IA carriers, whose life expectancy is many-fold longer. Importantly, reliable estimates of IA rupture risk among differing populations are few [121].

Evaluation of each patient's risk for IA rupture is based on individual risk factors. Risk-factor scores are based on generally known risk factors for IA rupture but do not necessarily reveal the IA rupture risk for an individual patient. Routine imaging methods provide data on the IA at macroscopic level, such as its size and shape, as well as its tendency for growth if followed up. However, even those IAs showing no risk features in macroscopic evaluation may rupture, if the IA wall is weak.

More detailed data on fragility of the IA wall requires more specific imaging methods. Despite not yet being in routine clinical use, methods such as contrast-enhanced MRI and dynamic flow simulations are promising options for prediction of IA rupture risk. However, to interpret data provided by molecular- and flow-model -based imaging methods, more knowledge is needed of the mechanisms in the IA wall prior to wall rupture. Development of more specific imaging methods requires complete understanding of the pathogenesis of IA formation and rupture, essential also in the development of pharmacological options for preventing rupture.

2.2 Saccular intracranial aneurysm pathogenesis

2.2.1 Normal artery wall structure

The normal arterial wall structure is divided into three histological layers: tunica intima, media, and adventitia. The innermost of the layers, the intima, represents the inner surface of the vessel wall from the basal lamina connecting the luminal endothelium to the hypocellular space between the endothelium and the media.

The intima contains negatively charged glycosaminoglycans secreted by the mural cells of the media. The middle layer, the media, consists mainly of smooth muscle cells (SMCs) responsible for the tensile strength of the artery wall and its capacity to adapt to blood-pressure changes, regulating vessel diameter through the cardiac-pulse cycle [154]. The outermost layer, the adventitia, is mainly of loose connective tissue collagen (type I and III) and elastin fibers and fibroblasts, which produce the components of the extracellular matrix (ECM) together with the mural SMCs. In arteries larger than the smallest capillaries, the adventitia contains vasa vasori, i.e. small vessels that supply oxygen to the cells of the media and the adventitia.

To support the media, elastic fibers are packed into two dense surrounding layers in peripheral artery walls (internal and external elastic lamina, IEL and EEL) [154,204,240]. In intracranial arteries, the EEL is only weakly developed compared to the IEL. The IEL regulates the diffusion of substances between the intima and media through its fenestrations, the size and density of which tend to increase with age. Degenerative changes in the IEL may also play a role in atherosclerotic diseases [194,219]. In intracranial artery bifurcation regions, the medial layer also has a narrow gap (medial raphe), which lacks smooth muscle cells (SMCs) and is filled instead with strong collagen fibers [65]. This anatomical defect may, however, not contribute to IA formation [229]. Figure 7 shows a schematic illustration of the layered structure of healthy intra- and extracranial artery walls.

2.2.2 Remodeling of and degeneration of the IA wall

An IA wall differs from a healthy intracranial artery wall, since it lacks the original defined arterial wall layers and the supporting IEL. Nevertheless, the remodeled structure of the IA wall does include intimal, medial, and adventitial portions, resembling the original layer-like structure. Altered hemodynamic forces and the subsequent increased shear stress in the lumen of an IA sack are likely contributors and triggers of such remodeling changes within the IA wall [70,71,116,230,231] (Figure 8).

2.2.2.1 Structural changes towards a rupture-prone IA wall

Along with the microscopic process of IA wall remodeling, macroscopic dilatation of the IA wall occurs. IA walls are classified according to histological morphology and signs of structural remodeling (Figure 9) [70,116].

Loss of functional endothelium, also known as endothelial erosion, is one of the main events triggering further aneurysm wall degeneration and inflammation in an experimental rat model [104], and possibly also in human IAs [70,71,242]. The site of endothelial erosion is instantly covered by a thrombocyte monolayer, fibrin, and erythrocytes. The thrombosis may develop further and become a thick layer of thrombus, which may organize and become an integral part of the IA wall by means of SCM or myofibroblast migration into the thrombus. An organized thrombus is a common finding in an IA [70,71].

The medial layer may rearrange itself through SMC proliferation, similarly to myointimal hyperplasia, and by SMC death through apoptosis or necrosis [70,116,133,217,230,245]. SMCs play a dynamic role in adaptation to hemodynamic and other stresses of the vascular wall [205], and their loss is deleterious for an IA [68]. In an experimental rat model of peripheral artery aneurysm, loss of SMCs led to aneurysm growth and rupture [153]. Importantly, SMC loss in patients has associated strongly with IA rupture [68,70,116,245]. Active remodeling of the ECM is also a central process occurring in the IA wall [32], with proteolytic activity by MMPs and serine proteases likely contributing to degradation of ECM components such as collagen, gelatin, and glycoproteins [32]. Disintegration of the ECM not only causes weakening of the tensile strength of the arterial wall but also induces apoptotic death of mural cells, whose

Intracranial artery wall

Adventitia

Media

IEL

Intima

Endothelium

Laminar (normal) blood flow in the artery lumen ⟶

Peripheral artery wall

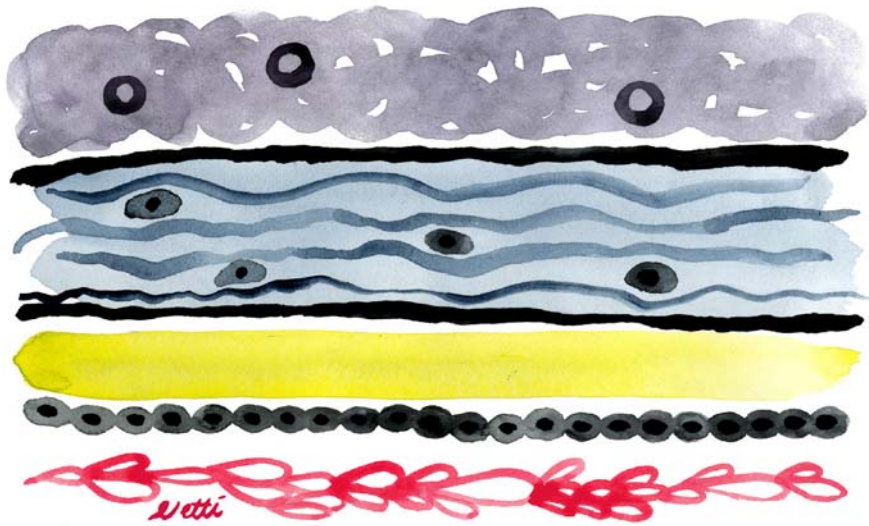

Adventitia

EEL

Media

IEL

Intima

Endothelium

Laminar (normal) blood flow in the artery lumen ⟶

Figure 7. Cross-sectional structure of a healthy intracranial artery wall vs. a peripheral (extracranial) artery wall. Normal intracranial artery wall differs from extracranial artery wall by its poorly developed external elastic lamina (EEL).

Intracranial aneurysm wall

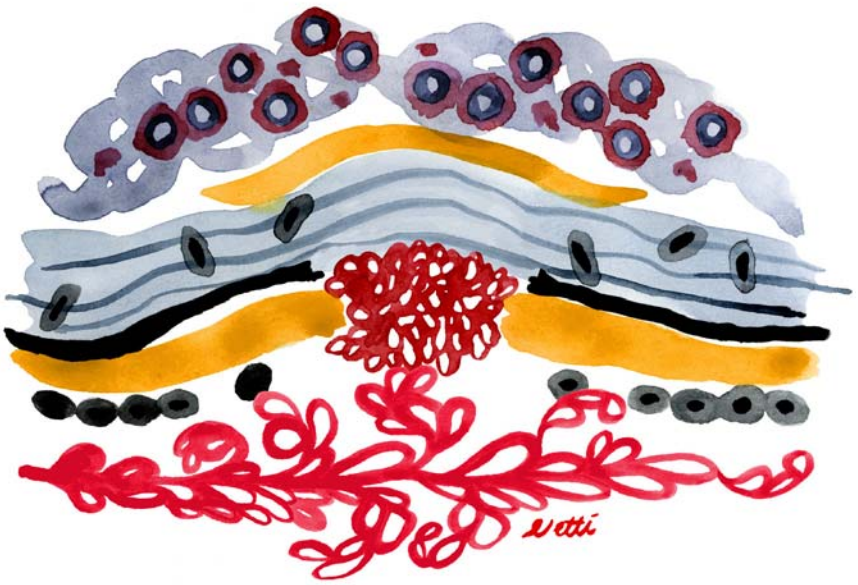

Adventitial layer

Medial layer

Intimal layer

Endothelium damaged, replaced by thrombosis

High wall shear stress

Turbulence

Diffuse flow

Abnormal blood flow in the artery lumen ⟶

Figure 8. Cross-sectional structure of an intracranial artery aneurysm (IA) wall which has undergone the process of wall remodeling and started pouching outwards. IA-wall structure is diffusely organized, lacking a clear layer-like division. The IEL has disappeared. Intraluminal thrombus covers the sites of endothelial damage or loss and slowly becomes an integral part of the IA wall structure. Abnormal neovascularization may occur. Oxidized lipid accumulation (dark yellow strands) is evident. Differing hemodynamic conditions in the artery lumen are hypothetized to associate with IA pathogenesis.

survival is physiologically dependent on connections to surrounding tissues [232].

The IA wall shows expression of various growth factors and their receptors [69,132], of which transforming growth factor (TGF) β-R2 and vascular endothelial growth factor (VEGF)-R1 associate with IA wall remodeling and rupture [69]. A gene expression profile of 11 ruptured IAs compared to that of 8 unruptured IAs has revealed a significant upregulation of signaling pathways responsing to processes such as turbulent blood flow, vascular remodeling, extracellular matrix degradation, oxidative stress, chemotaxis, and leukocyte migration, [132]. Upregulation of hypoxia-inducible factor-1A (HIF-1A) was detectable in ruptured IAs, suggesting occurrence of hypoxic conditions in the IA wall [132].

To prevent tissue hypoxia and necrosis in a variety of physiological conditions, including tissue repair and reproduction, wound healing, and inflammation, endothelial cells undergo neovascularization [170]. Typically, neovascularization is initiated via branching of adventitial vasa vasori. Recently, neovascularization has been demonstrated in the IA wall in association with inflammatory cell infiltration [90]. Chronic inflammation is present in IA lesions both pre- and post rupture, as reviewed by Tulamo et al. [242]). IAs show also marked lipid accumulation [72,125,244].

2.2.3 Inflammation in the IA wall

Inflammation is a defensive response of an organism to resist injurious stimuli [216]. The destructive effect of inflammation is thus targeted at the offending stimulus, such as infection, irritation, or injury. However, the defensive response also affects the tissue itself, causing the classical symptoms of an inflammatory reaction: “calor, dolor, rubor, tumor, et functio laesa,” heat, pain, redness, swelling, and loss of normal function [216]. Because of its essential task, inflammation occurs in a variety of human diseases: cancer, infections, and autoimmune and cardiovascular diseases.

Importantly, chronic inflammation plays a role in IA pathogenesis, where it associates with IA wall remodeling and rupture [47,70-72,116,133,243-245]. The IA wall is subjected to multiple stresses which likely trigger and regulate the

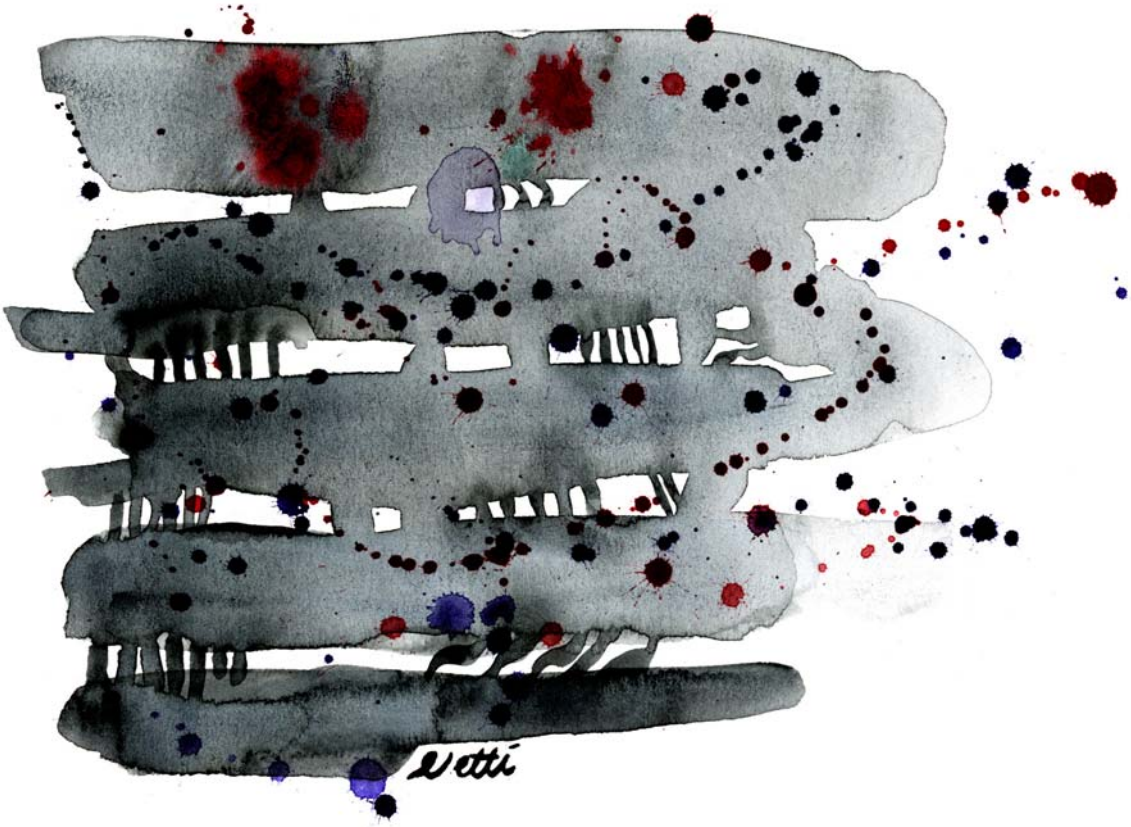

Figure 9. Classification of the wall structure (illustration is abstract). Kataoka et al. classified degree of IA wall remodeling in three categories: 1, disruption of endothelium, 2, remodeling of wall structure, and 3, magnitude of inflammatory cell infiltration. They scored the status of the IA endothelium from normal to completely disrupted (0-5), the IA wall structure from dense collagen and rich SMC-containing wall to hyaline-like structure (1-5), and the number of inflammatory cells from very few to many (0-3) [116]. In their comparison of 27 unruptured with 44 ruptured IAs, the latter showed significantly higher degree of pathological changes in all three categories, suggesting a more fragile wall structure in ruptured IA walls. Frösen et al. reported also an association between IA wall rupture and IA wall remodeling in 24 unruptured and 42 ruptured cases [70] and introduced an IA wall type classification as A, B, C, or D, taking the whole IA wall into account: type A resembled normal arterial wall containing intact endothelium and linearly organized SMCs, type B, a thickened wall with myointimal hyperplasia and disorganized SMC pattern, type C a degenerated and hypocellular wall with either additional myointimal hyperplasia or organizing luminal thrombosis, and type D an extremely thin wall with luminal thrombus [70]. Although the degeneration score (from A to D) correlated positively with IA wall rupture [70], it remains unclear whether in nature IA degeneration proceeds in this order, or whether different wall types represent different pathways of IA pathogenesis.

inflammatory response in the IA wall. Firm causal relations between IA-wall inflammation and potential proinflammatory stimuli such as hemodynamic stress, exposure to toxic compounds, accumulation of infectious particles, or atherogenic excess material in the wall are, however, not well known. Inflammatory cells present in the IA wall and potential proinflammatory roles of different stimuli are reviewed in the following sections.

In general, the immune response is divided into a less-specific innate immunity and a highly specific adaptive immunity. The innate immune response is mainly mediated by neutrophils, macrophages, and dendritic cells, which detect foreign material in their environment with pattern recognition receptors [101]. Adaptive immunity is mediated by a range of T and B lymphocyte subtypes, which are activated specifically by the stimulus presented by innate immune cells in their human leukocyte antigen (HLA) receptors. Figure 10 summarizes the basic features of inflammatory cells operating in arterial walls.

2.2.3.1 Inflammatory cells in the IA wall

Regardless of rupture status, inflammatory cells are present in the IA wall [51,71,242]. Polymorphonuclear leukocytes have been detectable in the IA wall [51,71,242], indicating the presence of neutrophils, an important population of innate immunity. Their extent in IAs is, however, unknown.

The IA wall also shows infiltration of small rounded cells, reflecting the presence of lymphocytes: both T ($CD3^+$ and $CD45RO^+$) and B ($CD20^+$) lymphocytes [47,70,71,245], suggesting the role of adaptive immunity in IA-wall pathobiology. Immunohistochemistry findings of immunoglobulins G and M in the IA wall [47,244] suggest involvement of B-cell activation in IA-wall pathogenesis. Natural killer T (NKT) cells have also been detectable in IAs [125]. Accumulation of T lymphocytes is most extensive in degenerated and ruptured IAs [70,245]. The potential role of these wide range T lymphocyte subsets for human IA formation and rupture has, however, remained unknown. One hemodynamically induced aneurysm model in rats showed no progressive response to the presence of or inhibition of $CD3^+$ T lymphocytes, suggesting that

their function was nonessential in that aneurysm model [167].

Several series of unruptured and ruptured IAs have demonstrated that the extensive presence of macrophages associates with IA-wall rupture [70,71,116]. The $CD163^+$ subtype appears the major leukocyte type in the IA wall, suggesting its significant role in the IA-wall pathogenesis [70]. $CD68^+$ macrophages are numerous as well in the IA wall, and thus are likely to play a role [47,71,116,245]. Notably, since macrophages appear in ruptured IA walls resected shortly after rupture, as well as in unruptured IAs, they seem to accumulate in IA walls even before rupture [70]. Their role in the IA wall has remained unestablished, however.

Mast cells (MCs) are proinflammatory and atherogenic cells in atherosclerotic artery walls [129] and in AAAs [160]. They also have been detectable in intracranial arteries close to ruptured IAs [59], and more recently also in IA walls [83]. In an experimental rat model, MCs contributed to formation and wall degeneration of an induced cerebral aneurysm [99].

2.2.3.2 Mediators of inflammation

Pro-inflammatory signaling in hemodynamic changes

NF-κB, a transcriptional factor expressed in human IAs [132], is located especially in the intima [13]. In cultured endothelial cells, wall-shear stress causes NF-κB activation through degradation of an associated IκB-component and translocation of normally cytoplasmic NF-κB into the nucleus [21]. NF-κB cause increased macrophage infiltration into the wall of an induced aneurysm rat model, potentially through induction of vascular cell adhesion molecule-1 (VCAM-1) –mediated leukocyte extravasation, and through MCP-1 expression [13], which attracts circulating monocytes to infiltrate into the tissue [115,182].

E26 Transformation-specific Sequence (Ets-1) is another transcriptional factor expressed in endothelial cells and arterial SMCs that can regulate arterial inflammation through MCP-1 [182]. Ets-1-mediated MCP-1 expression in SMCs also contributed to IA formation in an experimental rat model [9,10]. In ruptured human IAs, gene transcription factor analysis has revealed upregulation of both NF-κB- and Ets-signaling pathways [132].

According to one hypothesis regarding its mechanism, high fluid

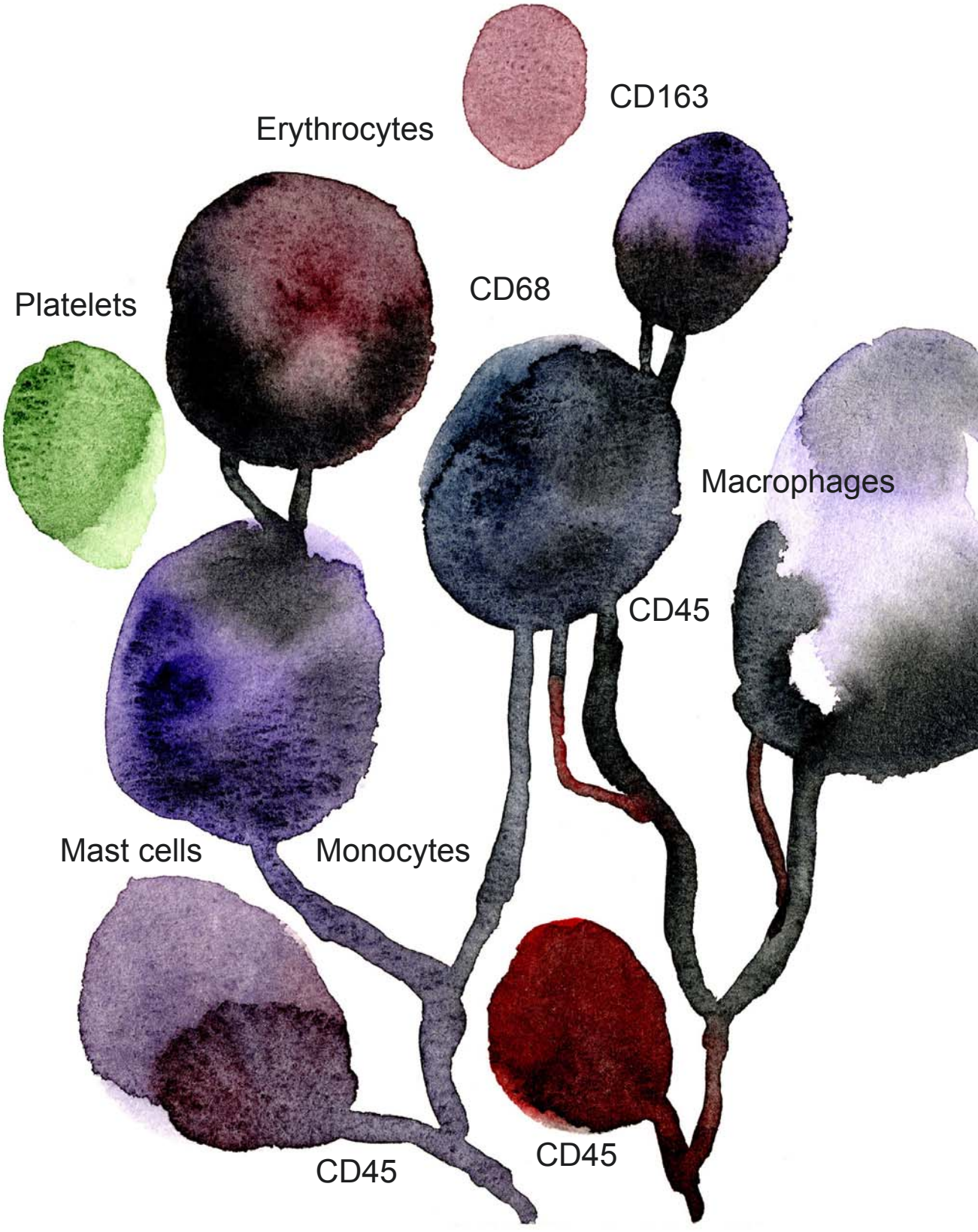
CD163
Erythrocytes
Platelets
CD68
Macrophages
CD45
Mast cells
Monocytes
CD45
CD45

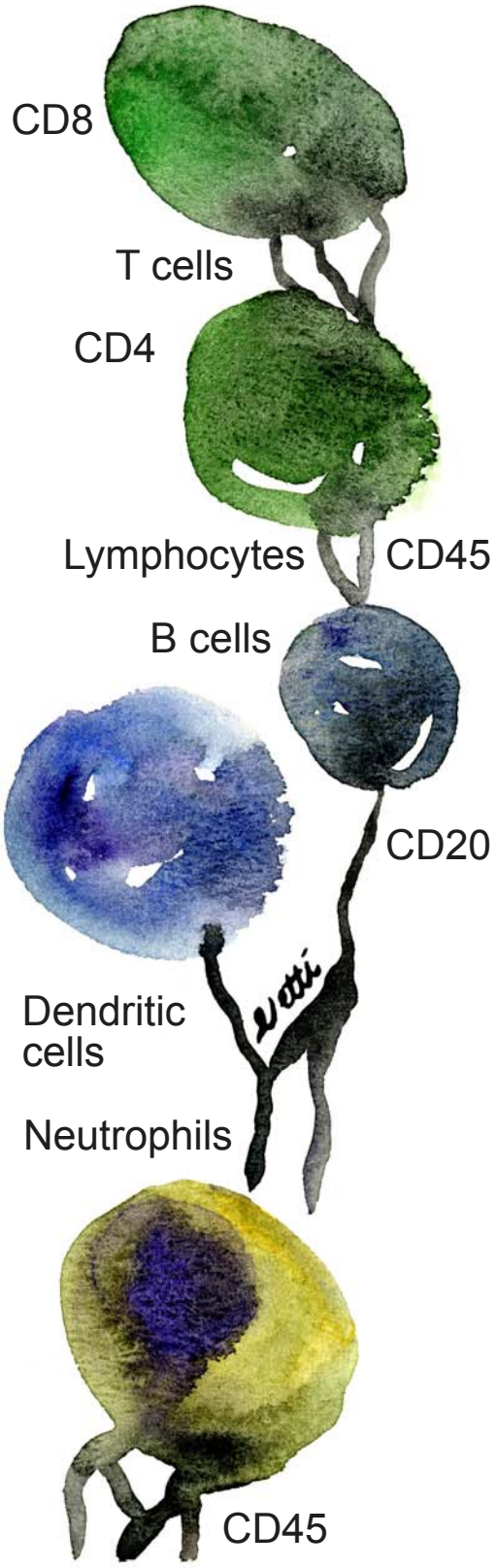

Figure 10. Overview of inflammatory cells in the arterial wall. Neutrophils are polymorphonuclear granulocytes classically arriving first at the location of acute infection or inflammation to fight pathogens through releasing antimicrobial granule proteins and catalyzing the formation of reactive oxygen species (ROS) [158,226]. Their activation is involved also in chronic inflammation [226]. Macrophages are monocyte-derived phagocytes of myeloid lineage [101,253], whose phenotype varies according to the environmental stimuli of the target tissue [41]. In the arterial wall, the pan-macrophage scavenger-receptor CD68 responds to oxidized low-density lipoprotein (ox-LDL) particles and apoptotic cells [44,247], whereas CD163 expression responds to erythrocyte-derived hemoglobin [66,130]. Various B and T lymphocyte subsets occur in the arterial wall, where they can have either an atherogenic or atheroprotective role, depending mainly on their immunoglobulin (B) or cytokine (T) profiles of secretion [42,143]. Dendritic cells link innate and adaptive immunity by presenting antigens via their major histocompability receptors (MHC) I and II (i.e., HLA receptors) to activate T lymphocytes. MHC-II (i.e. HLA-DR) –activated helper ($CD4^+$) T cells predominate over the MHC-I-activated cytotoxic ($CD8^+$) T cells in atherosclerotic lesions [143]. Th1 cells in lesions can activate natural killer T (NKT) cells and macrophages through their cytokines; Th2 cells can activate B cells to secrete specific antibodies against foreign material such as ox-LDL [42,143]. Mast cells (MCs) regulate various immune reactions through degranulation and by releasing histamine, heparin, neutral proteases, cytokines, and growth factors [23,129,131,152,202]. Rapid activation of MCs is involved in acute allergic, immunoglobulin-E-mediated reactions, whereas their long-term activation and slow secretion of proinflammatory mediators is associated with chronic inflammatory vascular diseases such as atherosclerosis [23,129,202] and abdominal aortic aneurysms [161,234]. All inflammatory cells express the leukocyte-common antigen CD45 [88].

shear stress could amplify the NF-κB- and ETS-signaling pathways, and also the prostaglandin E2 receptor (EP2)-COX-2-pathway described in cultured human endothelial cells [14]. The human IA wall also expresses COX-2, the expression of which is increased in ruptured walls [228]. In the rodent aneurysm model of Aoki et al., inhibition of EP2 or of COX2 suppressed NF-κB-mediated chronic inflammation. The authors therefore suggested the maintenance of chronic inflammation in the IA wall through these hemodynamic stress-induced inflammatory pathways [12,14].

Triggers of cell apoptosis

Apoptosis is programmed cell death, characterized by morphological changes in the dying cell and activation of caspases, cysteine protease enzymes, through their cleavage [232]. The trigger for apoptosis can originate either from inside the cell via a mitochondrial (intrinsic) signaling pathway, or outside the cell via the first apoptosis-signal (Fas) receptor-mediated (extrinsic) pathway. Expression of both Fas and its activating cytokine, TNF-α, have been increased in a series of 10 ruptured human IA walls compared to control cerebral artery walls [105]. This suggested a role for the extrinsic TNF-α-Fas-pathway in the induction of IA wall inflammation and apoptosis [105]. Another study reported, however, the complete absence of cleaved caspase-8, the extrinsically activated type of caspase, in protein lysates of 15 unruptured and 17 ruptured IAs [133]; instead, they found caspase-9 in 5 ruptured IA walls, indicating an intrisically activated apoptosis pathway. They suggest that caspase-9 activation originates from disturbed cellular homeostasis resulting from oxidative stress and the cytotoxic extracellular environment of the arterial wall [133].

Factors mediating oxidative stress

MPO is a neutrophil- and macrophage-derived enzyme that catalyzes oxidation of lipids, proteins, and lipoproteins [53,114,136]. Oxidation or any other type of modification of lipids predisposes their accumulation into tissues and their phagocytosis [43]. Due to its strong oxidative capacity, MPO is atherogenic in the arterial wall. MPO also occurs in the IA wall, and is associated with greater risk of rupture [76]. In an experimental mouse model of a cerebral

aneurysm, MPO contributed to aneurysm formation and rupture [46].

Heme oxygenase-1 (HO-1) is an anti-oxidating enzyme that degrades erythrocytes' oxidative hemoglobin to less-toxic metabolites [220]. Polymorphism of the HO-1 gene may play a role in IA formation [171]. A genotype-analysis of 39 IA patients and 230 age-matched controls revealed long dinucleotide repeats in HO-1 gene-promoter regions more likely in the IA patients than in controls, suggesting downregulation of the protective HO-1 in IAs [171]. Laaksamo et al. demonstrated by immunostaining the presence of HO-1 in the IA wall, showing that HO-1 expression is associated with wall degeneration and rupture [133].

Complement system activation

Complement activation is a hierarchical protein cascade which regulates inflammation [58]. It is associated with the pathogenesis of atherosclerosis [183,184], and with IA-wall degeneration and rupture [243-245]. The membrane attack complex of the complement occurs widely in decellularized and degenerated areas of the IA wall and in lipid-accumulation areas, suggesting the role of this complement system with chronic IA-wall inflammatory processes. The complement system in the IA wall becomes activated via a classical pathway with alternative pathway amplification. The classical pathway activation can be induced by C-reactive protein (CRP), immunoglobulins (Ig), and oxidized lipid, all detected also in IAs [244].

Infectious material in the IA wall

Chronic periodontitis is associated with cardiovascular diseases [2,52] and with AAAs [57], in which dental bacteria initiate the proteolytic and proinflammatory activity of neutrophils. Recently, studies have focused on potentially infectious material in the IA wall, with Pyysalo et al. finding evidence of dental bacterial DNA in 21 of 36 (58%) ruptured perioperatively-obtained IA specimens [197]. However, evaluation of unruptured IAs has revealed no significant difference in the distribution of bacterial DNA (unruptured: 20/28, 71%; ruptured: 29/42, 69%) [198]. The role of bacterial DNA in the IA pathobiology remains open.

2.2.4 Atherogenesis of the IA wall

In degenerated IA walls, a very common finding is lipid accumulation [72,125,244], occurring independently of plasma lipid levels [72]. It seems likely that endothelial erosion facilitates the entry of lipid particles into the IA wall [71,72]. Circulating lipid-transporter-particle apolipoprotein-B (apoB-100 [7]) occurs in the IA wall [72], reflecting transportation of lipids to the IA wall. Hydroxynonenal (HNE) and adipophilin in the IA wall [72,244] indicate the presence of oxidized lipids [188] and intracellular lipid accumulation there [87], suggesting lipid phagocytosis occurring in the IA wall. Kosierkiewicz et al. reported in atherosclerotic IAs also major histocompability complex type II (MHC-II, i.e. human leukocyte antigen-DR, HLA-DR) expression in macrophages and SMCs [125], reflecting their antigen-presenting function, potentially subsequent to lipid phagocytosis. These findings of lipid accumulation in IA walls suggest atherogenic mechanisms similar to those in atherosclerotic arterial wall pathologies.

2.3 Atherosclerosis of the arterial wall

Atherosclerosis is a chronic inflammatory disease of the arterial wall in which accumulation of lipids causes thickening, calcification, and degeneration of that wall [151]. The nature of this disease is systemic, but the most clinically relevant anatomical locations for atherosclerosis are coronary arteries, arteries of the lower limbs, and internal carotid artery bifurcations. Atherosclerosis commonly also affects intracranial arteries [89,265].

Classically, an atherosclerotic lesion causes stenosis in the arterial lumen, resulting in abnormal hemodynamic conditions at the lesion. Disturbed perfusion of the target organ may eventually cause symptoms including ischemic pain or dysfunction of the organ due to tissue hypoxia. Atherosclerotic disease may slowly advance until the affected arterial lumen becomes totally occluded. In such slowly progressing cases, a network of collateral vessels develops to supply blood to the target tissue suffering from chronic ischemia. Sudden intraluminal rupture of a fragile atherosclerotic

lesion of a coronary artery then causes thromboembolic acute occlusion of artery and a highly fatal myocardial infarct (reviewed in [218]). A similar mechanism may occur in atherosclerotic lesions of the internal carotid or intracranial arteries, whose intraluminal thrombosis and occlusion results in ischemic attack on the brain, i.e. ischemic stroke.

The main risk factors of atherosclerosis, including hyperlipidemia, hyperglycemia, aging, hypertension, and smoking, are in part the same as for IAs. In extracranial arteries, formation of an atherosclerotic lesion is characterized by accumulation of lipids in the intima, the innermost layer of the wall [82,128,143]. Lipids retained within the lesion become modified and phagocytozed by macrophages, causing chronic inflammation and contributing to arterial wall fragility (Figure 11).

2.3.1 Lipid metabolism in the arterial wall

The human body receives lipids such as cholesterol, phospholipids, and triglycerides either via dietary intake or via hepatic synthesis. Cholesterol is a physiological compound of cell membranes [222]. Tissues receive their essential cholesterol via either an endogenous or exogenous pathway; they either synthesize cholesterol themselves or internalize liver-derived cholesterol through apolipoprotein transportation. Bidirectional apolipoprotein traffic is responsible for systemic lipid transport in arterial walls [31,128,237,238].

2.3.1.1 Mechanisms of lipid traffic

These cholesterol-, phospholipid-, and triglyceride lipids shuttle in the circulation packaged within phospholipid-monolayered lipoprotein particles which carry them into target tissues. Liver-originated apoB-100-containing lipoproteins are classified according to their protein content as very low-, intermediate-, and low-density lipoproteins (VLDL, IDL, and LDL). These particles are relatively small in size (20-30 nm) and are responsible for lipid traffic towards the wall. Lipoproteins such as chylomicrons (over 500 nm) are too large to directly enter the arterial wall and require further processing in the liver

Atherosclerotic artery wall

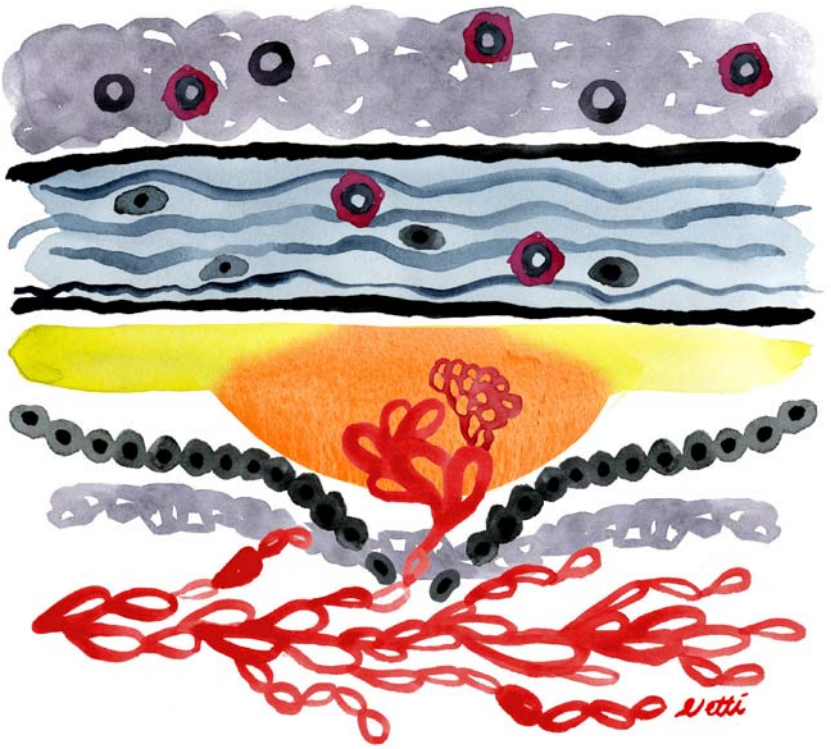

Figure 11. Schematic, simplified structure of an atherosclerotic plaque. In the extracranial artery wall, intimal lipid retention has led to intimal thickening and inbulging of the atherosclerotic lesion towards the arterial lumen, causing stenosis. Subsequent to endothelial erosion, a thrombosis has formed to cover the endothelial defect and the lesion is covered by a fibrocellular cap. Adventitial neovessels have spread towards the thickened part of the wall to provide arterial cells with oxygen. Some of the newly formed and fragile neovessels have leaked erythrocytes into the wall, causing microhemorrhages. Oxidative stress due to cytotoxic lipid retention, inflammatory response, and iron accumulation has caused cell death, and contributed to formation of the plaque's necrotic core. Among altered hemodynamic conditions, especially slow and diffuse flows with low wall-shear stress have been involved in this atherosclerotic process. [38,151,165,218].

before their lipid load can be mobilized [238]. The smallest of lipoproteins, apolipoprotein A-I (apoA-I)-containing high-density lipoprotein (HDL; 7-13 nm) particles are responsible for lipid clearance from the wall and for carrying lipids back to the liver through the circulation. Depending on the phase of lipid clearance, apoA-I may travel also in a solitary manner, without any associated lipids [129,144,178,238].

2.3.1.2 Development of atherosclerotic plaque

An adverse shift in the balance between lipid accumulation- and clearance mechanisms leads to lipid-laden foam-cell formation and progression of an atherosclerotic lesion, i.e. atherosclerotic plaque, in diseased arterial walls. Thus, the development of atherosclerotic plaque includes lipid accumulation in the intima, lipid phagocytosis, incomplete lipid clearance, and ultimate lipid retention in the arterial wall. The end result, a thickened arterial wall with a necrotic lipid core and chronic inflammation, is characteristic of atherosclerotic plaque [129,144].

Primary lipid accumulation in the arterial wall

Lipoprotein particles can enter the intact arterial wall via endothelial cell transcytosis or through endothelial cell junctions [7,129,144,227]. Endothelial erosion or loss causes dysfunction of its barrier function and leads to its increased permeability to lipid influx to the arterial vall via endothelial cell junctions [7,227]. Inbalance in lipid transportation causes excess lipid accumulation in the arterial wall, where apoB-100-associated lipoproteins have the affinity to bind to the negatively charged proteoglycans of the ECM [225].

Oxidation or other modification of accumulated apoB-100-containing lipid particles occurs in the ECM [141,192] and generates highly reactive fragments of oxidized fatty acids such as malonialdehyde, copper, or HNE, which can bind to apoB-100 [188,227]. Such lipid waste is cytotoxic and triggers inflammation.

Lipid phagocytosis in the arterial wall

Macrophages and SMCs in the arterial wall are activated to phagocytoze the retained, modified lipid particles [80]. To adapt to the circumstances of lipid load, SMCs may also express the pan-macrophage receptor CD68, as demonstrated in atherosclerotic aortas [6]. Antibodies can opsonize the lipid particles to facilitate phagocytosis [259]. Clearance of accumulated extracellular lipid debris by inflammatory cells within atherosclerotic plaques aims at stabilizing the arterial wall [80,129,143]. Subsequent intracellular lipid accumulation turns the lipid-ingesting phagocyte into a lipid-storing foam cell. After ingestion, apoB-100 is degraded in lysosomes [30]. The modified, cytotoxic lipid can, however, disturb normal lysosomal metabolism, leading to accumulation of apoB-100 and HNE in the cytoplasm of a phagocyte [106,150,237], where such a lipid load also disturbs other cellular functions [237]. Intracellular lipid droplets become covered by adipophilin [87], which has been demonstrated to prevent any lipid efflux from cultured macrophages and thus to enhance intracellular lipid accumulation in the foam cells of atherosclerotic plaques [135].

Lipid clearance in the arterial wall

To prevent any intracellular lipid overload in the tissues, the apoA-I- and HDL-mediated cellular lipid clearance mechanism transports lipids and cholesterol in reverse from the arterial wall back to the liver, where the excess cholesterol is excreted into the bile [129,144,178]. To perform lipid efflux from foam cells, the apoA-I lipoproteins operate via the adenosine-triphosphate-binding cassette A1 (ABCA1) or G1 cell-surface transporters, of which ABCA1 can deliver intracellular cholesterol to either lipid-rich or lipid-poor apoA-I particles [178]. In atherosclerotic arterial walls, ABCA1 is expressed on foam cells either of macrophage or of SMC origin [138].

Failure of intracellular lipid clearance leads to foam cell death and extracellular accumulation of lipids. Death of foam cells causes adipophilin-covered lipid material to be released in the extracellular space, where a necrotic lipid core of an atherosclerotic plaque forms [41,129,141,237]. Contrary to LDL and other atherogenic lipoprotein particles, HDL particles are not themselves retained in the arterial wall [7] unless attached to apolipoprotein E (apoE),

which can bind to ECM proteoglycans [181]. HDL may, however, become dysfunctional in an inflammatory environment, especially if MPO and oxidative stress occur [211]. Therefore, dysfunctional lipid clearance mechanisms may also facilitate atherogenesis.

2.3.2 Neovascularization and microhemorrhages in atherosclerosis

Neovascularization, a physiological mechanism to prevent tissue hypoxia [170], typically occurs in thickened atherosclerotic plaques. Oxygen can diffuse for approximately 250 to 500 micrometers in the vascular wall [206], and cells located at a greater distance from the lumen, if not supplemented by vasa vasori, demand neovascular oxygen sources. Infiltration of inflammatory cells into the atherosclerotic plaque cause increased oxygen use, thus triggering neovascularization. Neovascularization is initiated from vessel-sprouting under the regulation of HIF-1 and vascular endothelial growth factor (VEGF). MMPs, especially MMP1, promote endothelial cell detachment from mural SMCs. Chronically upregulated neovascularization may lead to formation of immature neovessels [170]. Plaque neovessels also contribute to lipid accumulation [139], serving as an optional route for excess lipids to enter the wall.

Immature neovessel walls are thin and lack a connection to the surrounding tissue, which predisposes them to leakiness [224]. Leaky neovessels are a major cause of intramural microhemorrhages [250]. In the arterial wall, the extravascular erythrocytes lyse and release their cholesterol-rich cell membranes, thus contributing to lipid load in the arterial wall [120,155,250]. Erythrocyte extravasation, marked by glycophorin A (GPA), an erythrocyte-specific membrane protein [18], is associated with atherosclerotic plaque vulnerability in coronary [120,139] and carotid [165] artery lesions.

Erythrocyte lysis also liberates the iron-containing oxidative heme into the arterial wall (Figure 12) [155,250]. Retention of iron has been considered a contributor to atherosclerotic pathologies, due to the high oxidative potential of free iron

ions ($Fe2^{+}$) [164,201,261]. To limit iron load in the tissue, synthesis of ferritin, an iron-storage protein, is upregulated by iron, oxidative stress, and inflammatory cytokines. Excessive nonbound iron is phagocytozed and stored in hemosiderin (FeIII, the Roman numeral referring to a bound form of iron) [164]. The free heme-derived iron is highly soluble and has a strong capacity to catalyze the formation of toxic reactive oxygen species (ROS) such as hydrogen peroxide (H_2O_2), hydroxyl radical ($OH.^{-}$), and superoxide ($O2.^{-}$). These free radicals may liberate more iron from hemoglobin and oxidize LDL, thus mediating deleterious, atherogenic effects in the arterial wall [155,164,165,201,261].

In addition to neovessel-derived erythrocyte leakage, thrombus-derived erythrocyte lysis has also been considered as a likely source of iron accumulation within the arterial wall [155,165]. Hemosiderin deposition, representing an intracellularly generated product of iron phagocytosis, has been detectable also in the IA wall [71,91].

2.4 Atherosclerosis in the IA wall – Summary

Atherosclerotic changes had already been detected in autopsied intracranial arteries of the Circle of Willis in 1961 [265]. Atherosclerosis is a common finding also in IAs. Atherosclerotic changes in the IA wall are notable, both in macroscopic observation in an intraoperative setting [189] and in microscopic evaluation after IA resection of the IA sack [70,72,125,244]. Indeed, various structural changes occur both in atherosclerotic plaques and in IA walls. Endothelial loss, i.e. erosion, and the subsequent thrombosis and remodeling of the media are characteristic for both pathologies. Chronic inflammation plays a significant role in regulation and maintenance of these remodeling changes. Similar to the atherosclerotic wall, IA also accumulates lipids, which oxidize. Oxidative stress, hemosiderin deposition, and neovascularization are involved in both pathologies. There are also differences, because the pathological process of atherosclerosis is mainly focused in the intima, whereas in the IA, the entire wall becomes

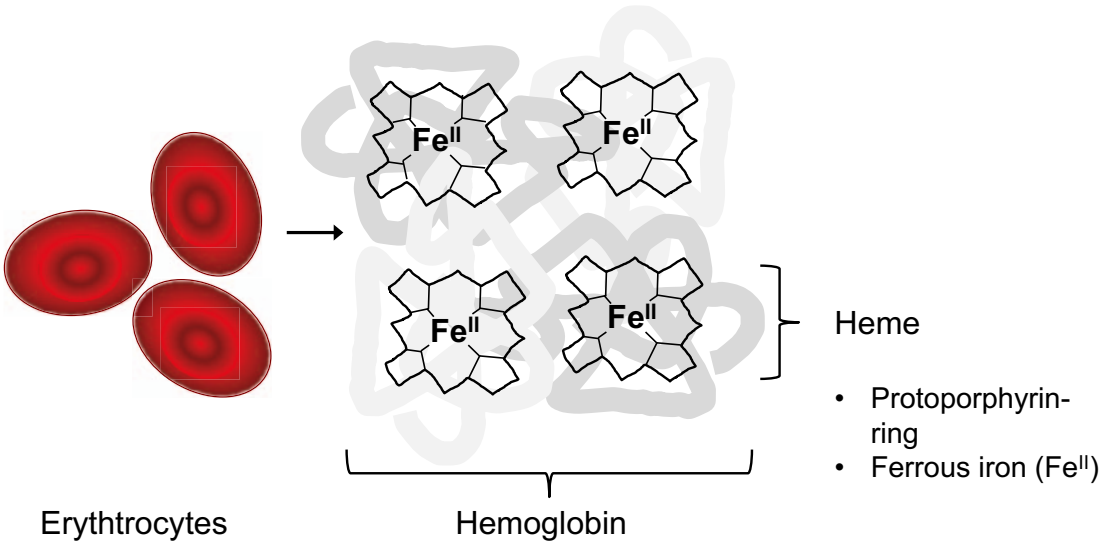

Figure 12. Composition of hemoglobin and a summary of human iron storage. In the human body, iron occurs either in the highly oxidative ferrous (Fe^{2+}) or less toxic ferric (Fe^{3+}) form. When bound to stabilizing proteins these are referred to as Fe^{II} or Fe^{III}. The protein-bound iron mediates various physiological functions such as oxygen transport in erythrocyte heme. In fact, a major part, approximately two-thirds, of iron in the body is complexed to hemoglobin in ferrous form. Erythrocytes contain hemoglobin, which consists of four peptide chains (two α- and two β-chains), each of which is complexed to the heme: a protoporphyrin ring bound to ferrous (bivalent) iron. Erythrocyte lysis thus releases free hemoglobin in the artery wall. In the ECM, the cytotoxic hemoglobin is bound to haptoglobin and is phagocytozed by $CD163^+$ macrophages. As HO-1 degrades the protoporphyrin ring, the released free iron is rapidly stored in ferritin or hemosiderin in the ferric form (trivalent ion, Fe^{III}). Finally, the remaining one-third of iron in the body occurs in the ferric form, mainly intracellularly stored. Small amounts of iron (Fe^{II} or Fe^{III}) may also be bound to circulating transferrin or loosely bound to various organic molecules in tissues [164].

weaker than a normal artery wall. The outcomes of the diseases differ accordingly: while the atherosclerotic lesion ruptures only partly from its luminal surface, causing acute occlusion of the affected artery by thrombosis or thromboembolism, the IA ruptures through its entire wall, causing often-fatal SAH. The role of atherosclerotic and other changes in the IA wall warrants our deeper understanding, allowing us to learn how to better prevent IA formation and rupture.

3. Aims of the Study

The purpose of this thesis was to deepen knowledge of human saccular intracranial aneurysm (IA) pathogenesis, especially from the perspective of atherosclerotic and inflammatory IA wall changes.

Specifically,

1) Is there a role for mast cells and neovascularization in IA wall degenerative remodeling, as there is in atherosclerosis (I)?

2) Does lipid accumulation contribute to IA wall remodeling and rupture, and what are the potential mechanisms of IA wall lipid accumulation and lipid clearance (II)?

3) Does intraluminal hemodynamic stress play a role in IA wall pathogenesis (III)?

4) What is the role for erythrocyte breakdown products in IA pathogenesis, and are they visualizable in small IAs with non-contrast ex vivo MRI (IV)?

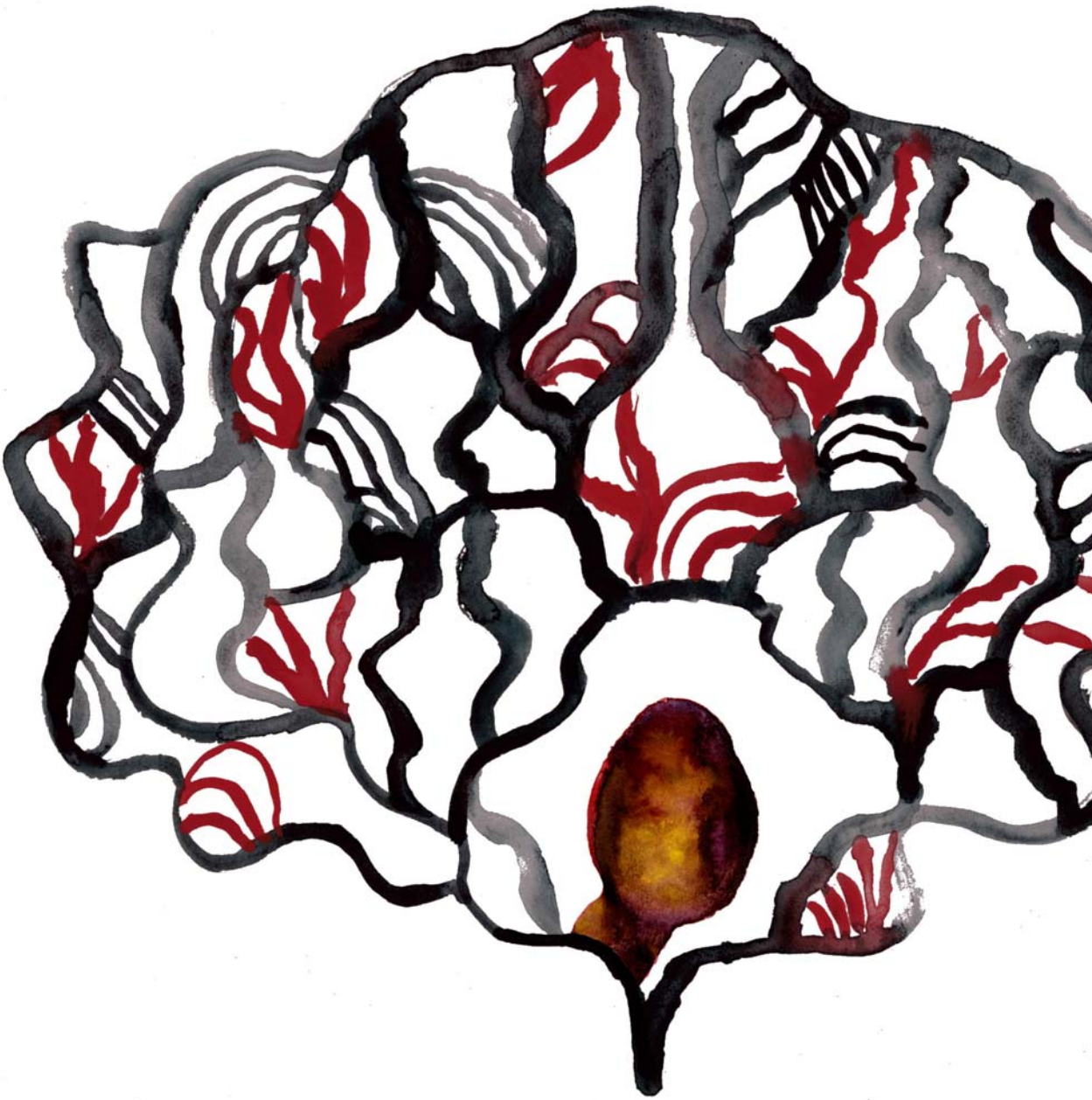

4. Materials and Methods

4.1 Aneurysm samples

This study covers in total 55 (25 unruptured and 30 ruptured) intraoperatively collected human saccular intracranial aneurysm (IA) samples. All IA specimens were studied by histological and immunohistochemical methods, and some of them were also scanned with ex vivo MRI to compare the radiological and histological findings of the IAs. The Hospital Ethics Committee approved the reasearch protocol.

4.1.1 IA sample collection and processing

Collection of IA fundi took place intraoperatively after clipping of the 55 IA neck at the Department of Neurosurgery, Helsinki University Central Hospital, Finland. After resection, 44 (Figure 13) of the IA fundi were immediately snap-frozen for further processing, and 11 (Figure 14) were fixed in formalin for magnetic resonance imaging (MRI) ex vivo.

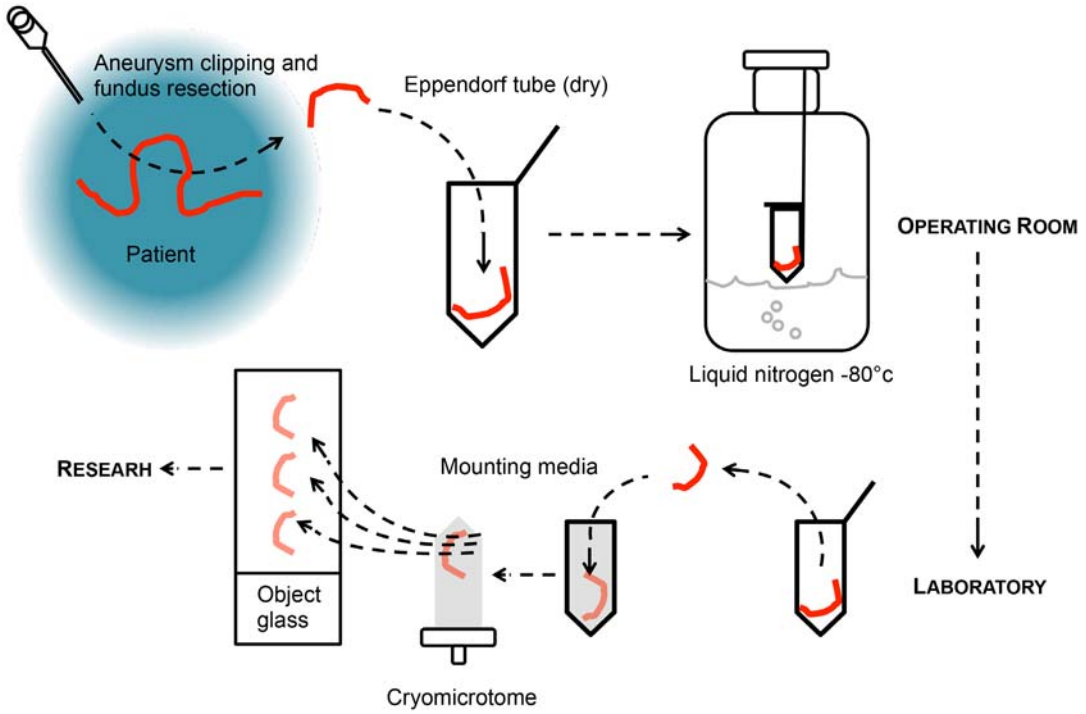

Figure 13. Aneurysm-sample processing after collection. In the routine protocol for 44 IAs, resected IA fundi were immediately snap-frozen in liquid nitrogen, and afterwards embedded in Tissue Tek (Sakura, Alphen aan den Rijn, The Netherlands) and stored at -80 C°. For histologic evaluation, the IA-sample blocks were serially cryosectioned at 4 µm.

4.1.2 Patients and IA studies

All 55 IA samples originated from different patients whose clinical data came from their medical records (Table 2). IA-dimension measurements were from preoperative computed tomography angiography (CTA) images. Table 3 specifies the use of IAs in the studies of the thesis. Samples 1 to 36 were the most extensively analyzed, being involved in Studies I, II, and IV. Of the 36 IA patients, 11 participated also in Study III, with the supplement of 9 additional IAs. Finally, Study IV was supplemented by 11 IAs that underwent ex vivo MRI scanning after resection.

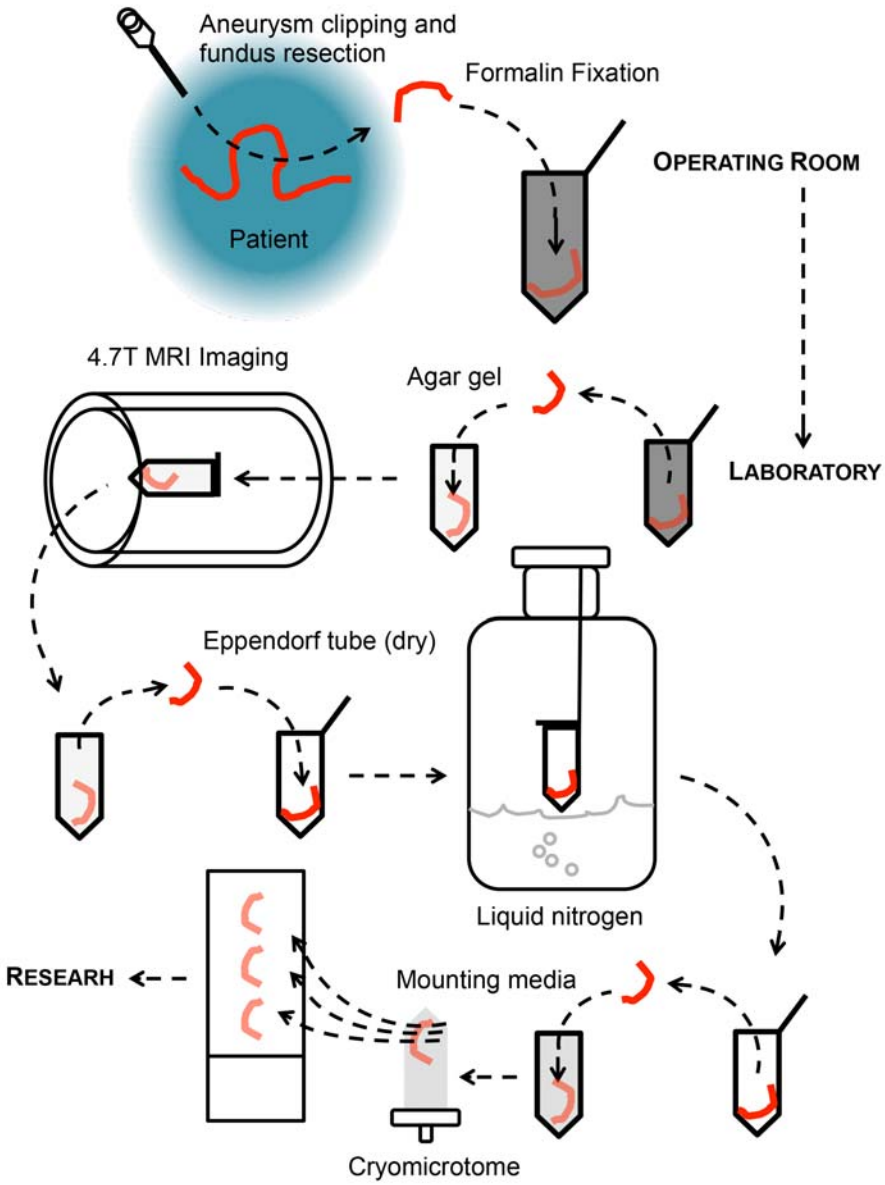

Figure 14. Aneurysm-sample processing prior to ex vivo MRI imaging. For imaging, the 11 IAs were first fixed in 10% formalin immediately after resection, and then embedded in 1% agar gel for scanning with 4.7 T MRI (Bruker Pharmascan, Bruker, Germany). After imaging, the IAs were gently removed from the agar and embedded in Tissue Tek, similarly as in the routine protocol described in Figure 13. Orientation of the IA fundus was maintained during handling. For histology, the IA sample blocks were thoroughly cryosectioned to produce 10-µm sections for histological and immunohistochemical stainings. The MRI-imaging protocol is described in detail in 4.4.1 and previously by Honkanen et al. [91].

Table 2. *Characteristics of IA patients and of samples.*

Variable	Number of IAs (n=55)
Patient	
Female (%)	38/55 (69)
Age (range)	55 (24-87)
Hypertension (%)	18/55 (33)
Current smoking (%)	28/55 (51)
Aneurysm	
Ruptured IA (%)	30/55 (55)
Size in mm (range)	
Fundus length	7 (2-19)
Fundus width	6 (2-20)
Neck diameter	4 (2-11)
Site (%)	
MCA	34/55 (62)
AcomA	11/55 (20)
PcomA	4/55 (7)
ICA	5/55 (9)
OA	1/55 (2)

* MCA, middle cerebral artery; AcomA, anterior communicans artery; PcomA, posterior communicans artery; ICA, internal carotid artery; OA, opthalmic artery.

Table 3. *IA samples studied.*

	Aneurysm		Patient		In Studies			
No.	Ruptured	Location*	Age	Sex	I	II	III	IV
1	No	AcomA	41	M	x	x		x
2	Yes	ICA	32	F	x	x		x
3	Yes	MCA	51	F	x	x	x	x
4	Yes	MCA	50	F	x	x		x
5	Yes	AcomA	29	F	x	x		x
6	Yes	AcomA	63	F	x	x		x
7	Yes	ICA	24	M	x	x		x
8	Yes	MCA	72	M	x	x		x
9	No	AcomA	55	M	x	x		x
10	Yes	MCA	63	F	x	x		x
11	No	AcomA	66	M	x	x		x
12	Yes	PcomA	41	F	x	x		x
13	No	MCA	55	F	x	x		x
14	No	MCA	49	F	x	x		x
15	No	MCA	44	F	x	x		x
16	Yes	PICA	74	F	x	x		x
17	Yes	MCA	46	M	x	x		x
18	No	MCA	55	F	x	x		x
19	No	MCA	67	F	x	x		x
20	Yes	MCA	43	M	x	x		x
21	Yes	ICA	87	F	x	x		x
22	No	MCA	62	F	x	x		x
23	No	MCA	41	M	x	x	x	x
24	No	MCA	58	F	x	x	x	x
25	No	MCA	59	F	x	x		x
26	No	AcomA	54	M	x	x	x	x
27	Yes	MCA	66	F	x	x	x	x
28	No	PcomA	36	F	x	x	x	x
29	Yes	MCA	63	F	x	x		x
30	No	MCA	55	F	x	x		x
31	Yes	MCA	37	M	x	x	x	x
32	Yes	OA	63	F	x	x	x	x
33	Yes	PcomA	53	F	x	x		x
34	Yes	AcomA	59	M	x	x	x	x
35	Yes	MCA	43	F	x	x	x	x
36	No	MCA	60	F	x	x	x	x
37	Yes	MCA	71	F			x	
38	Yes	MCA	46	F			x	
39	Yes	AcomA	43	F			x	
40	No	MCA	41	F			x	
41	No	AcomA	57	F			x	
42	No	MCA	38	F			x	
43	No	MCA	34	M			x	
44	No	MCA	64	M			x	
45	Yes	AcomA	59	M				x†
46	No	ICA	40	F				x†
47	Yes	ICA	53	F				x†
48	Yes	MCA	60	F				x†
49	Yes	Pcom	66	F				x†
50	Yes	MCA	63	F				x†
51	Yes	MCA	63	M				x†
52	No	AcomA	59	F				x†
53	Yes	MCA	55	M				x†
54	No	MCA	51	M				x†
55	No	MCA	63	F				x†

* Abbreviations as in Table 2.

† ex vivo MRI performed.

4.2 Histology and immunohistochemistry

4.2.1 Stainings

For histologic evaluation, IA sections underwent histological, immunohistochemical (IHC), and immunofluorescence (IF) stainings. Autopsied intracranial artery specimens and resected human tonsil tissue served as positive controls.

4.2.1.1 Histology

The IAs were stained for hematoxylin-eosin (HE), Oil Red O (ORO), and Perl's blue.

HE

All IAs were stained for Gill's hematoxylin-eosin G. The IA sections were fixed in -20c° acetone for 3 min, incubated in hematoxylin for 5 min, washed under running tap water until clear, and incubated in eosin G for 2 min. The sections were dehydrated by traveling through ethanol baths of rising precentages from 50% to absolute, and by incubation in Ultraclear, an iso-paraffin-based clearing reagent (J.T. Baker, Mallinckrodt Baker, Deventer, the Netherlands). The slides were then mounted with J.T. Baker's UltraKitt mounting medium.

ORO

Neutral lipids were stained with ORO for unfixed cryosections that underwent incubation in absolute propylene glycol (Sigma, St Louis, MO, USA) for 5 min, then an incubation in 0.5% ORO solution in propylene glycol for 7 min, and then two rounds of washes in 85% propylene glycol, running tap water, and aqua. Mayer's Hematoxylin (Sigma) background-stained the nuclei. Faramount aqueous mounting medium (Dako) served for embedding the slides.

Prussian blue

Nonheme ferric (Fe^{3+}) iron deposition, cellularly stored as ferritin or hemosiderin [164], was stained for Prussian blue using Perl's method [164] or a modification of it by the Artisan Iron Stain Kit (Dako, Glostrup, Denmark) according to the manufacturer's protocol. IA sections 1 to 36 were stained by the latter method in collaboration with the Department of Pathology, Helsinki University Hospital. IA sections 45 to 55 were incubated in 1% potassium ferrocyanide in acidic pH [164], and Nuclear Fast Red background-stained the nuclei.

4.2.1.2 IHC and IF

All IAs were by immunohistochemistry (IHC)-stained and an immunofluorescence (IF) technique served for double-stainings (Table 4). Phases of staining protocol are explained in chronological order below. All incubations were performed at room temperature (RT) and finished, unless otherwise stated, with rinsing of the IA sections three times in phosphate-buffered saline (PBS).

Fixation

The IA sample sections were first fixed in either ice-cold (-20°c) acetone for 3 min, 4% paraformaldehyde for 5 to 10 min, formalin for 10 min, methanol for 10 min, or for 1 min in Carnoy's fixative (60% EtOH, 30% chloroform, and 10% acetic acid [113]). Of the fixatives, acetone served as the main fixative for most IHC stainings, with a few exceptions: formalin was used for double-stainings with ORO, methanol for CD34 staining, Carnoy's solution for mast cell tryptase- and chymase stainings, and paraformaldehyde for all IF stainings. Because IAs 45 to 55 were originally fixed in formalin, their IHC staining was performed after antigen retrieval in citrate buffer.

Blocking

For IHC, the endogenous peroxidase was blocked with either 0.9% hydrogen peroxide (Merck, Espoo, Finland) in PBS for 20 min, or commercial peroxidase block solution according to the protocol

(EnVision kit, Dako). For IHC and IF, non-specific binding of mouse monoclonal antibodies was blocked with 3 to 5% normal horse serum (Vector Laboratories, Burlingame, CA, USA). Rabbit or guinea-pig polyclonal antibodies were blocked with 3-5% normal goat serum; 1% fish skin gelatin (fatty acid-free; Sigma) completed the block in selected IHC stainings. All blocks were diluted in room-temperature buffer solution (in PBS 3% bovine serum albumin and 0.1% Tween, both from Sigma). Incubation time was 30-60 min.

Antibodies

All antibodies (Table 4) were diluted in the buffer solution described above, and incubated for 30 to 60 min at RT, or overnight at 4°C. As negative controls, irrelevant IgG-class-specific monoclonal antibodies (IgG1 or IgG2a; Serotec, Oxford, UK) served as a substitute for monoclonal primary antibodies. Polyclonal primary antibodies were omitted in negative controls. In IHC, the primary antibodies were secondarily detected with either the EnVision kit or the Vectastain Elite ABC kit (Vector) according to manufacturers' protocols. Diaminobenzidine (Vector or EnVision kit) incubation for 1 to 5 min visualized the signal. In IF, Alexa's fluorescent-labeled antibodies were at 1:100 dilution for secondary detection of unconjugated primary antibodies. For the first round of double staining, either Alexa 488 (green) F(ab')2 fragment of goat anti-rabbit or goat anti-mouse IgG (Molecular Probes, Eugene, OR, USA) was used with 30 min of incubation. For the second round, IAs were first re-incubated with primary mouse anti-human antibodies similarly to the first round, and then with Alexa 546 (red) F(ab')2 fragment of goat anti-mouse IgG secondary antibodies. Double staining combinations are in Table 5.

Background staining and embedding

For IHC, Mayer's hematoxylin served for pan-nuclei staining, after which the IA sections were embedded either in Faramount aqueous mounting medium or, after an EtOH bath, in J.T. Baker's UltraKitt mounting medium as described above. In IF, all nuclei were detected with DAPI (4',6-diamidino-2-phenylindole; 1mg/ml, Sigma) in 5-min incubation, and finally the IA sections were mounted with a fluorescent mounting medium (Dako).

Table 4. *Antibodies and dilutions for immunohistochemistry.*

Epitope**	Antibody clone	Dilution	Origin#
CD31	JC70A*	1:100	Dako
αSMA	1A4†	1:100	Dako
CD45	2B11_PD7/26*	1:400	Dako
CD163	5C6-FAT*	1:100	Acris; Novus
	Ab87099‡	1:100	Abcam
CD68	EBM11*	1:100	Dako
CD3	F7.2.38*	1:500	Dako
HLA-DR	CR3/43*	1:100	Dako
Tryptase	AA1*	1:500	Dako
Chymase	CC1*	1:500	Serotec
CD34	QBEnd/10*	1:100	Novocastra
GPA	JC159*	1:100	Novus
ApoA-I	1C5*	1:5000	Monosan
ApoB-100	MB47†	1:10000	[262]
ApoE	WU E-4*	1:500	Santa Cruz Biotechnology
HNE	HNE§	1:300	[188]
Adipophilin	AP125*	1:10	R&D
ABCA1	NB400-105‡	1:100	Novus
HO-1	ADI-SPA-896‡	1:500	Enzo
IgG1	MCA928*	‖	Serotec
IgG2a	MCA929*	‖	Serotec

** αSMA, α-smooth muscle cell actin; HLA-DR, Human leukocyte antigen-DR; GPA, Glycophorin A; ApoA-I, Apolipoprotein A-I; ApoB-100, Apolipoprotein B-100; ApoE, Apolipoprotein E; HNE, Hydroxynonenal; ABCA1, ATP-binding cassette A1; HO-1, Heme oxygenase-1.

* mouse monoclonal IgG1

† mouse monoclonal IgG2a

‡ rabbit polyclonal antibody

§ guinea-pig polyclonal antibody

‖ IgG1 and IgG2a, Irrelevant antibodies for controls, diluted to the same concentration as the primary mouse monoclonal antibody of interest

Dako, Glostrup, Denmark; R&D Systems, MN, USA; Acris, Herford, Denmark; Novus Biologicals, CO, USA; Abcam, Cambridge, UK; Serotec, Oxford, UK; Novocastra, Newcastle, UK; Monosan, Uden, Netherlands; Santa Cruz Biotechnology, TX, USA; Enzo Life Sciences, Farmingdale, NY, USA; LSBio, Seattle, WA, USA; Merck Millipore, Darmstadt, Germany.

4.2.1.3 IHC and ORO double-staining

Lipid-containing either $CD163^+$, $CD68^+$, or αSMA^+ cells, foam cells, were identified by IHC and ORO –double-stainings, where ORO staining was performed on IA sections before hematoxylin incubation of IHC. To avoid lipid dilution, the buffer solution was prepared without Tween, and formalin served as fixative.

4.2.2 Histological evaluation

For analysis, the histological and IHC stains were microscoped and photomicrographed with a Zeiss Axioplan 2 imaging microscope (Flokal Bv Micro-optik, Deursen, The Netherlands) and a Progres C7 USB digital camera (Jenoptik, Jena, Germany). The stained IA sections of the MRI-imaged IAs were imaged with a Hamamatsu Nano-Zoomer XR digital histo scanner, and the Hamamatsu viewer program. The IF stains were photomicrographed with a 3DHISTECH Pannoramic 250 FLASH II digital slide scanner (Genome Biology Unit, University of Helsinki) and the Pannoramic viewer program. See Table 5 for the histological analysis.

IA wall structure

Three blinded observers (E.O., R.T., and J.F.) evaluated the wall structure for the dominant wall type. IAs 1 to 44 were classified as A, B, or C in type according to Frösen criteria [70] (details in Figure 9). Of the IAs, only two samples were representative for type D, and thus were excluded from wall-type analysis. Another three IA samples were poorly oriented for wall-type evaluation, and thus excluded from this analysis.

Additionally, the IAs were scored for the presence or absence of myointimal hyperplasia, decellularization, fibrosis, and fresh or organized thrombosis. The status of luminal endothelium was scored according to the presence or absence of an intact monolayer of CD31 (platelet endothelial cell adhesion molecule-1, PECAM-1 [256]) -positive cells on the luminal surface of the IA wall.

Number of Inflammatory Cells

The number of $CD68^+$, $CD163^+$, $CD3^+$, and $CD45^+$ cells and MCs (tryptase$^+$ cells) were counted in three standard-sized (0.613 mm^2) areas of hot spots, representing the areas most intensely stained for the

cells of interest. In a few IAs, the number of analyzed hot spots had to be restricted because of small sample size. Any thrombus present was excluded from the cell-count analysis. Additionally, distribution density of MCs in the IA wall was defined as MCs per mm^2 using ImageJ, NIH Software. $Chymase^+$ MCs were counted separately. Degranulated MCs were identified as cells showing pericellular staining positive for either tryptase or chymase [117]. IAs 1 to 36 were analyzed for all the leukocyte markers, and IAs 37 to 44 for $CD45^+$ cells.

Extent and pattern of lipid accumulation markers

The presence or absence of ORO-positive neutral lipid accumulation was defined as was its intracellular or extracellular localization. The extent of ORO-positive area in the IA wall was measured as a percentage of the total surface area of an IA wall section (ImageJ). The relative positively stained areas for apoA-I, apoB-100, HNE, and adipophilin underwent measurement similarly to that of ORO. ApoE was analyzed for the presence or absence of colocalization or partial colocalization with apoA-I and apoB-100 in consecutive sections. All lipid markers were analyzed from IAs 1 to 36.

Iron deposition

To identify the presence of iron deposits, a Prussian blue-positive signal was sought from several serial IA sections from IAs 1 to 36 and 45 to 55. IAs with strong, widespread iron deposition with large deposits were considered to contain significant deposition of iron, whereas IAs containing only a few spots of faint positive staining underwent separate analysis.

Presence and density of neovascularization

Neovascularization, i.e. the presence of CD31- or CD34-positive capillary-like structures with lumens [107,159,179,256], was analyzed from the IAs 1 to 36. The number of neovessels per mm^2 (ImageJ) defined their distribution density, similar to that of MCs. CD34-positive structures showing a branching morphology without a lumen were analyzed separately.

Semiquantitative Analyses

Each variable was scored for the presence or absence of positive staining in the IA wall, the localization: intracellular or extracellular or both, of the positive staining, as well as whether the signal was located in the IA wall or in the thrombus or both. Several variables were further scored semiquantitatively to define the extent of positive signal in the IA wall. Thereafter, IAs stained for αSMA, HLA-DR, ABCA-1, GPA, or HO-1 were divided into 3 to 5 categories based on the presence and extent of the variable analyzed.

Of the semiquantitatively scored variables, the cellularly localized ones: αSMA^+, $HLA\text{-}DR^+$, and $ABCA^+$, were scored based on the amount or extent of positively stained cells. For αSMA^+ cells, the IAs were divided into five groups: 1, none; 2, a small group or a few scattered or both; 3, scarce; 4, extensive presence; or 5, increased density of αSMA^+ cells (SMCs) throughout the wall. $HLA\text{-}DR^+$ cells were always present, either 1, in a retricted wall area; 2, widely spread or densely in parts of the wall; 3, densely throughout the wall. The score of $ABCA1^+$ cells was either: 1, none; 2, a few; 3, a small dense group or few scattered positively stained cells or both; 4, dense accumulation in half the wall area or numerous scattered cells in the whole wall area or both; or 5, dense accumulation in the whole wall area.

The amount of either GPA^+ or $HO\text{-}1^+$ signal in the IA wall was scored based on the extent of positive staining, due to either intracellular or extracellular localization of these variables. For GPA, the extent of positive stainings was either: 1, none, 2, faint in a restricted wall area; 3, less than half the sIA wall area; or 4, more than half the sIA wall area. For HO-1, the scores were: 1, no positive staining; 2, scattered positive cells in a restricted wall area; 3, either scattered positive cells throughout the wall or intracellular and extracellular staining in parts of the wall; 4, positive staining throughout the wall.

Colocalizations of the positively stained areas were defined from adjacent sections of IHC stainings of the variables: GPA, HO-1, and HLA-DR stains were scored for colocalization with $CD163^+$, $CD68^+$, or αSMA^+ cells as absent, partial, or complete.

The number of ORO^+ lipid-containing $CD163^+$, $CD68^+$, or αSMA^+ foam cells was scored either as 1, none; 2, a few < 5; 3, a small dense group or solitary scattered cells or both; or 4, numerous and widely spread double-positive cells in the IA wall.

Table 5. *Histological and immunohistochemical evaluation of stainings.*

Staining	Function	Analysis	Study
CD31	Endothelium and inflammatory cells	†	I
αSMA*	Smooth-muscle cells	†‡	I, II
CD45	Pan-Leukocyte Marker	§	III
CD163*	Hemoglobin-haptoglobin-scavenger receptor	§	I
CD68*	Pan-macrophage scavenger receptor	§	I
CD3	T Lymphocytes	§	I
HLA-DR*	Antigen presentation, MHCII	†‡	IV
Tryptase	Mast-cell tryptase, all mast cells	†#	I
Chymase	Mast-cell chymase	†	I
CD34	Cells of hematopoietic origin, neovessels	†#	I
GPA*	Erythrocyte membrane protein	†‡	IV
ApoA-I	HDL particles	‖	II
ApoB-100	VLDL, IDL, or LDL particles	‖	II
ApoE	HDL, VLDL, IDL, or LDL particles	†	II
HNE	Oxidized lipid	‖	II
Adipophilin	Intracellular lipid accumulation	‖	II
ABCA1*	Removal of intracellular lipids	†‡	II
HO-1*	Heme catabolism	†‡	IV
ORO*	Neutral lipid	†‖	I
Prussian blue	Ferric iron, hemosiderin or ferritin	†	I, IV

* Double-stainings: αSMA with CD163, ABCA1, GPA, HO-1, and ORO; CD163 with αSMA, ABCA1, GPA and ORO; CD68 with ABCA1 and ORO.
† binary; presence or absence
‡ semiquantitative
§ number of cells in 1-3 hotspots, each 0.613 mm^2
# distribution density in the whole IA wall section, i.e. number of cells or structures per mm2
‖ percentage of positively stained area in the IA section

4.3 Computational Flow Dynamic models

Patients' preoperative 3D CTA images of approximately 250 axial sections (512 x 512 pixels and 0.4 x 0.4 x 0.6 mm voxel resolution) served as a data source for computational fluid dynamics (CFD) models (III). The flow models were constructed in the Bioengineering Departments of George Mason University, Fairfax, Virginia, USA. The geometrics of the IAs and parent arteries were segmented from CTA raw data at 0.625-mm slice thickness. Mesh generation and computational fluid modeling were as described previously [36,37]. The mathematical simulations of pulsatile flows [176] and the fluid dynamic variables for intra-aneurysmal environment were as described by Mut et al. [177]. Principles for inflow and outflow rates were defined according to the Murray law [174], and inflow boundary conditions according to Taylor et al. [239]. Flow waveform models originated from healthy subjects, as described by Cebral et al. [36].

To define the degree of wall shear-stress (WSS), the IAs were divided into three groups with different levels of WSS according to the median WSS (8.9 dyne/cm2, SD 12.6 dyne/cm2). Low-WSS level was <4.5 dyne/cm2, mid-WSS level was between 4.5 dyne/cm2 and 18.0 dyne/cm2, and high-WSS level was >18.0 dyne/cm2. The WSS-level groups were correlated with IA wall type and number of inflammatory cells. Degree of inflammation was characterized as little or substantial according to the number of $CD45^+$ cells (lower or higher than the median) to compare the hemodynamic changes in different stages of inflammation.

Blood flow was characterized over time (systole-diastole) and space (IA volume from neck to fundus) and determined focally in various regions within the IA sack. The flow was defined as homogenous according to mean flow over time spatial average <0.5 dyne/cm2 or the average <3 dyne/cm2; otherwise, flow was considered heterogeneous. The degree of inflammation was considered as homogenous, if the number of $CD45^+$ cells in the two or three hotspots of the IA wall remained constant (between the threshold values 10 and 200). Of the 20 IAs, 2 were excluded from this analysis due to small sample size, and only one hotspot was analyzed.

4.4 Ex vivo MRI

After their resection, fixation, and embedding, IAs 45 to 55 were imaged with MRI (Figure 14) by Petri Honkanen, MD, similarly as earlier [91] with two iron-sensitive sequences: 1. A T1- or T2-weighted fast-spin echo sequence with rapid acquisition and relaxation enhancement (RARE), and 2. A T2* gradient echo sequence with a fast low-angle shot (FLASH) in a linear birdcage radiofrequency coil with inner diameter of 60 mm.

4.4.1 Imaging protocol

The factors for T1-weighted RARE images were TE 10 ms, TR 600 ms, 5 excitations, echo train length 4; and for T2-weighted RARE images: TE 40 ms, TR 2600 ms, 10 excitations, flip angle 900, echo train length 8; and for proton-density-weighted RARE images: TE 10 ms, TR 3000 ms, 3 excitations, echo train length 4. For T2*-weighted FLASH images, the factors were TE 8 ms, TR 500 ms, 4 excitations, flip angle 400. For all MRI sequences, matrix size was 265 x 265, and slice thickness 1 mm. The MR images were reviewed with OsiriX software (free version).

4.4.2 Analysis of MRI-scanned IA subseries

After imaging, the IAs were cryosectioned each in the same orientation into 10µm sections. Corresponding to each MRI image, the positive signal of GPA and Prussian blue were evaluated from the serial histological sections, for GPA using immunostaining and Perl's method.

For comparison of histology with MR images, each MR image was paired with its corresponding histological section. In this MR image series of each IA, the first and last images of the series of adjacent sections were usually images of tangentially cut IA sections. Since these peripheral pieces of the IA wall showed no informative crosscut of the wall structure, they were excluded from further analysis. Finally, in total 48 MR images from 11 IAs were evaluated.

4.4.2.1 Visuospatial comparison of histology and MRI presentation

All histological sections, stained either for GPA or Prussian blue, were compared with their corresponding MRI images to assess the appearance of these two erythrocyte markers in MRI. Orientation of the IA wall section and the localization of corresponding wall areas were identified to find correlations between the histological and MRI presentations.

4.4.2.2 Statistical comparison of histology and MRI signal intensity

In the MR images, the presence or absence of susceptibility artifacts, considered as black areas within the IA, was observed. Additionally, areas showing heterogenous signal intensities wihin the total IA section area were defined as either 1, hypointense: darker than the background; 2, isointense: similar to the background; 3, or hyperintense: brighter than the background. By "background" this means the agar gel surrounding the IA section in the image. The extent of areas showing different signal intensities within the IAs in MR images were scored semiquantitatively. Thus, all 48 MR images were scored for the presence or absence of any particular signal intensity. If present, the extent of the IA wall area showing the particular signal intensity was scored either as 1, less than half the IA wall area; or 2, more than half the IA wall area of the section. Finally, MRI signal intensity scores were compared with the histological scores of GPA and Prussian blue in the corresponding sections, independent of their visuospatial colocalization or lack of it.

4.5 Statistics

IBM SPSS Statistics Software (version 21; IBM Corporation) served for data analysis. Fisher's exact test served for calculating the proportions of categorical variables, and the Mann-Whitney U-test and Kruskall-Wallis multiple comparison tests compared categorical and continuous variables. Continuous and semiquantitative variables were correlated by the Spearman correlation test. Median and range were calculated for continuous variables. The α-level was 0.05.

5. Results and Discussion

5.1 Clinical and macroscopic features of the IAs

5.1.1 Risk factors and IA rupture

The 55 patients with saccular intracranial aneurysms (IAs), 25 unruptured (45%), and 30 ruptured (55%), studied for degenerative wall changes in histology (I-IV), flow conditions in the IA lumen (III), or magnetic resonance imaging (MRI) of the IA wall (IV), did not significantly differ in sex, age, smoking status, or hypertension (Table 6). These findings suggest that in this group of patients, the main clinical risk factors for IA prevalence and rupture did not associate with IA rupture. Values for plasma total cholesterol, triglycerides, and low- and high-density lipoproteins (LDL and HDL) were available for 21 patients with 12 unruptured and 9 ruptured IAs (II), and these levels similarly failed to associate with IA rupture (Table 6).

Among the 36 samples studied in I-II and IV, the location and size of an IA neither associated with wall rupture (I), nor did the PHASES score [185], which sums up the effect of selected risk factors for IA rupture: Population, Hypertension, Age, Size of an aneurysm,

Earlier SAH from another aneurysm, or Site of an aneurysm [77] (Table 6). Thus, the risk factors studied could not have predicted IA rupture in this series of patients and IAs. This supports a demand for other tools for risk prediction, ones requiring better knowledge of potential risk factors and biomarkers predictive for aneurysm rupture.

5.1.1.1 Multiple IAs

Of the patients, those with an unruptured IA showed IA multiplicity more often than did those with a ruptured IA (I) (Table 6) (Figure 15). Previous subarachnoidal hemorrhage (SAH) showed no association with IA multiplicity (p=0.144, unpublished data). Selection bias should therefore not explain the finding of multiple incidental IAs due to imaging of the previous SAH. A possibility exists that patients showing multiple unruptured IAs would have a systemic etiology or a risk factor behind their IAs more often than would those patients who develop only one IA. However, IA multiplicity did not associate with these classical risk factors (p>0.086 for all), and this does not therefore seem to offer an explanation for any potential systemic cause. The cause for multiple IAs thus remains unknown.

5.2 Degenerative remodeling of the IA wall

Histological changes in the IA wall were most extensively studied in IA samples 1 to 36 (I, II, IV). Wall type and thrombosis were identified also in IAs 37 to 44 (III).

5.2.1 Structural changes in IA walls

Most IAs showed IA wall changes such as loss of endothelium, degenerative or proliferative remodeling of the wall or both, and a luminal thrombus [70,116] (Figure 16).

5.2.1.1 Endothelial erosion, thrombosis, and SMC remodeling

Most IAs (26 of 36; 72%) had lost their intact luminal endothelium, based on the absence of a $CD31^+$ cell monolayer

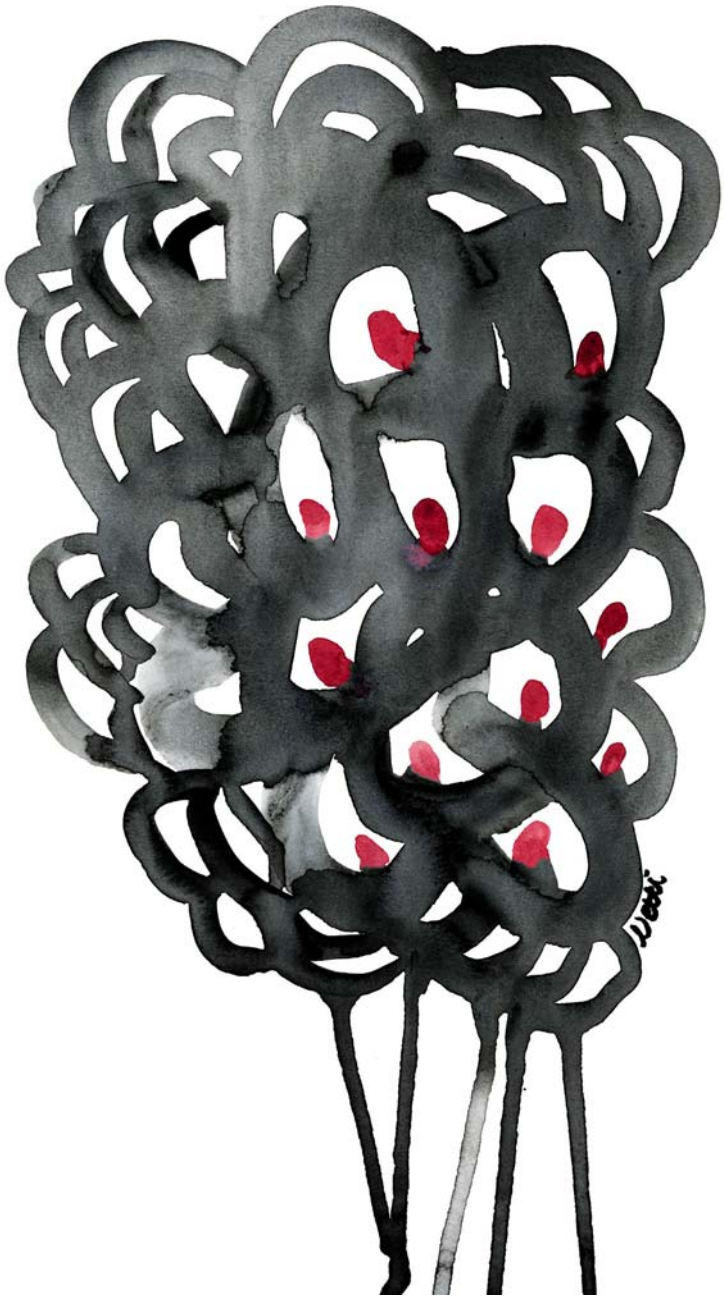

Figure 15. An artistic representation of multiple IAs. Of interest, one of the IAs studied was derived from a patient with a total of eight IAs. The patient also had a history of a SAH, although the one of her IAs studied in this thesis was unruptured. That IA wall showed of the total area of the IA wall section, a remarkable accumulation of lipids: the wall area positive for neutral lipids was 67%, oxidized lipids 6.9%, apolipoprotein A-I 100%, and B-100 89%, and adipophilin 89%. Plasma cholesterol values were also high in this patient, total cholesterol being 6.6, triglycerides 1.05, LDL 4.3, and HDL 1.49 mmol/l. No clinical evidence of hypertension existed, but she smoked. The contribution of potential systemic atherosclerosis, of smoking, hyperlipidemia, or other factors in this particular patient, remains unknown in this setting.

Table 6. *Clinical characteristics of 55 (unruptured 25 or ruptured 30) saccular intracranial artery aneurysms (IAs).*

Variable	Bleeding status: Unruptured IAs (n=25)	Bleeding status: Ruptured IAs (n=30)	p value
Patient			
Female† (%)	17/25 (68)	21/30 (70)	1.000
Age (years) ‡	55 (34-67)	57 (24-87)	0.374
Patient with multiple (≥2) IAs†§ (%)	10/16 (63)	4/20 (20)	0.016*
Patient with previous SAH†§ (%)	2/16 (13)	0/20 (0)	0.190
Hypertension† (%)	8/25 (32)	10/30 (33)	1.000
Smoker† (%)	15/25 (60)	13/30 (43)	0.282
Serum cholesterol value‡# (range)			
Total cholesterol	5.4 (4.2-7.1)	5.4 (3.8-6.6)	0.702
LDL-cholesterol	2.8 (2.1-4.8)	2.7 (1.7-3.9)	0.422
Triglycerides	1.8 (0.6-3.5)	1.2 (0.6-5.4)	0.345
HDL-cholesterol	1.5 (1.1-2.0)	1.6 (0.9-3.0)	0.422
Aneurysm			
Size (mm) ‡			
Fundus length	6 (2-19)	7 (2-13)	0.429
Fundus width	6 (3-20)	6 (3-16)	0.850
Neck diameter	4 (2-8)	4 (2-11)	0.856
Site‡ (%)			0.701
MCA	17/25 (68)	16/30 (5%)	
AcomA	6/25 (24)	6/30 (20)	
PcomA	1/25 (4)	2/30 (7)	
ICA	1/25 (4)	4/30 (13)	
OA	0/25 (0)	1/30 (3)	
PICA	0/25 (0)	1/30 (3)	
PHASES Score‡‖ (range)	9 (7-15)	12 (5-14)	0.678

* $p \leq 0.05$ considered significant.
† Fisher's exact test, proportions given.
‡ Mann-Whitney U-test, median and range for continuous variables.
§ N=36 (samples 1-36)
# N=21
‖ N=44 (samples 1-44)

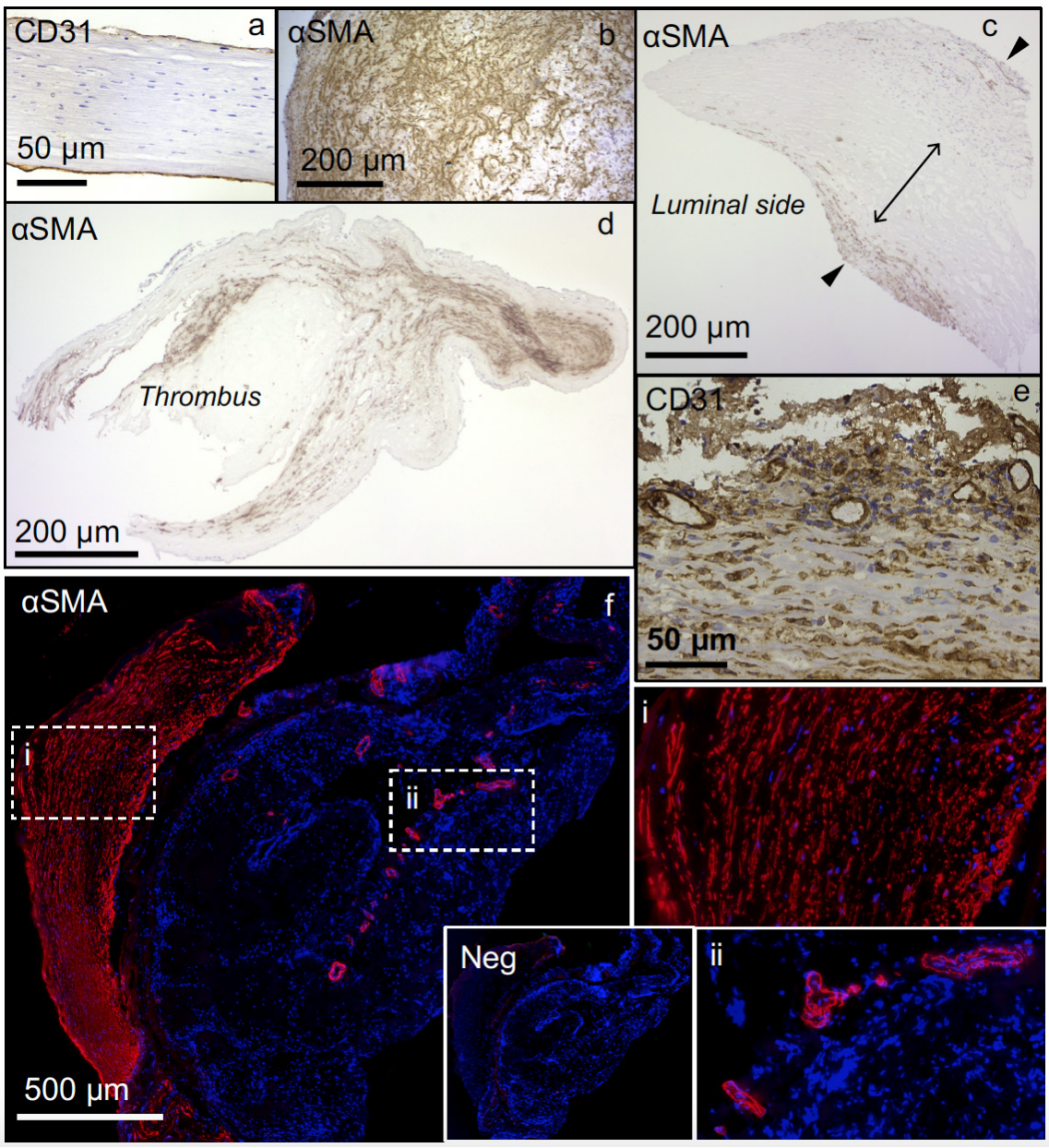

Figure 16. Images of IA wall structural features. a, CD31⁺ endothelium (brown) in the luminal surface of a type A aneurysm with a linearly organized wall structure; b, hyperproliferative and disorganized αSMA⁺ SMC pattern (brown) in type B wall; c, an unruptured type C IA wall, showing a thick, hypocellular wall structure (arrow) and αSMA⁺ cells (arrowheads) in both luminal and adventitial sides of the wall; d, another unruptured IA wall with a thrombus; e, CD31⁺ adventitial vasa vasori or neovessels in the IA wall and a high number of surrounding inflammatory cells also staining positive for CD31; f a ruptured IA, stained for αSMA (red, immunofluorescence staining). Negative control (DAPI) is the inset of f, and i and ii show close-up images of αSMA⁺ cells, likely SMCs, and αSMA⁺ small vessels. Descriptions for IA wall types are in 5.2.1.2.

in the luminal surface of the IA wall (I). Ruptured IAs showed such endothelial erosion more often than did unruptured IAs, supporting previous findings [71], although the finding here did not reach statistical significance (Table 7). The platelet endothelial cell adhesion molecule-1 (PECAM-1, i.e. CD31), together with the vascular cell adhesion molecule-1 (VCAM-1) [142], mediates various regulatory functions of endothelial cells responding to vascular wall shear stress, leukocyte transmigration, and thrombosis [256]. Regulation of these barrier functions may thus be disturbed in those IAs lacking an intact endothelium.

An intraluminal thrombus was present in 17 of 42 (40%) of the IAs (I, III). Two of the 44 IAs remained unclear for the presence (or absence) of thrombosis, due to their complex wall orientation. Of the thrombosed IAs, 14 showed a fresh (young) thrombus and 14 an organizing (older) thrombus. Notably, thrombus organization suggested that thrombosis was not only secondary to the acute IA bleeding, but instead, it had occurred slowly during IA formation. Any thrombus, whether fresh or organized, was associated with IA wall rupture (Table 7).

Mural α-smooth muscle cell actin (αSMA) -expressing cells were present in the wall, but also in the organized thrombus. Even though macrophages can express αSMA in a murine model of atherosclerosis [1,63] and potentially also in humans [74], the αSMA^+ cells were considered to be smooth-muscle cells (SMCs), based on their morphology in relation to the general histological appeareance of the samples. SMCs located in the thrombus seemed to originate from the adjacent aneurysm wall. In atherosclerotic arteries, the thrombus is known to secrete growth factors such as platelet-derived growth factor (PDGF) and transforming growth factor beta (TGF-b), which can potentiate SMC proliferation and migration [142]. Frösen et al. demonstrated the expression of PDGF and TGF-b receptors in the area of myointimal hyperplasia and organizing thrombus of ruptured IA walls [69], proposing the activity of these growth factors in the IA wall, thus potentially triggering SMC migration and proliferation. Loss of SMCs occurred to a variable degree in the majority of IAs (26/36, 72%), but the semiquantitative SMC score did not associate with IA rupture ($p=0.321$, Fisher) (II). SMC disorganization was, however, more common in ruptured than in unruptured walls (I) (Table 7). Changes in SMC organization may reflect a shift in SMC

Table 7. *Histological changes in unruptured and ruptured saccular intracranial artery aneurysms (IAs). Modified from data in tables of Studies I and II.*

Variable	Bleeding status of the IA		p value
	Unruptured	Ruptured	
Structural wall remodeling† (%)			
Endothelium not intact	9/16 (56)	17/20 (85)	0.073
Intraluminal thrombus	3/21 (14)	14/21 (67)	0.001*
Intraluminal fresh thrombus	2/21 (10)	12/21 (57)	0.003*
Intraluminal organizing thrombus	2/21 (10)	12/21 (57)	0.003*
Smooth muscle cell disorganization	4/16 (25)	12/20 (60)	0.049*
Neovascularization	7/16 (44)	8/20 (40)	1.000
Iron deposition	6/16 (38)	3/20 (15)	0.146
Ratio of lipid-rich area, % ‡			
ApoA-I	57 (0-100)	56 (6-100)	0.604
ApoB-100	9 (0-89)	23 (0-56)	0.158
Oxidized lipid	7 (0-92)	20 (0-88)	0.089
Adipophilin	4 (0-87)	21 (0-80)	0.020*
Total number of inflammatory cells‡§			
$CD68^+$ macrophages	7 (0-228)	67 (0-527)	0.042*
$CD163^+$ macrophages	33 (5-185)	132 (28-443)	0.005*
$CD3^+$ T lymphocytes	8 (0-137)	30 (2-357)	0.058
$Tryptase^+$ mast cells	0 (0-24)	0 (0-32)	0.262
Mast cells present† (%)	6/16 (38)	3/20 (15)	0.146

† Fisher's exact test, proportions given.
‡ Mann-Whitney U-test, median and range for continuous variables.
§ In standard-sized areas of 0.613 mm^2.

phenotype from the contractile to the synthetic type [39,49], which may occur in the IA wall and contribute to wall fragility.

5.2.1.2 Distribution of IA wall types

Aneurysm walls 1 to 44 were classified according to wall-type criteria described by Frösen et al. [70] (I, III). Three IAs were excluded from analysis due to their unfavorable orientation in the tissue block. Among the other 41 IAs, 9 (22%) represented type-A walls, with an intact endothelium and linearly organized SMCs; 17 (41%) represented type-B walls, with a thickened, hyperproliferative wall with disorganized SMCs; and 13 (32%) type-C walls, showing a hypocellular wall, accompanied by either myointimal hyperplasia or an organizing luminal thrombus. Only 2 (5%) of the IAs were representative of the most degenerated type-D walls, showing an extremely thin, hypocellular wall with a luminal thrombus. Due to the small number of type-D samples, they were excluded from wall-type analysis. Both type-D IAs were ruptured.

Wall type did not associate with IA clinical risk factors (Table 8). Notably, the presence of clinical risk factors was associated neither with IA rupture (see 5.1.1) nor with wall type, the latter of which may also predict the rupture risk of an IA, based on degree of degenerative IA-wall changes [70]. IAs have indeed demonstrated a gradual risk increase for IA rupture from type A to D [70]. In this IA series, wall type did not associate with IA rupture statistically significantly (Table 8), although the evident trend suggests these findings as in line with those [70].

5.2.2 Neovascularization in the IA wall

Of 36 IAs, 15 (42%) contained $CD34^+$ or $CD31^+$ capillarylike structures, indicating the presence of neovessels (I) (Figure 17). Hematopoietic progenitor cells of immature endothelial structures express CD34 [107], whereas CD31 is expressed by mature endothelial cells [256]. Therefore, both $CD34^+$ and $CD31^+$ capillaries sought from adjacent histological sections were considered to be neovessels of potentially different maturation stages [159,170]. The final quantitative analysis of these neovessels was based on the number of $CD34^+$ neovessels alone, since they predominated

Table 8. *Distribution of clinical characteristics in saccular intracranial artery aneurysm (IA) wall types A, B, and C.*

Variable	Wall type A (n=9)	Wall type B (n=17)	Wall type C (n=13)	p value
Patient				
Female† (%)	7/9 (78)	12/17 (71)	9/13 (69)	1.000
Age (years)‡	62 (41-87)	53 (29-64)	50 (24-74)	0.122
Patient with multiple (≥2) sIAs†§ (%)	5/9 (56)	2/12 (17)	5/11 (45)	0.199
Hypertension† (%)	4/9 (44)	3/17 (18)	4/13 (31)	0.355
Smoker† (%)	6/9 (67)	11/17 (65)	5/13 (38)	0.354
Serum cholesterol value‡#				
Total cholesterol	5.8 (4.3-7.1)	5.2 (4.2-5.7)	5.6 (3.9-6.6)	0.443
LDL-cholesterol	2.9 (2.1-4.8)	2.8 (2.2-3.9)	2.8 (1.7-4.3)	0.899
Triglycerides	1.2 (0.6-2.2)	1.2 (0.9-2.7)	2.7 (0.6-5.4)	0.215
HDL-cholesterol	1.8 (1.6-2.0)	1.5 (1.1-2.2)	1.5 (0.9-3.0)	0.225
Aneurysm				
Size (mm) ‡				
Fundus length	7 (5-19)	7 (3-12)	7 (2-13)	0.764
Fundus width	7 (5-13)	5 (3-9)	6 (4-13)	0.253
Neck diameter	4 (3-11)	4 (3-8)	4 (2-7)	0.420
Site‡ (%)				0.149
MCA	7/9 (78)	9/17 (53)	9/13 (69)	
AcomA	1/9 (11)	7/17 (41)	1/13 (8)	
PcomA	0/9 (0)	1/17 (6)	0/13 (0)	
ICA	1/9 (11)	0/17 (0)	1/13 (8)	
OA	0/9 (0)	0/17 (0)	1/13 (8)	
PICA	0/9 (0)	0/17 (0)	1/13 (8)	
PHASES Score‡‖	13 (7-14)	9 (7-13)	8 (5-15)	0.510
Ruptured IA (%)	2/9 (22)	9/17 (53)	9/13 (69)	0.104

† Fisher's exact test, proportions given.
‡ Kruskal-Wallis test, median and range for continuous variables.
§ N=36 (samples 1-36)
# N=21
‖ N=44 (samples 1-44)

in 14 of the 15 IAs, with only one IA showing a single $CD31^+$ vessel without any $CD34^+$ neovessels. This single IA was excluded from quantitative analysis. In the IA walls adjacent to neovessels, additional $CD34^+$ continuous structures without a capillary lumen were abundant. These were often located adventitially in the IA wall. In the neovascularization process known to occur in atherosclerotic artery walls, neovascularization starts as endothelial sprouting from the adventitial vasa vasori [170], and the newly developed neovessel branches invade through the media towards the thickened intima [170,206]. Thus, the branching $CD34^+$ structures in neovascularized areas of the IA walls are interpreted as early-stage neovessels [56,170]. These findings suggest ongoing neovascularization in the majority of the IA walls, in 28 of 36 (78%).

The presence of or density of neovessels and the other $CD34^+$ structures considered as pre-vessels was not associated with IA rupture (Table 7) However, neovascularization did associate with IA wall degeneration, with the density of neovessels being the highest in type-C walls (Table 9). The IA is likely to suffer from hypoxic conditions, based on its expression of hypoxia inducible factor-1 (HIF-1) [132], a potential trigger for neovascularization. In addition to HIF-1, activity of angiogenic growth factors PDGF and vascular endothelial growth factor (VEGF) may occur in the IA wall [69], and thus they may mediate neovascularization there.

In the present study (I), neovessel density correlated with the presence of mast cells (MCs, $p<0.001$) and with the number of $CD163^+$, $CD68^+$, and $CD3^+$ inflammatory cells in the IA wall ($r=0.617$-0.669, $p<0.001$, Spearman, unpublished correlation). The presence of neovessels in human IAs has been reported in association with leukocytes [90]. These findings suggest the contribution of inflammation to neovascularization. In atherosclerotic arterial walls, inflammatory cells secrete several pro-angiogenic factors among their cytokines and chemokines, ones such as VEGF, PDGF, TNF-α, and MMPs [206], which may mediate neovascularization also in the IA walls. On the other hand, neovessels can facilitate the entry of circulating inflammatory cells into the IA wall [224,250], which thus may cause neovessel rupture and microhemorrhages in the vascular wall [206], as described in the following section.

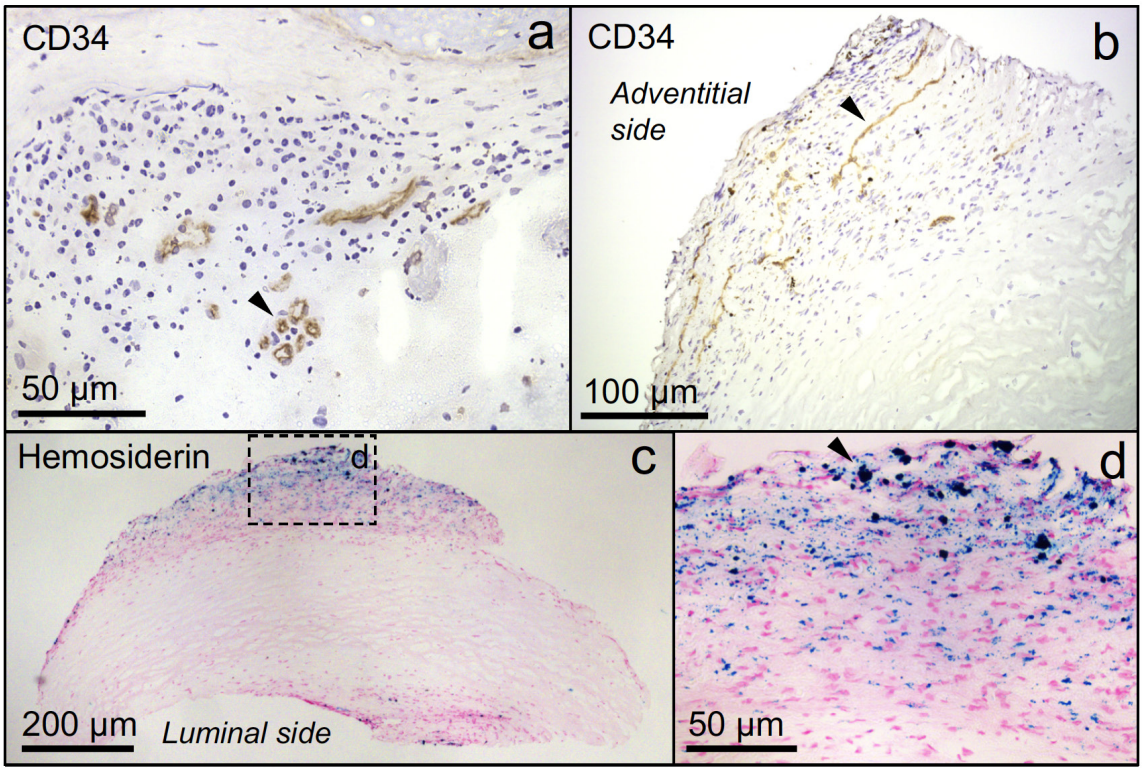

Figure 17. Neovessels and microhemorrhages in the IA wall. a, $CD34^+$ structures with a lumen (arrowhead), considered as neovessels; b, $CD34^+$ continuous structures without a lumen (arrowhead), considered as developing neovascular structures or early neovessels, potentially sprouting from adventitial vasa vasori (not shown here); c, strong iron (hemosiderin) deposition in the area of the suspected early neovascularization; d, inset, close-up of iron deposition.

Table 9. *Distribution of wall remodeling changes, ones not included in the wall type criteria, in saccular intracranial artery aneurysm (IA) wall types A, B, and C. Modified from tables of Studies I and II.*

Variable	Wall type			p value
	A (n=9)	B (n=12)	C (n=11)	
Neovascularization and iron				
Neovessels present† (%)	0/9 (0)	5/12 (42)	9/11 (82)	0.001*
Density of neovessels (neovessels/mm^2) ‡	0 (0-0)	0 (0-21)	4 (0-50)	0.001*
Iron deposition† (%)	2/9 (22)	2/12 (17)	5/11 (45)	0.293
Strong iron deposition† (%)	0/9 (0)	1/12 (8)	5/11 (45)	0.016*
Ratio of lipid-rich area, % ‡	16 (1-32)	5 (0-32)	25 (4-69)	0.036*
ApoA-I	38 (0-69)	38 (0-69)	86 (35-100)	0.011*
ApoB-100	7 (0-17)	15 (0-56)	32 (8-89)	0.001*
Oxidized lipid	8 (0-22)	8 (0-55)	43 (4-92)	0.034*
Adipophilin	4 (0-21)	8 (0-58)	30 (0-87)	0.005*
Total number of inflammatory cells‡§				
CD68$^+$ macrophages	0 (0-57)	74 (0-302)	124 (0-527)	0.010*
CD163$^+$ macrophages	23 (7-132)	115 (5-443)	185 (74-417)	0.002*
CD3$^+$ T lymphocytes	5 (0-21)	39 (0-261)	52 (11-357)	0.004*
Tryptase$^+$ mast cells	0 (0-0)	0 (0-32)	0 (0-24)	0.074
Mast cells present† (%)	0/9 (0)	3/12 (25)	5/11 (45)	0.081

† Fisher's exact test, proportions given.
‡ Kruskal Wallis test, median and range for continuous variables.
§ In standard-sized areas of 0.613 mm2.

5.2.2.1 Microhemorrhages from leaky neovessels

Of the 47 IAs, Prussian-blue-positive staining occurred in 20 (43%), reflecting deposition of ferric iron in the form of hemosiderin (I, IV). Notably, hemosiderin was sought systematically from several IA wall levels throughout IA sample blocks 45 to 55, and all of these IAs showed positive staining, whereas from IAs 1 to 36 only two sections stained, and of these 36, 9 IAs showed hemosiderin deposition. Thus, the number of stained sections possibly affected the sensitivity of finding hemosiderin. Nevertheless, the amount of hemosiderin per section in most cases was small.

Of the 20 IAs, 7 showed local, strong iron positivity in their large hemosiderin deposits, whereas the other 13 IAs showed weak positive staining. That some of the large iron deposits were located intracellularly suggests the intracellular storing of hemosiderin following lysosomal degradation of hemoglobin [164,165,195]. The presence of extracellular iron deposition in the IA wall indicates phagocytic release of hemosiderin [263].

The strong iron deposition colocalized with neovessels in the 6 of the 36 IAs that stained for both (I), and strong iron deposition associated with neovessel density ($p<0.001$) and wall degeneration (Table 9). Newly formed neovessels can leak erythrocytes into the arterial wall, producing microhemorrhages [165,224], which implies that leaky neovessels are a cause for microhemorrhages in the IA walls. Another potential source of iron accumulation is the hemoglobin originating from erythrocytes trapped in the luminal thrombus.

5.3 Lipid load as a possible promoter of IA wall rupture

Lipid accumulation, a core phenomenon of atherosclerotic plaque formation, is known to occur in the IA wall and may play a role in IA wall pathogenesis [71,72,125,244].

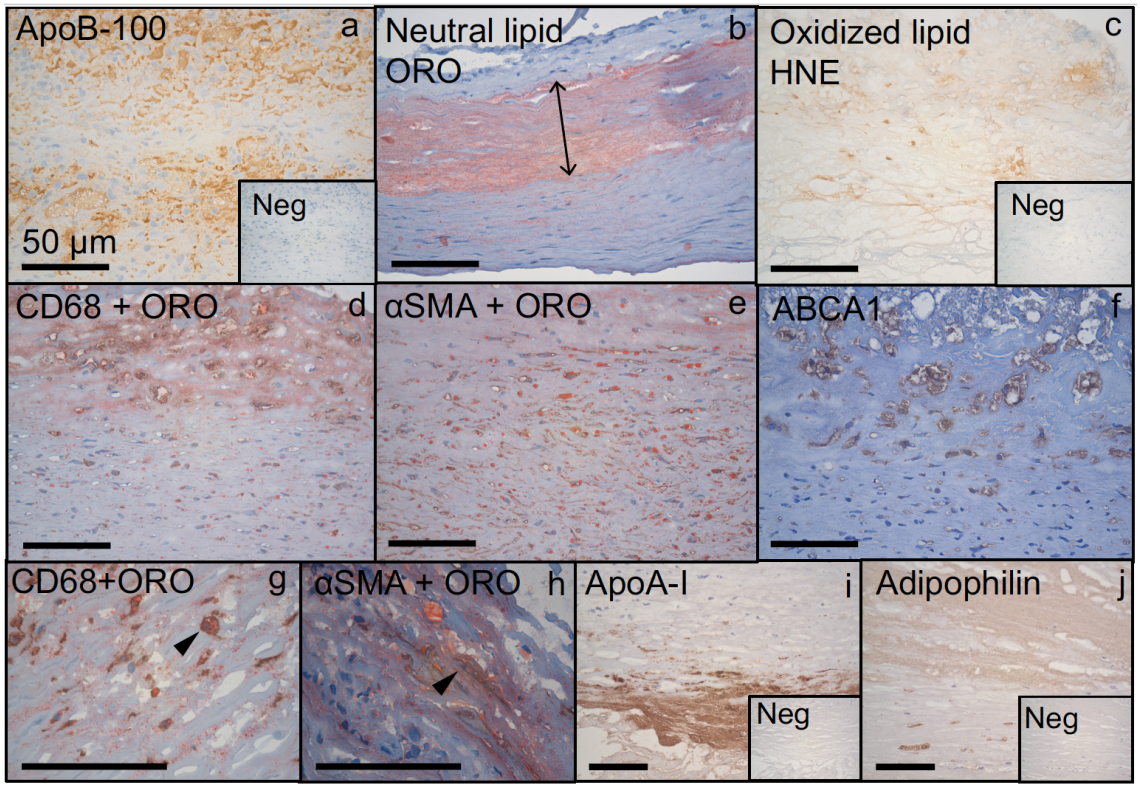

Figure 18. Lipid accumulation in the IA wall. Representative images of a, apoB-100^{+} lipoprotein particles, b, ORO^{+} neutral lipid (arrow), and c HNE^{+} oxidized lipid retention in the IA wall. Images d-f show adjacent sections from the same area of an IA wall. Double-stainings of ORO with d, CD68^{+} and e, aSMA^{+} cells demonstrate intracellular lipid accumulation in these cells; and f, expression of ABCA-1 lipid transporter suggests its upregulation potentially by foam cells in the IA wall; g and h show intracellular lipid accumulation at higher magnification. i ApoA-I was focally distributed in the IA wall, and j, adipophilin often showed widespread extracellular accumulation in hypocellular wall areas, suggesting foam cell death in that area. All scale bars 50 µm.

5.3.1 Lipid accumulation broadly present in degenerated IA walls

Accumulation of lipids or their circulatory carrier particles, apolipoproteins, appeared to a variable extent in all 36 IA walls (II). These lipid or apolipoprotein particles were retained both intracellularly and extracellularly, irrespective of plasma lipid levels, as in earlier observations [72]. This suggests that the local pathological conditions in the IA wall, like its structural remodeling and proinflammatory microenvironment, contribute to the influx and retention of lipids, favoring a non-physiological accumulation of lipids. Figure 18 demonstrates accumulation patterns of the lipid markers in the IA wall.

5.3.1.1 Apolipoprotein B and lipid influx in the IA wall

Apolipoprotein B-100 (apoB-100) was present in all 36 IA walls, reflecting retention of atherogenic very low-, intermediate-, and low-density lipoprotein particles (VLDL, IDL, and LDL) (II). These lipoproteins carry lipids from the circulation to the arterial walls [129,144], and apparently also to the IA walls. Tulamo, and Frösen, et al. have shown apoB-100 in the IA wall [72,244] and this study highlights its extensive retention in the wall. The median proportion of IA wall area staining positive for apoB-100 was 16%, ranging from 0 to 89%. In three IAs (8.3%), the positive staining was restricted only intracellularly to a few positively staining mural cells.

Especially those IA walls lacking intact endothelium showed the most extensive accumulation of apoB-100 (median area 25% vs. 8%, p=0.001). Disturbed barrier function or total loss of luminal endothelium predisposes the arterial wall to lipoprotein influx from the circulation [7], indicating that endothelial erosion may contribute to apoB-100 lipoprotein accumulation in the IA wall. An organized thrombus associated with apoB-100 accumulation (p=0.009), indicated endothelial erosion prior to thrombosis and thus supports this interpretation. Moreover, the thrombus itself may become a source of lipids by trapping erythrocytes whose lysis releases cholesterol from cell membranes [250].

5.3.1.2 Neutral lipid accumulation

The vast majority of the IAs showed an accumulation of Oil red O (ORO) positive lipid, reflecting accumulation of cholesterol esters and triglycerides, i.e. neutral lipids. Specifically, of 36, 28 (78%) showed extracellular ORO$^+$ lipid when stained at one section level per sample (I), and 33 (92%) showed ORO$^+$ when stained at several IA section levels (II). The atherogenic LDL particles contain high quantities of triglycerides and cholesterol covered by a phospholipid layer and integral apoB-100 [73]. The association of ORO$^+$ lipids with apoB-100 ($r=0.400$, $p=0.016$, unpublished correlation) suggests that at least some neutral lipids in the IA wall have derived from apoB-100-containing lipoprotein particles.

Accumulation of neutral lipids did not associate with IA wall rupture, nor did the apoB-100 retention in the IA wall (Table 7). However, ORO$^+$ lipid was particularly retained in hypocellular areas and was spread most extensively in degenerated (C-type) IAs (Table 9). Tulamo et al. have shown that a similar ORO$^+$ lipid retention area colocalizes with the terminal complement activation complex C5b-9 that is associated with chronic inflammation and IA rupture [244]. Frösen et al. have demonstrated that accumulation of neutral lipids in the aneurysm wall is associated with loss of mural cells, suggesting that a lipid-induced proinflammatory or cytoxic stimulus may trigger degenerative remodeling of the aneurysm wall [72].

5.3.1.3 Oxidized lipids, lipid phagocytosis, and foam cell death

That 35 IA walls (97%) showed the presence of extracellular and intracellular hydroxynonenal (HNE) (II) indicates the presence of oxidized lipids in the IA wall [188]. The median extent of HNE retention was 10% (range 0-92%) of the IA wall area. Retention of oxidized lipids was the highest in type-C walls (Table 9), reflecting the association of retention with IA wall degeneration. Oxidative stress causes modification of proteoglycan-bound lipids and lipoproteins [225], facilitating their retention, and triggering their phagocytosis by macrophages and mural SMCs in the arterial wall [141].

The IAs contained an intracellular accumulation of ORO, apoB-100, and HNE, indicating the presence of lipid-laden foam cells. Immuno-double-stainings with ORO revealed ORO$^+$/ CD68$^+$,

CD163$^+$, and aSMA$^+$ cells, suggesting lipid ingestion by both macrophages and SMCs in the IA walls (II). Macrophage-driven phagocytosis is an essential mechanism for lipid clearance from the arterial wall, preventing the formation of a necrotic lipid core in the atherosclerotic plaque [80,129,143]. Notably, of the 36 IAs, 16 (44%) contained SMC foam cells (II). SMCs containing HNE$^+$ oxidized lipids have also been detectable in the IA wall [72]. These findings suggest a role for SMCs as lipid-phagocytosing cells in the IA walls.

IAs containing SMC foam cells showed a marked loss of mural SMCs ($p=0.011$), suggesting the cytotoxicity of intracellular lipid accumulation. Furthermore, loss of SMCs was associated with accumulation of neutral lipids ($p=0.027$) and oxidized lipids ($p=0.009$). Ingestion of cytotoxic lipids may contribute to the death of SMCs by disturbing their normal cellular functions [237]. The finding that not only oxidized lipid but also apoB-100 was occasionally present in the cell cytoplasm (II) suggests that lipoprotein oxidation and retention possibly disturbs lysosomal processing of lipoprotein particles [30,106,150]. In short, excess lipid load may cause intracellular lipid retention and associated cell death in the IA wall.

Once phagocytozed, intracellular lipid droplets become covered by adipophilin [87]. Adipophilin was expressed also in 35 (97%) of the 36 IAs, where it was located mainly extracellularly (II), suggesting the release of adipophilin-containing lipids from the cells either by active exocytosis or at their death. Extent of adipophilin (median 13%, range 0-87%) associated also with loss of SMCs ($p=0.011$) and IA wall rupture (Table 7). The observation of extracellular adipophilin surrounding adipophilin-expressing foam cells indicates the release of adipophilin-attached lipid droplets into the ECM, most likely as a result of lipid-laden foam-cell death [41,129,141,237], potentially predisposing to IA wall rupture, in line with findings by Frösen et al. [72].

5.3.2 Cellular lipid clearance pathway in the IA wall

Apolipoprotein A-I (apoA-I), the protein component of high-density lipoprotein (HDL), existed in all IAs (II). ApoA-I was mainly located in the ECM, and its presence was most widespread in the degenerated IA walls (Table 9), which also contained an abundant

accumulation of lipids. The widespread presence of apoA-I (median 56%, range 0-100%) indicated the presence of the reverse cholesterol transport pathway of intracellularly accumulated lipids [7]. To perform the cellular lipid clearance, apoA-I itself does not enter the foam cell, as it operates through the cell membrane transporter ATP binding cassette-1 (ABCA-1) [7,211]. Of the IA walls, 33 (92%) expressed also ABCA-1 (II), indicating the capacity for release of intracellular lipids via interaction with apoA-I. The amount of ABCA-1 associated with oxidized lipids and adipophilin suggests that intracellular lipid accumulation was associated with the presence of apoA-I and the ABCA-1 clearance pathway.

5.3.2.1 Impaired apolipoprotein A-mediated lipid clearance

Contrary to the lipid clearance function of apoA-I, those IAs with massive infiltration of apoA-I also showed massive lipid accumulation and wall degeneration. Such a finding indicates insufficient function or failure of the apoA-I–ABCA-1-mediated clearance mechanism, especially as apoA-I and ABCA-1 accumulated in different wall areas in nearly half of the IAs expressing them both. These observations indicated lack of the apoA-I–ABCA-1 interaction in those wall areas. The colocalization of ABCA-1-expressing and apoA-I-containing wall areas associated with a higher amount of SMCs in the IA wall ($p=0.003$), whereas the supposed functional lack of this colocalization associated with wall degeneration ($p=0.017$) (II). This finding supports the interpretation that failure of intracellular lipid clearance predisposes SMCs to death by lipids.

In part, the supposed failure of apoA-I function could be explained by the observed non-physiological distribution observed of apoA-I in the IA wall. Normally the small-sized apoA-I particle diffuses freely through the arterial wall, without binding to the ECM [7,211]. However, apoA-I showed focal distribution in the IA wall, raising the suspicion of its abnormal retention in the IA wall. Binding of apoA-I to ECM is possible via the apoE particle [181]. In the IAs, however, apoA-I$^+$ wall areas colocalized only partly with apoE$^+$ staining, and thus attachment of apoA-I to apoE could not fully explain the localized apoA-I pattern (II). Other factors may therefore be disturbing apoA-I function in the IA wall, factors such as oxidative stress. Thus, besides lacking interaction with ABCA-1, apoA-I

may have become dysfunctional itself, due to the pro-oxidative environment of the IA wall. ApoA-I has normally anti-oxidant and anti-inflammatory properties in the arterial wall in addition to its anti-atherosclerotic function [7,211]. The shift of apoA-I into its dysfunctional and proinflammatory form has been described in atherosclerotic arteries and AAAs, especially in the presence of oxidizing myeloperoxidase (MPO) [93,178,211]. Since MPO has been detectable in human IAs [76], and these IAs also contain MPO [185], oxidation of apoA-I may have occurred in the IA wall, thus triggering the apoA-I retention.

Another potential mechanism for impaired lipid clearance from SMCs is their downregulated ABCA-1 expression. In the IA wall, ABCA-1 expression correlated positively with the number of $CD68^+$ ($p=0.005$) and $CD163^+$ ($p=0.001$) macrophages, suggesting upregulation of ABCA-1 by macrophages. However, because high expression of ABCA-1 did not correlate with high amount of SMCs in the IA wall ($p=0.075$), intracellular lipid accumulation may upregulate ABCA-1 expression in macrophages, but not necessarily in SMCs in the IA walls; this is a phenomenon recently demonstrated in advanced atherosclerotic lesions, where intimal SMC foam cells showed reduced ABCA-1 expression in comparison to myeloid lineage inflammatory cells [5]. Such a reduced capacity for upregulated ABCA-1 expression by SMC foam cells may occur also in the IA walls, since only solitary cells double-positive for αSMA and ABCA-1 appeared (II).

In short, apoA-I function via ABCA-1 may be a significant lipid clearance mechanism in the IA wall, and the lack or dysfunction of this protective mechanism may contribute to excess lipid load and to SMC death.

5.4 Erythrocytes as a source of oxidative stress

Of the IAs, 40% contained fresh or luminal thrombus and a thrombus associated with IA rupture (see 5.2.1.1). Thrombi appear as a potent source of oxidative stress in the IA walls, since they contained erythrocytes. Erythrocyte-derived heme is an effective oxidant.

5.4.1 Eryhtrocytes originating from the thrombus and neovessels

Glycophorin A (GPA), an erythrocyte-specific cell membrane component [120], was present in the majority (34 of 36, 94%) of the IA walls, reflecting the accumulation of either intact or lysed erythrocytes (IV). Erythrocyte accumulation was abundant in the luminal thrombus in the IAs, suggesting the thrombus as a significant source of erythrocyte membrane fragments, as it is in intraplaque hemorrhages in atherosclerotic arteries [165]. In the IAs especially, organized thrombus associated strongly with GPA score ($p<0.001$). This finding highlights erythrocyte accumulation as a long-term factor in IA wall pathogenesis as a component of old thrombus, rather than as representing acute repair of intraluminal wall injury or its eventual rupture. GPA was associated also with the iron deposition adjacent to neovessels ($p=0.014$), reflecting intramural microhemorrhages as another apparent source for erythrocytes (5.2.2.1).

5.4.2 Heme-derived iron may cause IA wall degeneration and rupture

Accumulation of erythrocytes or the fragments of erythrocyte cell membrane correlated with loss of SMCs ($r=0.59$, $p<0.001$), with IA wall degeneration ($p=0.008$), and with its rupture (0.005), suggesting a contribution of erythrocyte accumulation towards a rupture-prone IA wall (IV). This finding may imply the deleterious effect of erythrocytes in the IA wall, being in line with earlier findings in coronary [120,139] and carotid [165] arteries, where GPA accumulation associates with fragility of an atherosclerotic lesion. The destructive effect of erythrocytes is known to originate from their lysis and their subsequent release of highly oxidizing hemoglobin-derived ferrous iron in the vascular wall [120,155,166,250,263]. Due to the extensive presence of GPA, it is evident that the IA wall also contains hemoglobin-derived ferrous iron, which may contribute to oxidative stress for that wall. Laaksamo et al. demonstrated oxidative stress in the IA wall and suggested that oxidation creates a cytotoxic extracellular environment leading to apoptotic cell death [133]. In short, a significant cause of this devastating oxidative stress in the IA wall appears to be erythrocytes (IV).

5.4.2.1 Erythrocytes in the IA wall contributing to lipid oxidation

The erythrocyte lysis products GPA ($r=0.58$, $p<0.001$, IV) and iron ($p=0.018$, II) correlated with the accumulation of oxidized (HNE^+) lipid. Thus, erythrocyte accumulation in the IA wall may contribute to lipid accumulation via the retention of erythrocyte membrane remnants, rich in phospholipids and cholesterol, and also may trigger lipid oxidation via their released heme. GPA accumulation did not, however, associate with retention of apolipoproteins A-I and B-100, with adipophilin expression, or with the extent of neutral (ORO^+) lipid accumulation ($p>0.056$, unpublished finding). This indicates that cholesterol-containing erythrocyte-membrane degradation is another, parallel source for lipid accumulation in the IA wall, one independent of lipid transport by apolipoproteins.

5.5 Inflammatory response to IA wall damage

Inflammatory cells had infiltrated all 44 IAs stained for such cells. More specifically, all of the IAs 1 to 36 contained $CD163^+$ macrophages, most of the IAs contained $CD68^+$ macrophages (34 of 36, 94%) and $CD3^+$ T lymphocytes (32 of 36, 89%), and a quarter of the IAs contained mast cells (MCs, $tryptase^+$ cells; 9 of 36; 25%) (I). Single polymorphonuclear cells were also present in these IA walls, representing neurophils. To study the presence of inflammatory cells in general, samples 37 to 44 were stained only for leukocyte-common antigen CD45, and this was present in each of them (III).

The observation of abundant inflammatory cells in the IA walls supports earlier findings suggesting the contribution of chronic inflammation to IA pathogenesis [47,70,116,125,244,245]. In atherosclerotic pathologies, as well, chronic inflammation appears as the driving force of remodeling of the arterial wall [143]. In the present study (I), among the inflammatory cells, macrophages were the most numerous in ruptured IAs (Table 7), and their number was associated with wall degeneration (wall type, Table 9). The number of T lymphocytes also correlated with wall degeneration. These findings support the earlier interpretation that chronic inflammation is involved in IA wall remodeling.

5.5.1 Mast cells associated with neovessels and microhemorrhages

In the IA wall, MCs were rare and their number lower than for T lymphocytes and macrophages (Table 7). Their presence associated neither with wall rupture nor with wall type at a statistically significant level, although most of the MC-containing IAs were representative of the degenerated wall type C (Table 9). The rarity of MCs in the IA walls suggests that the role of MCs in IAs is not as pivotal as in atherosclerotic diseases of the extracranial arteries such as coronary atherosclerosis [129] and abdominal aortic aneurysms (AAAs) [161,234], where MCs have played an important role as regulators of chronic inflammation and vascular wall degeneration.

Prior to this study (I), MCs had been demonstrated in the arteries of the Circle of Willis in patients who had died of SAH [59], and more recently in samples of intraoperatively obtained IAs [83]. In the latter study, the authors found MCs in all ten IAs studied, and the semiquantitative score of MCs was higher in the five ruptured IAs than in the five unruptured ones [83]. This suggested MCs as being part of the proinflammatory response leading to IA rupture. Although the present finding of MCs in IAs does not support the hypothesis of a central role for MCs in IA pathogenesis, several significant IA wall remodeling changes may be facilitated by MC actions.

First, all IAs containing MCs lacked intact endothelium ($p=0.039$), suggesting that the MC-specific neutral proteases tryptase and chymase may cause detachment of endothelial cells from the basement membrane of the IAs, similarly to the case in atherosclerotic lesions [129] and in AAAs [161]. Both proteases also have the ability to activate MMPs [129], capable of degrading the ECM.

Second, MCs were strongly associated with the occurrence of neovascularization, with neovessels present in all nine MC-positive IAs in proximity to MCs ($p<0.001$). The density of neovessels was also associated with MC occurrence ($p<0.001$). These findings suggest that MCs may induce neovascularization in the IA wall, similarly as in atherosclerotic plaques, aortic valves, and AAAs [67,107,112,161,234,236,255]. In addition to the actions of proteases, MCs also secrete histamine and other angiogenic factors such as VEGF, basic fibroblast growth factor (bFGF) [134],

TNF-α, and heparin [206,236], all of which may contribute to IA neovascularization (5.2.1.1).

Third, MCs in the IA wall associated with and colocalized with microhemorrhages (p=0.003), suggesting that they may also induce neovessel leakage via their histamine and proteases [23,24,112,206]. Finally, the majority (67%) of MCs in the IA walls showed degranulation, suggesting that they were in the active state.

The MC proteases can also contribute to LDL modification and HDL degradation in the ECM, and thus trigger foam cell formation of the arterial wall [128,137]. In the IAs, MCs associated with the extent of lipid accumulation, suggesting their potential contribution to lipid accumulation in those IA walls where they exist. However, the extensive lipid accumulation compared with the minor MC accumulation in the IA walls implies other atherogenic mechanisms in the IA walls that are in general more significant than are the actions of MCs.

5.5.2 Inflammation directed to the clearance of hemoglobin

Extensive GPA accumulation correlated with the numbers of $CD163^+$ and $CD68^+$ phagocytes (r=0.65 and 0.54, p≤0.001) but not with the number of T lymphocytes (r=0.25, p=0.136) (IV), suggesting that macrophage-driven phagocytosis is a more important mechanism for the clearance of erythrocytes from the IA walls than is a potential T-lymphocyte-driven adaptive immunity response to erythrocytes. Macrophages are known to phagocytose intact or lysed erythrocytes in the arterial wall to protect it from the oxidizing effect of extracellular hemoglobin [140,166,186]. In addition to macrophages, SMCs are also capable of phagocytosing erythrocytes [119]. However, that a minor amount of GPA was present intracellularly in the IA wall may indicate either the GPA's rapid lysosomal degradation after phagocytosis or indicate that phagocytes in the IA wall are more focused on ingesting the intracellular contents of erythrocytes after lysis than on ingesting erythrocyte membrane fragments. Hemosiderin in the IA wall reflected the prior phagocytosis of hemoglobin, supported also by the association of strong hemosiderin deposition with number of $CD163^+$ and $CD68^+$ phagocytes (p=0.016 and 0.017) (I).

5.5.2.1 Hemoglobin-phagocytozing CD163+ macrophages in the IA wall

Phagocytes expressing CD163, the scavenger receptor for hemoglobin [130], were evident in all 36 IA walls, representing the most numerous type of inflammatory cells there (I). The massive infiltration of $CD163^+$ cells in the IA wall appears to play a role in IA wall pathogenesis, since the number of $CD163^+$ cells associates strongly with IA wall degeneration, (wall type, Table 9) and rupture (Table 7) (I), as in other studies [70,71,245]. To further study the phenotype of $CD163^+$ cells in the IA wall, these cells were doublestained for human leukocyte-DR (HLA-DR) and αSMA (IV). The latter double-staining revealed only single $CD163^+/\alpha SMA^+$ cells in only 3 of the 36 (8.3%) IA walls, implying that $CD163^+$ cells were of myeloid origin rather than being SMC derived. Double-staining for four selected phagocyte-rich IAs revealed only single $CD163^+/HLA\text{-}DR^+$ cells in one IA, showing that the main portion of the $CD163^+$ macrophages were $HLA\text{-}DR^-$. This finding suggests in IAs a macrophage population specialized in hemoglobin phagocytosis, similar to the situation suggested in atherosclerotic coronary arteries [26] and abdominal aortic aneurysms (AAAs) [212]. Since the IA wall contains much erythrocyte-derived oxidizing hemoglobin accompanied by infiltration of $CD163^+$ cells, it is likely that a similar hemoglobin-induced macrophage population plays an important role in IA pathogenesis.

5.5.2.2 Hemeoxygenase-1 involved in IA pathogenesis

The vast majority of the 36, 35 (97%), expressed hemeoxygenase-1 (HO-1), and its expression was significantly higher in degenerated IAs ($p=0.041$, IV). This finding is in line with the observation of HO-1 expression as being higher in ruptured than in unruptured IAs [133]. $CD163^+$-mediated phagocytosis of hemoglobin, usually complexed with the circulating acute-phase protein haptoglobin, leads to degradation of the complex in lysosomes and subsequent degradation of the protoporphyrin ring of heme by HO-1. This reaction produces anti-inflammatory carbon monoxide and biliverdin, along with the ferrous iron [172,220]. HO-1 in the IA wall and its correlation with extensive GPA accumulation ($r=0.57$, $p<0.001$) thus reflects the degradation of hemoglobin in the IA wall.

Both oxidative stress and hemoglobin upregulate HO-1 expression [100,187]. High HO-1 expression correlated with the numbers of $CD163^+$ and $CD68^+$ macrophages in the IA wall ($r=0.74$ and 0.67; $p<0.001$ for both), suggesting that inflammatory cells likely express HO-1 there. Moreover, of 28 IA walls, half showed solitary SMCs expressing HO-1 (IV), an observation in line with earlier findings in AAAs [212].

5.5.3 Inflammation directed to the clearance of lipids

The presence of apoB-100, oxidized lipid, and adipophilin was associated with high numbers of $CD68^+$ and $CD163^+$ macrophages ($r=0.564$-0.695, $p<0.001$ for each), suggesting that excess lipid load is proinflammatory and widely handled by phagocytosis in the IA wall (II), as it is in atherosclerosis [80]. Phagocytes expressing the pan-macrophage scavenger receptor CD68 were the second most numerous cells of inflammatory cells in the IA wall (I). Generally, CD68 action is not significant in tissue response to bacterial or viral pathogens [44], but CD68 has a high affinity for oxidized low-density lipoprotein particles and apoptotic cells, thus showing its importance in the atherosclerotic inflammatory processes of arterial walls [247]. In the IA wall, the $CD68^+$ phagocyte was the dominant foam-cell type in the majority (20 of 36) of IA walls in comparison to $aSMA^+$ or to $CD163^+$ cells (II). Moreover, foam cells in human atherosclerotic plaques have shown a predominance of CD68 over CD163 expression [247]. Therefore, $CD68^+$ macrophages appear important in the primary clearance of lipids from IA walls, as important as they are in atherosclerotic walls.

In addition to foam cells, all IA walls expressed HLA-DR (IV), the major histocompatibility complex class II protein responsible for antigen presentation to T-lymphocytes after phagocytosis [81]. The finding that extensive HLA-DR expression in the IA wall correlated with extensive lipid accumulation: apoB-100, oxidized lipid, and adipophilin ($r=0.455$-0.522, p£0.005), means that lipid intake is likely one of the triggers of HLA-DR expression in the IA wall. The extensive expression of HLA-DR also correlated with high numbers of $CD68^+$ ($r=0.525$, $p=0.001$) and $CD163^+$ ($r=0.422$, $p=0.012$) macrophages, and T lymphocytes ($r=0.413$, $p=0.012$), suggesting their involvement in the acquired immunity response to lipid

clearance from the IA wall. Interestingly, double-stainings revealed that also solitary SMCs, in addition to macrophages, expressed HLA-DR, which may reflect their adaptation to lipid-ingesting cells, similar to the situation in atherosclerotic plaques [81,109].

Adaptive immunity is potentially involved in the protection of the IA wall from atherosclerotic processes also humorally, because in patients carrying unruptured IAs, serum levels of immunoglobulin G antibodies reactive to oxidized lipids are higher than in patients with a history of aneurysmal SAH [72]. In IAs, as well, oxidized lipids may activate the complement system in the presence of CRP [244], as they do in atherosclerosis. In addition, the majority of naturally occurring IgM antibodies are capable of binding to oxidized epitopes, activating the complement system [45], and they are detectable in IAs [47,244]. The humoral or other mechanisms of adaptive immunity were not further assessed in this study, but, based on the presence of T lymphocytes and HLA-DR in the IA wall, adaptive immunity is likely an important support for innate immunity in lipid clearance from the IA wall.

5.5.4 Possible role of macrophages in the IA wall

Degenerated IA walls appear to suffer from a load of waste material, such as lipids, lipoprotein particles, and erythrocyte-remnants including toxic hemoglobin-derived iron. The fundamental role of macrophages is to protect tissues by phagocytozing pathogens and other foreign material from disturbed area and thus supporting the tissue's physiological function [101]. To effectively prevent the retention of harmful material in the arterial wall is the reason for the existence of various subpopulations of macrophages [41,50].

Human macrophages commonly express CD68 and may co-express CD163 as a response to hemoglobin ingestion [66]. Traditionally, macrophages have been classified into proinflammatory M1- and anti-inflammatory M2 subtypes. Of these, the M1 type is activated through Th1 and is predominantly $CD68^+$, whereas the M2 type is activated through Th2 and is predominantly $CD163^+$ [41,66,175]. However, the M1/M2 classification of macrophages may be too much simplified, due to the existence of a dynamic range of differing macrophage subtypes in the human vasculature [66,175,247].

Finn et al. have demonstrated in cultured human monocytes that monocytes exposed to hemoglobin-haptoglobin complexes express CD163, showing resistance to lipid accumulation by upregulating ABCA1 [66]. This hemoglobin-induced population was further characterized as a hemorrhage-induzed macrophage population [26]. In atherosclerotic plaques, these "non-foamy" macrophages were suggested to have locations distinct from $CD68^+$ macrophages, suggesting separate macrophage populations induced by stresses of the local microenvironment [66].

Based on the findings of erythrocytes, microhemorrhages, lipids, and foam cells in the IA wall, it seems likely that similar mechanisms of macrophage polarization may occur also in the IA wall. Most likely, the IA-wall phagocyte population also includes a variety of different macrophage populations with different, but partly overlapping subspecializations. The defensive functions of macrophages in the clearance of lipids and other waste products appear to be supplemented by those of inflammation-adapted SMCs, potentially to compensate for the insufficient function of macrophages. Thus, the essential role of macrophages would be the protection of mural SMCs from toxic lipid- and erythrocyte waste, which may thus be the primary cause of IA wall degeneration and rupture, rather than the cause as being the inflammatory response itself. Therefore, especially the widespread infiltration of the $CD163^+$ macrophages strongly associated with IA wall degeneration and rupture may indicate the potentially destructive effect of erythrocyte accumulation in the IA wall.

5.6 Hemodynamic models and IA remodeling

A subseries of 11 unruptured and 9 ruptured IAs was studied with CTA-derived flow simulations for any correlation between histopathological changes and intraluminal hemodynamic conditions (III). Of the IAs, 4 showed high wall-shear stress (WSS), 7 showed low WSS, and 9 mid-WSS. Neither WSS nor other hemodynamic variables (viscous dissipation, VD, oscillatory shear index, OCI, flow complexity, or flow instability) differed between unruptured and ruptured IAs. However, flow conditions were associated with IA wall structural remodeling and inflammation.

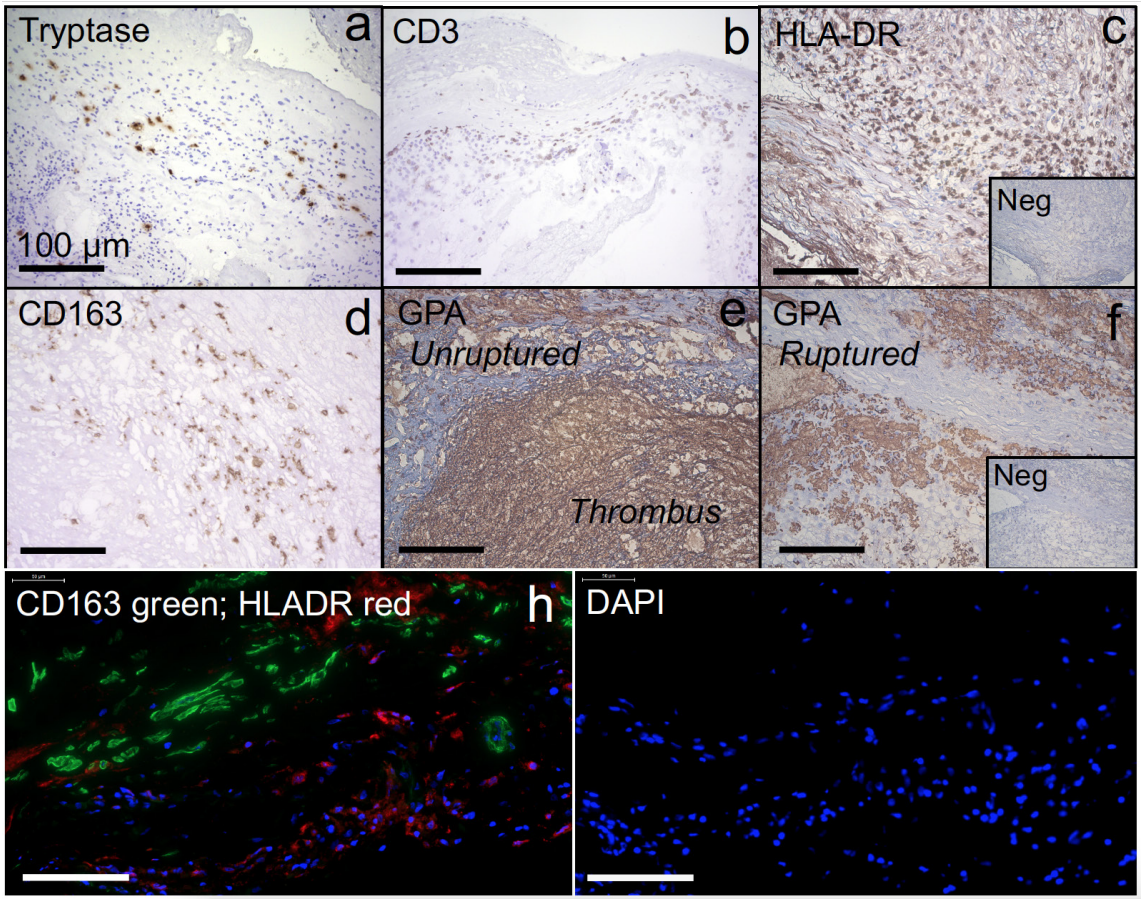

Figure 19. Inflammatory cell infiltration in the Ia wall: a, tryptase^{+} cells, i.e. mast cells; b, CD3^{+} T lymphocytes; c, HLA-DR^{+} inflammatory cells; d, CD163^{+} macrophages. E and f show accumulation of GPA in the IA wall, indicating erythrocytes or their cell membrane fragments. In e, an unruptured and in f, a ruptured IA wall. These images demonstrate erythrocytes in the IA wall independent of IA-rupture status. CD163^{+} macrophages were mainly HLA-DR- in the IA wall, suggesting the hemoglobin-phagocytozing phenotype detectable in AAAs and coronary arteries.

5.6.1 Flow conditions and IA wall remodeling

In the flow-modeled IAs, simple and stabile flows were associated with the 10 type-B walls, indicating the association of such flow conditions with hyperplastic IA walls. In contrast, slow and diffuse flows were associated with the 8 type-C walls, meaning a degenerated, decellularized IA wall structure. Type-B and -C walls also showed a lower OCI than did the 2 type-A walls, suggesting that a less transient flow associated with wall remodeling, whereas multidirectional flows associated with a more linearly organized IA wall composition.

Flow conditions have been studied in a mouse carotid artery by means of a surgically created stenosis [40,191]. In that model, Cheng showed that low and oscillatory WSS induces atherosclerotic plaque formation, whereas particularly low WSS induces large, outward, and vulnerable lesions, but oscillatory shear stress induces more stabile lesions with fibrous caps and a proliferation of SMCs [40]. Pedrigi further demonstrated, in the same mouse model, that the low-WSS-induced vulnerable plaques were located in the prestenotic region of the artery, whereas the complex flow-induced advanced plaques were located in the post-stenotic region of the artery [191]. Apparently, the experimental model of a stenotic artery is not geometrically applicable to the outwards-pouching IA, which can present with a variety of different morphologies. However, based on the variable geometries, histological findings, and flow parameters, it could be assumed that similar flow-induced areas were present regionally in the IA wall. Thus, the different regional flow patterns in the IA lumen, affected by the geometrical shape of the IA pouch, could affect histology in specific regions of the wall.

5.6.1.1 Flow, endothelial erosion, and inflammation in the IAs

The condition of the endothelium was analyzed from 10 flow-modeled IAs, of which 7 lacked intact endothelium. Defective or absent endothelium was associated with non-physiological flows such as low OCI, high vorticity, high VD, and high shear rate ($p=0.020$-0.034). Functioning as a barrier between the arterial wall and the circulation, the endothelium is sensitive to changes in blood flow which affect the morphology, alignment, and function of endothelial cells [54,207]. The altered flow conditions in the

IA lumen may trigger an endothelium-driven proinflammatory signaling cascade [246]. Pedrigi et al. simulated in vitro how a multidirectional (oscillatory) endothelial cell stretch caused increased expression of the proinflammatory mediator NF-kB in the stretched cells [190]. Flow-induced inflammation mediated by NF-kB has been demonstrated in a rodent aneurysm model, and a similar mechanism has been proposed to occur also in human IAs [14]. It is likely that the barrier mechanism of the luminal endothelium in the IAs has become disturbed due to the nonphysiological flow, which could also have triggered endothelial loss and inflammation.

Similar to an endothelial defect, inflammation in the IA walls was associated with high vorticity, high VD, and high shear rate ($p=0.046$ for all). Those IAs with low or high WSS showed a greater number of $CD45^+$ inflammatory cells than did the IAs with mid-WSS. Variability in $CD45^+$ cell distribution was associated with WSS levels in different areas of the IA sac ($p=0.035$), supporting the possibility that focal WSS level may play a role in that area's inflammatory cell infiltration.

5.7 Visualization of erythrocyte remnants with MRI

In MRI, hemosiderin causes a hypointense signal or signal loss, i.e. a susceptibility artifact [60]. Honkanen et al. demonstrated in three giant IAs their MRI sensitivity for Prussian blue-positive iron [91]; in the current study (IV), eleven small IAs were similarly imaged with MRI, using two iron-sensitive sequences [91].

All 11 IAs showed susceptibility artifacts in both T2*-weighted (FLASH) and T2-weighted (RARE) sequences. Their histology showed in all these IAs also hemosiderin deposition, and 10 showed GPA^+ staining; the orientation of 9 IAs was identifiable in MRI, and these were thus included in the histologic comparison. After the correlation of histological specimens with their corresponding MR images (in total 48 MRI-slice-histological section pairs; 3 to 9 per IA), no exact spatial correlation of histology with distribution of the MRI signal in that slice was, however, identifiable.

Challenges in identifying the corresponding specific wall areas

in each MR image and its histological section were in part related to MRI-signal heterogeneity; this did not provide a specific signal pattern in the corresponding histological region of interest, i.e. a GPA^+- or $iron^+$ area of the wall. Furthermore, the smaller sample size of the present IAs in comparison with the earlier series of giant IAs (median length 11 vs. 40 mm and width 10.5 vs. 30 mm) [91] may have predisposed unintentional changes in IA sample orientation in MRI and histology during sample processing, thus further challenging accurate spatial comparison.

Due to current limitations, all MRI and histological section pairs were compared, also irrespective of spatial analysis. Interestingly, extensive GPA accumulation correlated positively with a hyperintense (bright) signal in both RARE ($r=0.444$, $p=0.004$) and FLASH ($r=0.519$, $p=0.001$) sequences of MRI presentation, whereas extensive hemosiderin deposition correlated positively with hypointense (dark) signal ($r=0.373$, $p=0.015$, Spearman) and negatively correlated with a hyperintense signal ($r=-0.404$, $p=0.008$) in the RARE sequence of MRI.

To conclude, this study did not succeed in demonstrating the erythrocyte degradation products in MRI of the IA wall. However, the statistical association found between MRI signal intensity and the presence of erythrocyte degradation products in the IA wall implies that further studies, potentially utilizing high-resolution MRI, could provide more knowledge on the relevance of MRI in visualizing IA wall erythrocyte accumulation and microhemorrhages.

Matsushige et al. recently imaged 7 giant IAs in vivo with 7T MRI, showing high spatial resolution which also allowed visualization of IA wall microstructure [157]. In histological evaluation of 2 of the giant IAs, Prussian blue-positive hemosiderin was located in the adventitial layer and also in the luminal region of the wall adjacent to the thrombus. These same areas showed a hypointense signal in time-of-flight (TOF)-MRA and susceptibility-weighted imaging (SWI) sequences, demonstrating that the MRI presentation can show iron deposition [157]. Thus, high-field MRI up to 7T, in comparison to lower magnetic fields, may serve as a sensitive method for IA wall imaging iron deposition. Wrede et al. compared the images acquired between 7T MR angiography and standard digital subtraction angiography (DSA) in 64 unruptured IAs, proposing the combination of TOF-MRA and magnetization-prepared rapid acquisition

gradient-echo sequences as a promising clinical application for imaging of IAs [257].

Collectively, it appears that MRI techniques have the potential for detailed imaging of IA structure. As the availability of high-field MRI increases, promisingly also smaller IAs can be visualized. Thus, MRI may serve as a tool for evaluating the individual-IA rupture risk, more specifically than does current risk analysis based on IA size, shape, or growth in follow-up. However, first the meaning of various different signal intensities and visualizing enhancements, whether the biomarker of interest is tissue iron or something else, and whether a contrast agent should be used or not, call for elucidation. Histological studies are essential tools to be coupled with radiological imaging in future studies.

5.8 Limitations of the study

For this series of IAs, several limitations should be noted.

Challenges of IA sample collection

Obtaining IA sample tissue material is always limited. First of all, only a portion of all IAs are treated surgically, and those treated endovascularly do not allow any aneurysm tissue sampling. Nor during surgery do circumstances always allow sample collection. The smallest IAs cannot be collected after clipping due to insufficient amount of tissue. Closed with a clip, the neck region of an IA remains in the patient. The present series is therefore quite selected and restricted to those IAs that could be collected with consideration of patient safety and IA size.

Histological autopsy studies of small IAs may be able to supplement the histological analysis, but factors potentially important in IA pathogenesis may be undetectable after death due to tissue autolysis.

Avoiding sample selection bias when using perioperative or other in vivo IA tissue collection techniques is impossible. To study also the wall composition of the smallest IAs, ones likely representative of very early lesions or pre-IAs, will require

development of detailed imaging methods such as high-field MRI. Once enough data exist on visualization of histological changes in imaging studies, it may be possible to extrapolate from comparisons of histological and imaging studies of large IAs to the smallest ones.

Small number of samples

The small series of IAs is, naturally, a shortcoming in terms of weak statistical power, sensitivity to bias, and the likelihood of selection and other confounding coincidences. However, collection of a large IA series is challenging and time-consuming. Although it is important to study large IA series to ensure increased the statistical power of the potential findings, smaller series can provide important new data in a feasible length of time.

Time progress of IA pathogenesis remains unknown

Sample collection is only one moment in time which does not reveal the slow dynamic wall remodeling process that, at the moment of sample resection, may have already lasted years or decades. Thus, the natural history of IAs is still poorly known. To follow the pathogenesis of an IA through histology would require regular biopsies or other methods of tissue collection, all of which are impossible; thus the chronological order of histological changes in the IA wall remains unknown. For the same reason, control tissue from the patients' intracranial arteries is rarely, if ever, available. Importantly, the present research does not reveal causative mechanisms in IA pathogenesis.

To further study the causal connections involved in IA pathogenesis and to place events in a time-line of pathogenesis warrants the best possible experimental models representing human pathogenesis. Meanwhile, when assessing the rupture probability of these human IAs, it seems valuable not to rely only on the known rupture status of a particular IA, since the walls of unruptured IAs may also be rupture-prone. IAs that still were unruptured at the moment of sample collection might have ruptured the following day. Finding those features which may predict wall rupture is therefore vital.

Clinical data may be outdated

The amount of clinical information available concerning each IA patient's risk factors may vary greatly. Here, the clinical data were collected retrospectively from patient medical records which did not always reveal for all patients current or accurate data on smoking status, blood pressure, or cholesterol levels. These are shortcomings that can affect results and final interpretations as to clinical correlations with IA wall histopathology.

One solution for improvement of clinical data collection would be a prospective questionnaire and accurate IA measurements. However, this type of data collection would still miss those patients entering a hospital with acute aneurysmal SAH and receiving emergency surgery for a ruptured IA.

Simplification of heterogenous IA wall structures

Histological analyses were in almost all cases performed at only one sample-section level of the IA block. Since wall composition may be highly heterogenous within one IA, the location of many degenerative factors may also vary within the IA wall. In addition, there may even exist different areas representing different wall types within a single IA section. In those cases, the sample was classified according to the dominant (i.e. the most apparent) wall type. Another option would be to study several histological parameters based on a focal representation of a certain wall type, resulting in several subanalyses for various wall types within one IA sample. This method would have given more detailed data on wall-type-based histologal parameters; it would not, however, have allowed inter-sample analysis and comparisons.

Since no two IA walls are identical, evaluation of individual IAs through imaging and possibly other detailed methods should allow assessment of their individual rupture risks. Histological-sample analysis regionally should find the weakest spot of the wall, which could determine the fate of the entire wall. As knowledge of the histological markers of IA wall fragility accumulates, finding the most rupture-prone focal sites within the IA lesion should also become easier.

The rupture site often undefined

In the histological sections, the actual rupture site in ruptured IAs was neither sought nor identified. The exact orientation of any IA sample during its mounting and freezing and its placement in the cryotome is, indeed, challenging. The site of rupture in the IA macroscopic inspection is not always definite, either. In comparison with an atherosclerotic lesion, an IA may not clearly show any specific region of interest such as the shoulder region in an atherosclerotic plaque. It is most likely, however, that the rupture site is included in the collected IA sample specimen, since Crompton showed already in the 1960s in an autopsy study of 289 SAH patients that most often (84%) an IA ruptures through its apex i.e. the IA fundus [51]. This suggests that in surgically acquired samples, the rupture site will be included in the sample studied.

6 Conclusions

1) Mast cells (MCs) appear in only a minority of IA walls, and when they do, they are scanty. The role of MCs is thus, in general, likely less important in IAs than in extracranial atherosclerotic diseases, where they are important regulators of vascular wall atherogenesis and inflammation. Pro-angiogenic factors of MCs may, however, in this fraction of IA walls contribute to IA wall neovascularization, detectable in nearly half of the walls. Neovessels were associated with hemosiderin deposition, implying their leakiness and subsequent microhemorrhages, which may release hemoglobin-derived pro-oxidative iron in the sIA wall. MC proteases are one potent factor that may contribute to rupture of neovascular newly formed endothelia in sIA walls, thus increasing the likelihood of deleterious intramural microhemorrhages.

2) Lipids accumulate in all IA walls, which also show accumulation of circulatory apoliporoteins. Lipid transport by pro-atherogenic apoB-100-containing lipoprotein particles seems likely to be the major mechanism for IA-wall lipid entry. The macrophages and SMCs in the IA wall show foam cell formation, suggesting clearance

of lipids via phagocytosis. Lipids that have once been phagocytosed, however, appear to end up back in the IA wall's extracellular space, a phenomenon associated with wall rupture. That finding, together with the finding of abnormal accumulation of normally anti-atherogenic apoA-I, suggests the contribution of an impaired ABCA-1–apoA-I-mediated cellular lipid clearance to lipid-laden foam cell death. Such cytotoxic intracellular and extracellular lipid accumulation may thus contribute to IA wall rupture.

3) IA intraluminal hemodynamic conditions are associated with wall remodeling and inflammation. These wall changes may, at least in part, be mediated by endothelial cells that are responsive to vascular-wall shear stress. Pathological flow factors in IAs, obtained from CT-angiography-derived hemodynamic simulations, may serve as a marker for IA wall degeneration, and are thus a potential tool for diagnostics of rupture-prone IAs.

4) Erythrocyte-membrane-component GPA accumulates in degenerated IA walls independent of IA rupture status, implying chronic accumulation of erythrocytes in IA walls. The extent of such accumulation associates with IA wall rupture, suggesting the deleterious effect of erythrocyte breakdown products. Iron-containing hemoglobin, released from lysed erythrocytes, is pro-oxidative and pro-inflammatory. $CD163^{+}$/$HLA\text{-}DR^{-}$ phagocytes are abundant especially in degenerated and ruptured IA walls suggesting a macrophage population specialized in hemoglobin clearance there. A macrophage-derived product of hemoglobin, hemosiderin is detectable by MRI. Here, both hemosiderin and GPA were associated with signal intensity changes in ex vivo MRI, suggesting their role as promising biomarkers for diagnostics of rupture-prone IAs. Neither the areas of hemosiderin accumulation nor those of GPA accumulation were, however, spatially identifiable in ex vivo MR images, suggesting that imaging of small-sized IAs requires further development of methods prior to any clinical application.

7 Summary

The subarachnoid hemorrhage (SAH) is a highly fatal disease threatening all who harbor saccular intracranial aneurysms (IAs). Rupture of the IA wall occurs due to a complex process of IA wall degeneration that tissue-protection mechanisms failed to repair. Only a fraction of IAs rupture during a lifetime, but timely identification of those IAs prone to rupture and demanding surgical or endovascular treatment remains a clinical challenge. Known clinical risk factors for IA formation and rupture, including smoking and high blood pressure, suggest a role for vascular risk factors in IA-wall pathogenesis. Non-physiological blood flow conditions contribute to the formation of atherosclerotic plaques, and likely also of IAs, both typically located in arterial bifurcations. This thesis evaluated the potential role and imaging of hemodynamics and atherosclerotic changes in IAs.

Histopathology of the IAs studied represented a variety of structural wall-remodeling changes accompanied by thrombosis, chronic inflammation, and accumulation of lipids, in line with earlier IA series. These changes were associated also in this series with IA wall degeneration and rupture, demonstrating their clinical importance. The majority of the IAs showed endothelial erosion indicative of loss of the intraluminal barrier.

The endothelial erosion was associated with an abundance

of accumulated circulatory apoB-containing LDL- and other atherogenic lipoproteins. Thus, dysfunctional endothelium may allow increased lipid influx from the circulation into the IA wall as in atherosclerotic diseases. Degenerated IAs showed extensive retention of neutral and oxidized lipids. Especially the extracellular space of degenerated and ruptured IA walls contained an abundance of once-phagocytozed lipid material, likely derived from dead macrophage- and smooth-muscle-cell foam cells. HDL-mediated cellular lipid clearance by the apoA-I-ABCA-1-pathway seemed to occur in the IA wall, but most likely functioned inefficiently. Accumulation of cytotoxic lipid in the IA wall may therefore be a potent mechanism of IA degeneration and rupture.

Degenerated and ruptured IA walls also showed the widespread erythrocyte-membrane component GPA, reflecting wall accumulation of intact erythrocytes or erythrocyte membrane fragments. Organized intraluminal thrombus appeared as the major source of GPA and may thus chronically induce oxidative stress in the IA wall, via the release of hemoglobin from lysed erythrocytes. Neovessels appeared as another potential source of erythrocyte leakage, since some fraction of the IAs showed adjacent iron deposition indicative of microhemorrhages. The role of erythrocyte waste material in the IA wall is potentially deleterious, due to the accumulation of cholesterol-rich atherogenic cell membranes and oxidative heme-derived iron.

A pro-oxidative environment and the presence of hemoglobin were considered to be pro-inflammatory in the IA wall, because among inflammatory cells, macrophages expressing hemoglobin-haptoglobin scavenger receptor $CD163^+$ were most frequent in the wall. Their predominance in the IA wall may result from their upregulation in the presence of hemoglobin, similarly as in atherosclerotic plaques and AAAs. In the IAs, a high number of $CD163^+$ cells associated strongly with wall rupture. $CD68^+$ macrophages also associated with degeneration and rupture, likely playing an important role in the inflammatory response to clearance of various excess substances from the wall. T lymphocytes may have played some role in the adaptive immunity response in the IA wall, although their identities were not further specified in the this study. Mast cells were present in the areas of neovascularization and microhemorrhages, indicating their proangiogenic potential

and their adverse effect on neovascular endothelium in the IA wall, similar to that of atherosclerotic lesions. However, the scattered presence of MCs in only some of the IAs suggest their minor role in IA pathobiology.

In sum, atherogenic processes are apparently present in IAs, indicating that IAs may show mechanisms of degeneration and inflammation similar to those of atherosclerotic lesions. These mechanisms may contribute to IA wall rupture.

Both imaging methods utilized here: computational fluid dynamics and ex vivo MRI, showed changes in correlation with some IA wall changes. Intra-aneurysmal flow models suggested abnormal wall-shear stress in the IA wall as a potential trigger of degenerative changes and inflammation, hypothetically mediated by endothelial injury. Non-contrast ex vivo MRI appeared promising in visualizing degenerative IA wall changes. Finding a relevant marker of high sensitivity and specifity for IA rupture risk requires, however, further work. This study will be, hopefully, of aid in guiding future studies, and development of novel diagnostic methods and preventive treatment for IAs.


Lotti

Acknowledgements

This study originated from the Neurosurgery research group, Biomedicum Helsinki, and the Wihuri Research Institute during 2011-2018. Aneurysm sample collection took place in the Neurosurgery Department of Helsinki University Hospital, Helsinki, Finland, prior to that period. I sincerely thank all those who guided, supported, or inspired me during the journey and anyone who otherwise contributed to this work. You are plentiful.

Especially, my gratitude goes to

Mika Niemelä, the head of the Neurosurgery Department and the Neurosurgery research group. Your positive energy and tireless encouragement have been an essential driving force throughout the project. Despite your busy clinical work, varying hours, or traveling on the other side of the globe, you have always been available for answering promptly any practical questions. Your understanding and support have meant a lot in times when things were challenging and took forever. Working in such a lab atmosphere has been a privilege, for which I'm deeply thankful to you.

Riikka Tulamo and **Juhana Frösen**, my supervisors. You are two super human beings, from whom I have learned hugely about aneurysm pathobiology and the scientific world, and to whom I look up. Riikka, your dedication has been invaluable. You have guided me in all kinds of matters such as how to understand histology, how to present results, how to write articles, and what are the best tips for a holiday trip. You have regularly taken your time also to remind me about the essence of free time and life outside of the lab – it is more than I could ever have expected from a research supervisor. Thank you for your friendship along the way. Juhana, discussions with you have always been extremely inspiring and eye-opening. I admire your knowledge, which is undoubtedly endless. Still, you have shown extensive patience in explaining complicated things and guiding me through many difficult questions. You have the talent to motivate people to work hard and do their best. I sincerely thank you both for this journey, especially Juhana for showing the map of the right path, and Riikka for holding the torch and making sure that we get all the way to the goal.

Petri Kovanen and **Satu Lehti** from Wihuri Research Institute. Our collaboration has been absolutely fruitful. I'm happy for your involvement in one part-project after another, always with new and fresh ideas to bring up. You deserve all credit for what became of this work's atherosclerosis aspect; your expertise and devotion have been pivotal in shaping this project into what it is. I'm grateful for all I have learned from you in our Biomedicum group-writing sessions. Petu, you are a superstar in science. I am impressed by the passion and playfulness you bring into any project you participate in. Satu, your methodological knowledge and biochemistry lessons at a microscope have been important for this work from the start. Having learned from you has given me more confidence to analyze histology that may appear messy. Your calm and practical approach have saved me from many moments of frustration. It has been a delight to learn from the best, for which I cordially thank you both. I could not skip thanking also Petu's wife **Marja-Terttu** for her generousity to let Petu work so late at night for the project, and for honoring our research meetings with her lovely cinnamon rolls, baked with oil to maintain healthy cholesterol levels.

Sami Tetri and **Anne Räisänen-Sokolowski** as the reviewers of this thesis. I highly respect your firm and insightful comments and am thankful for all your input, which significantly improved this thesis.

Tiit Mathiesen; it is a great honor that you have agreed to act as the opponent. I'm looking forward to welcoming you in Helsinki and to our scientific discussion.

All co-authors; without your contribution the project could not have succeeded. I want to express my appreciation to Juha Hernesniemi for his warm, supportive attitude and exceptional surgical skills which enabled aneurysm sample collection. I'm truly thankful to **Salla Kaitainen, Timo Liimatainen,** and **Seppo Ylä-Herttuala,** as well as to **Miriam Lee-Rueckert, Juan Cebral, Anne Robertson, Bong Jae Chung, Fernando Mut, Visa Sippola,** and **Behnam Rezai Jahromi** for their expertise and hard work. I warmly recall **Petri Honkanen**, whose time here was tragically left too short. I'm deeply grateful for our good times in the lab, his friendliness, teachings, and also all helpful technical tricks he shared. Remembering his ideas has been and will be an important root for continuation of the lab's research.

Mikko Mäyränpää and **Petri Mattila** for your excellent help in providing the cerebral artery and tonsil tissues used as controls, and **Anders Paetau**, for your valuable methodological help. Your contribution was significant for the project to succeed.

The Neurosurgery Research group members. I'm particularly thankful to **Aki Laakso**, a senior scientist of the group and an experienced clinician. Your constructive comments and supportive feedback in our lab meeting discussions have been of great importance to this study. I also thank our former lab members **Johan, Emilia, Elisa,** and **Serge** for their great company and good example. Accordingly, I thank fellow-researchers **Antti** and **Henrik A**, and former visiting stars **Henrik B, Arto, Visa, Siiri, Anni**, and **Heikki**, for their vital peer support and lab entertainment. I'm delighted by our current

members **Benkku, Rahul,** and **Vladimir**, and our heartly welcomed new students. It has been a pleasure to work with you all.

Other research colleagues. I warmly thank all lab members of the old Wihuri group for your hospitality and for welcoming me as your lab's regular visitor. Thank you for your invaluable practical and methodological help and for always sharing reagents and a corner of your bench if needed. I thank our fourth-floor neighbors, the Lindsberg lab colleagues as well as the Hematology group's folks for their always cheery chatter. I thank **Olli Mattila** for his helpful advice in the use of the microscope. Colleagues from the Doctoral Programme in Biomedicine, thank you for your precious company and support.

Laboratory technicians **Nancy Lim, Suvi Sokolnicki, Mari Jokinen, Kaisa Laajanen, Susanna Räsänen,** and **Sisko Juutinen** for your excellent technical assistance. Special thanks I want to aim toward Suvi, who thoroughly taught me the method of immunohistochemical staining in Kalliolinnantie lab during the first summer of the project. I thank **Kirsi Weckström, Jessica Knaapila, Ira Kiviniemi,** and Biomedicum Info for secretarial and logistic help.

Carol Norris, whose language revision service is one of a kind. This thesis' presentation improved light-years after your experienced touch. I also thank you for that one dramatic winter night in the snow and the final warm dinner in your house. I have enjoyed following your personalized way of working and fantastic skills in editing scientific texts.

Eveliina Netti and **Eetu Leppälä**, who deserve grateful thanks for this book's appearance. Your team's expertise in layout and Eve's artistic work for covers and all painted illustrations on the pages have completed this book to its fullest. Your talent has inspired and given me strength to do my own part in the preparation of this book. I'm extremely grateful to have such professionals in the family.

My dear friends, who have frequently put all possible research struggles in their proper scale with your presence and simple excellence. I heartly thank all school friends with whom our friendship has only deepened; I respect you as colleagues and adore you as friends. I can't resist a happy smile when recalling times after school with our legendary clinic group, our deathly laughs around a dinner table and those many nights when you sweetly put aside food for me when I had to stay late in the lab. I feel happiness about the wonderful community we make today, with a growing number of people and many traditions of all getting along together. I'm also thankful to some precious dance- and ashtanga yoga circles in Helsinki and abroad for providing a safe zone where I can always go for balance, and where I feel that a part of me belongs.

My Relatives. I'm sincerely grateful for all the support I've received from you. I'm lucky for having around me such a big extended family, who spends quite a lot of time together. It feels grounding to know that many generations have gathered in Mäntyniemi for Midsummer celebrations for over 30 years. Your presence is a gift not to be taken for granted. Special well-deserved thanks go to my god-parents **Airi, Sepi, Eero, Virpi, Sari,** and **Jopi** for their steady support and care. I thank our god-sons **Pirkka** and **Perttu** for many play days together and hope that they also get inspired about science someday. I'm also greatly thankful to the whole family **Helminen** for their support. I value our times together in both Kirkkonummi and London residences.

Family. I'm profoundly thankful to my parents **Hanna** and **Seppo** for their part in everything. You have shown with your own example of a positive and hardworking attitude that there is no giving up in life; I deeply respect you both for that. You also have encouraged me to achieve things I want, without pushing me to follow any potential dreams of your own. Thank you for your open-mindedness and priceless support. I could not have asked for better parents. I thank my dream-sister **Eve**. I admire you simply as a person. You are one of the funniest! We share so many interests that it is always a pleasure to spend time with you. Thank you for all of your help and for our friendship. I'm also grateful to **Eetu** and the cats **Merri** and **Pippin** for their support.

Anttu. You have been there for me in exactly the way I have needed, not only during these years, but always. You have lifted me up from many situations of despair without judging whether they are big or tiny. You have floated with me when life has been nice and easy and shared many unforgettable travels. You have lately waked me up in the early morning with your coffee service, not only when I "needed" it, but every day. That's how you are. I know I'm spoiled by you. What matters to me is that you are my superhero and I love you endlessly. Getting this book out of the house means more time for us. I have waited for that.

This work received financial support from Helsinki University Hospital EVO grants, Kuopio University Hospital research grants, the Doctoral Programme in Biomedicine of the University of Helsinki funding, the Finnish Medical Foundation, the Orion Research Foundation, the Petri Honkanen Foundation, and the Wihuri Research Institute maintained by the Jenny and Antti Wihuri Foundation.

References

1. Albarran-Juarez J, Kaur H, Grimm M, Offermanns S, Wettschureck N (2016) Lineage tracing of cells involved in atherosclerosis. Atherosclerosis 251: 445-453.

2. Alfakry H, Malle E, Koyani CN, Pussinen PJ, Sorsa T (2016) Neutrophil proteolytic activation cascades: a possible mechanistic link between chronic periodontitis and coronary heart disease. Innate Immun 22: 85-99.

3. Alg VS, Sofat R, Houlden H, Werring DJ (2013) Genetic risk factors for intracranial aneurysms: a meta-analysis in more than 116,000 individuals. Neurology 80: 2154-2165.

4. Algra AM, Klijn CJ, Helmerhorst FM, Algra A, Rinkel GJ (2012) Female risk factors for subarachnoid hemorrhage: a systematic review. Neurology 79: 1230-1236.

5. Allahverdian S, Chehroudi AC, McManus BM, Abraham T, Francis GA (2014) Contribution of intimal smooth muscle cells to cholesterol accumulation and macrophage-like cells in human atherosclerosis. Circulation 129: 1551-1559.

6. Andreeva ER, Pugach IM, Orekhov AN (1997) Subendothelial smooth muscle cells of human aorta express macrophage antigen in situ and in vitro. Atherosclerosis 135: 19-27.

7. Annema W, von Eckardstein A, Kovanen PT (2015) HDL and atherothrombotic vascular disease. Handb Exp Pharmacol 224: 369-403.

8. Aoki T, Kataoka H, Ishibashi R, Nozaki K, Hashimoto N (2008) Simvastatin suppresses the progression of experimentally induced cerebral aneurysms in rats. Stroke 39: 1276-1285.

9. Aoki T, Kataoka H, Nishimura M, Ishibashi R, Morishita R, Miyamoto S (2010) Ets-1 promotes the progression of cerebral aneurysm by inducing the expression of MCP-1 in vascular smooth muscle cells. Gene Ther 17: 1117-1123.

10. Aoki T, Kataoka H, Ishibashi R, Nozaki K, Egashira K, Hashimoto N (2009) Impact of monocyte chemoattractant protein-1 deficiency on cerebral aneurysm formation. Stroke 40: 942-951.

11. Aoki T, Kataoka H, Ishibashi R, Nakagami H, Nozaki K, Morishita R, Hashimoto N (2009) Pitavastatin suppresses formation and progression of cerebral aneurysms through inhibition of the nuclear factor kappaB pathway. Neurosurgery 64: 357-65.

12. Aoki T, Frösen J, Fukuda M, Bando K, Shioi G, Tsuji K, Ollikainen E, Nozaki K, Laakkonen J, Narumiya S (2017) Prostaglandin E2-EP2-NF-kappaB signaling in macrophages as a potential therapeutic target for intracranial aneurysms. Sci Signal 2017 Feb 7;10(465).

13. Aoki T, Kataoka H, Shimamura M, Nakagami H, Wakayama K, Moriwaki T, Ishibashi R, Nozaki K, Morishita R, Hashimoto N (2007) NF-kappaB is a key mediator of cerebral aneurysm formation. Circulation 116: 2830-2840.

14. Aoki T, Nishimura M, Matsuoka T, Yamamoto K, Furuyashiki T, Kataoka H, Kitaoka S, Ishibashi R, Ishibazawa A, Miyamoto S, Morishita R, Ando J, Hashimoto N, Nozaki K, Narumiya S (2011) PGE(2) -EP(2) signalling in endothelium is activated by haemodynamic stress and induces cerebral aneurysm through an amplifying loop via NF-kappaB. Br J Pharmacol 163: 1237-1249.

15. Arsenault BJ, Boekholdt SM, Kastelein JJ (2011) Lipid parameters for measuring risk of cardiovascular disease. Nat Rev Cardiol 8: 197-206.

16. Backes D, Rinkel GJ, Laban KG, Algra A, Vergouwen MD (2016) Patient- and Aneurysm-Specific Risk Factors for Intracranial Aneurysm Growth: A Systematic Review and Meta-Analysis. Stroke 47: 951-957.

17. Bak AA, Grobbee DE (1990) A randomized study on coffee and blood pressure. J Hum Hypertens 4: 259-264.

18. Ballas SK, Krasnow SH (1980) Structure of erythrocyte membrane and its transport functions. Ann Clin Lab Sci 10: 209-219.

19. Bekelis K, Smith J, Zhou W, MacKenzie TA, Roberts DW, Skinner J, Morden NE (2015) Statins and subarachnoid hemorrhage in Medicare patients with unruptured cerebral aneurysms. Int J Stroke 10 Suppl A100: 38-45.

20. Berge J, Blanco P, Rooryck C, Boursier R, Marnat G, Gariel F, Wavasseur T, Desal H, Dousset V (2016) Understanding flow patterns and inflammatory status in intracranial aneurysms: Towards a personalized medicine. J Neuroradiol 43: 141-147.

21. Bhullar IS, Li YS, Miao H, Zandi E, Kim M, Shyy JY, Chien S (1998) Fluid shear stress activation of IkappaB kinase is integrin-dependent. J Biol Chem 273: 30544-30549.

22. Blok KM, Rinkel GJ, Majoie CB, Hendrikse J, Braaksma M, Tijssen CC, Wong YY, Hofmeijer J, Extercatte J, Kerklaan B, Schreuder TH, ten Holter S, Verheul F, Harlaar L, Pruissen DM, Kwa VI, Brouwers PJ, Remmers MJ, Schonewille WJ, Kruyt ND, Vergouwen MD (2015) CT within 6 hours of headache onset to rule out subarachnoid hemorrhage in nonacademic hospitals. Neurology 84: 1927-1932.

23. Bot I, van Berkel TJ, Biessen EA (2008) Mast cells: pivotal players in cardiovascular diseases. Curr Cardiol Rev 4: 170-178.

24. Bot I, de Jager SC, Zernecke A, Lindstedt KA, van Berkel TJ, Weber C, Biessen EA (2007) Perivascular mast cells promote atherogenesis and induce plaque destabilization in apolipoprotein E-deficient mice. Circulation 115: 2516-2525.

25. Boulouis G, Rodriguez-Regent C, Rasolonjatovo EC, Ben Hassen W, Trystram D, Edjlali-Goujon M, Meder JF, Oppenheim C, Naggara O (2017) Unruptured intracranial aneurysms: An updated review of current concepts for risk factors, detection and management. Rev Neurol (Paris). 2017 Nov;173(9):542-551.

26. Boyle JJ, Harrington HA, Piper E, Elderfield K, Stark J, Landis RC, Haskard DO (2009) Coronary intraplaque hemorrhage evokes a novel atheroprotective macrophage phenotype. Am J Pathol 174: 1097-1108.

27. Brisman JL, Song JK, Newell DW (2006) Cerebral aneurysms. N Engl J Med 355: 928-939.

28. Broderick JP, Viscoli CM, Brott T, Kernan WN, Brass LM, Feldmann E, Morgenstern LB, Wilterdink JL, Horwitz RI, Hemorrhagic Stroke Project Investigators (2003) Major risk factors for aneurysmal subarachnoid hemorrhage in the young are modifiable. Stroke 34: 1375-1381.

29. Bromberg JE, Rinkel GJ, Algra A, van Duyn CM, Greebe P, Ramos LM, van Gijn J (1995) Familial subarachnoid hemorrhage: distinctive features and patterns of inheritance. Ann Neurol 38: 929-934.

30. Brown MS, Goldstein JL (1986) A receptor-mediated pathway for cholesterol homeostasis. Science 232: 34-47.

31. Brown MS, Kovanen PT, Goldstein JL (1981) Regulation of plasma cholesterol by lipoprotein receptors. Science 212: 628-635.

32. Bruno G, Todor R, Lewis I, Chyatte D (1998) Vascular extracellular matrix remodeling in cerebral aneurysms. J Neurosurg 89: 431-440.

33. Buchanan MR, Hirsh J (1986) Effect of aspirin on hemostasis and thrombosis. N Engl Reg Allergy Proc 7: 26-31.

34. Calcagno C, Ramachandran S, Millon A, Robson PM, Mani V, Fayad Z (2013) Gadolinium-Based Contrast Agents for Vessel Wall Magnetic Resonance Imaging (MRI) of Atherosclerosis. Curr Cardiovasc Imaging Rep 6: 11-24.

35. Can A, Castro VM, Ozdemir YH, Dagen S, Dligach D, Finan S, Yu S, Gainer V, Shadick NA, Savova G, Murphy S, Cai T, Weiss ST, Du R (2017) Alcohol Consumption and Aneurysmal Subarachnoid Hemorrhage. Transl Stroke Res. 2018 Feb;9(1):13-19.

36. Cebral JR, Castro MA, Putman CM, Alperin N (2008) Flow-area relationship in internal carotid and vertebral arteries. Physiol Meas 29: 585-594.

37. Cebral JR, Castro MA, Appanaboyina S, Putman CM, Millan D, Frangi AF (2005) Efficient pipeline for image-based patient-specific analysis of cerebral aneurysm hemodynamics: technique and sensitivity. IEEE Trans Med Imaging 24: 457-467.

38. Cecchi E, Giglioli C, Valente S, Lazzeri C, Gensini GF, Abbate R, Mannini L (2011) Role of hemodynamic shear stress in cardiovascular disease. Atherosclerosis 214: 249-256.

39. Chaabane C, Coen M, Bochaton-Piallat ML (2014) Smooth muscle cell phenotypic switch: implications for foam cell formation. Curr Opin Lipidol 25: 374-379.

40. Cheng C, Tempel D, van Haperen R, van der Baan A, Grosveld F, Daemen MJ, Krams R, de Crom R (2006) Atherosclerotic lesion size and vulnerability are determined by patterns of fluid shear stress. Circulation 113: 2744-2753.

41. Chinetti-Gbaguidi G, Colin S, Staels B (2014) Macrophage subsets in atherosclerosis. Nat Rev Cardiol. 2015 Jan;12(1):10-7.

42. Chistiakov DA, Orekhov AN, Bobryshev YV (2016) Immune-inflammatory responses in atherosclerosis: Role of an adaptive immunity mainly driven by T and B cells. Immunobiology 221: 1014-1033.

43. Chistiakov DA, Melnichenko AA, Orekhov AN, Bobryshev YV (2017) How do macrophages sense modified low-density lipoproteins? Int J Cardiol 230: 232-240.

44. Chistiakov DA, Killingsworth MC, Myasoedova VA, Orekhov AN, Bobryshev YV (2017) CD68/ macrosialin: not just a histochemical marker. Lab Invest 97: 4-13.

45. Chou MY, Fogelstrand L, Hartvigsen K, Hansen LF, Woelkers D, Shaw PX, Choi J, Perkmann T, Backhed F, Miller YI, Horkko S, Corr M, Witztum JL, Binder CJ (2009) Oxidation-specific epitopes are dominant targets of innate natural antibodies in mice and humans. J Clin Invest 119: 1335-1349.

46. Chu Y, Wilson K, Gu H, Wegman-Points L, Dooley SA, Pierce GL, Cheng G, Pena Silva RA, Heistad DD, Hasan D (2015) Myeloperoxidase is increased in human cerebral aneurysms and increases formation and rupture of cerebral aneurysms in mice. Stroke 46: 1651-1656.

47. Chyatte D, Bruno G, Desai S, Todor DR (1999) Inflammation and intracranial aneurysms. Neurosurgery 45: 1137-46.

48. Clarke M (2008) Systematic review of reviews of risk factors for intracranial aneurysms. Neuroradiology 50: 653-664.

49. Coen M, Burkhardt K, Bijlenga P, Gabbiani G, Schaller K, Kovari E, Rufenacht DA, Ruiz DS, Pizzolato G, Bochaton-Piallat ML (2013) Smooth muscle cells of human intracranial aneurysms assume phenotypic features similar to those of the atherosclerotic plaque. Cardiovasc Pathol 22: 339-344.

50. Colin S, Chinetti-Gbaguidi G, Staels B (2014) Macrophage phenotypes in atherosclerosis. Immunol Rev 262: 153-166.

51. Crompton MR (1966) Mechanism of growth and rupture in cerebral berry aneurysms. Br Med J 1: 1138-1142.

52. Damgaard C, Kantarci A, Holmstrup P, Hasturk H, Nielsen CH, Van Dyke TE (2016) Porphyromonas gingivalis-induced production of reactive oxygen species, tumor necrosis factor-alpha, interleukin-6, CXCL8 and CCL2 by neutrophils from localized aggressive periodontitis and healthy donors: modulating actions of red blood cells and resolvin E1. J Periodontal Res. 2017 Apr;52(2):246-254.

53. Daugherty A, Dunn JL, Rateri DL, Heinecke JW (1994) Myeloperoxidase, a catalyst for lipoprotein oxidation, is expressed in human atherosclerotic lesions. J Clin Invest 94: 437-444.

54. Davies PF (1995) Flow-mediated endothelial mechanotransduction. Physiol Rev 75: 519-560.

55. de Rooij NK, Linn FH, van der Plas JA, Algra A, Rinkel GJ (2007) Incidence of subarachnoid haemorrhage: a systematic review with emphasis on region, age, gender and time trends. J Neurol Neurosurg Psychiatry 78: 1365-1372.

56. De Spiegelaere W, Casteleyn C, Van den Broeck W, Plendl J, Bahramsoltani M, Simoens P, Djonov V, Cornillie P (2012) Intussusceptive angiogenesis: a biologically relevant form of angiogenesis. J Vasc Res 49: 390-404.

57. Delbosc S, Rouer M, Alsac JM, Louedec L, Al Shoukr F, Rouzet F, Michel JB, Meilhac O (2016) High-density lipoprotein therapy inhibits Porphyromonas gingivalis-induced abdominal aortic aneurysm progression. Thromb Haemost 115: 789-799.

58. Dunkelberger JR, Song WC (2010) Complement and its role in innate and adaptive immune responses. Cell Res 20: 34-50.

59. Faleiro LC, Machado CR, Gripp A,Jr, Resende RA, Rodrigues PA (1981) Cerebral vasospasm: presence of mast cells in human cerebral arteries after aneurysm rupture. J Neurosurg 54: 733-735.

60. Fazekas F, Kleinert R, Roob G, Kleinert G, Kapeller P, Schmidt R, Hartung HP (1999) Histopathologic analysis of foci of signal loss on gradient-echo T2*-weighted MR images in patients with spontaneous intracerebral hemorrhage: evidence of microangiopathy-related microbleeds. AJNR Am J Neuroradiol 20: 637-642.

61. Feigin V, Parag V, Lawes CM, Rodgers A, Suh I, Woodward M, Jamrozik K, Ueshima H, Asia Pacific Cohort Studies Collaboration (2005) Smoking and elevated blood pressure are the most important risk factors for subarachnoid hemorrhage in the Asia-Pacific region: an overview of 26 cohorts involving 306,620 participants. Stroke 36: 1360-1365.

62. Feigin VL, Rinkel GJ, Lawes CM, Algra A, Bennett DA, van Gijn J, Anderson CS (2005) Risk factors for subarachnoid hemorrhage: an updated systematic review of epidemiological studies. Stroke 36: 2773-2780.

63. Feil S, Fehrenbacher B, Lukowski R, Essmann F, Schulze-Osthoff K, Schaller M, Feil R (2014) Transdifferentiation of vascular smooth muscle cells to macrophage-like cells during atherogenesis. Circ Res 115: 662-667.

64. Fessler RD, Esshaki CM, Stankewitz RC, Johnson RR, Diaz FG (1997) The neurovascular complications of cocaine. Surg Neurol 47: 339-345.

65. Finlay HM, Whittaker P, Canham PB (1998) Collagen organization in the branching region of human brain arteries. Stroke 29: 1595-1601.

66. Finn AV, Nakano M, Polavarapu R, Karmali V, Saeed O, Zhao X, Yazdani S, Otsuka F, Davis T, Habib A, Narula J, Kolodgie FD, Virmani R (2012) Hemoglobin directs macrophage differentiation and prevents foam cell formation in human atherosclerotic plaques. J Am Coll Cardiol 59: 166-177.

67. Freeman AF, Crawford SE, Cornwall ML, Garcia FL, Shulman ST, Rowley AH (2005) Angiogenesis in fatal acute Kawasaki disease coronary artery and myocardium. Pediatr Cardiol 26: 578-584.

68. Frösen J (2014) Smooth muscle cells and the formation, degeneration, and rupture of saccular intracranial aneurysm wall--a review of current pathophysiological knowledge. Transl Stroke Res 5: 347-356.

69. Frösen J, Piippo A, Paetau A, Kangasniemi M, Niemelä M, Hernesniemi J, Jääskeläinen J (2006) Growth factor receptor expression and remodeling of saccular cerebral artery aneurysm walls: implications for biological therapy preventing rupture. Neurosurgery 58: 534-41.

70. Frösen J, Piippo A, Paetau A, Kangasniemi M, Niemelä M, Hernesniemi J, Jääskeläinen J (2004) Remodeling of saccular cerebral artery aneurysm wall is associated with rupture: histological analysis of 24 unruptured and 42 ruptured cases. Stroke 35: 2287-2293.

71. Frösen J, Tulamo R, Paetau A, Laaksamo E, Korja M, Laakso A, Niemelä M, Hernesniemi J (2012) Saccular intracranial aneurysm: pathology and mechanisms. Acta Neuropathol 123: 773-786.

72. Frösen J, Tulamo R, Heikura T, Sammalkorpi S, Niemelä M, Hernesniemi J, Levonen AL, Hörkkö S, Ylä-Herttuala S (2013) Lipid accumulation, lipid oxidation, and low plasma levels of acquired antibodies against oxidized lipids associate with degeneration and rupture of the intracranial aneurysm wall. Acta Neuropathol Commun 1: 71-5960-1-71.

73. Goldstein JL, Brown MS (1977) The low-density lipoprotein pathway and its relation to atherosclerosis. Annu Rev Biochem 46: 897-930.

74. Gomez D, Owens GK (2012) Smooth muscle cell phenotypic switching in atherosclerosis. Cardiovasc Res 95: 156-164.

75. Gounis MJ, van der Bom IM, Wakhloo AK, Zheng S, Chueh JY, Kuhn AL, Bogdanov AA,Jr (2015) MR imaging of myeloperoxidase activity in a model of the inflamed aneurysm wall. AJNR Am J Neuroradiol 36: 146-152.

76. Gounis MJ, Vedantham S, Weaver JP, Puri AS, Brooks CS, Wakhloo AK, Bogdanov AA,Jr (2014) Myeloperoxidase in human intracranial aneurysms: preliminary evidence. Stroke 45: 1474-1477.

77. Greving JP, Wermer MJ, Brown RD,Jr, Morita A, Juvela S, Yonekura M, Ishibashi T, Torner JC, Nakayama T, Rinkel GJ, Algra A (2014) Development of the PHASES score for prediction of risk of rupture of intracranial aneurysms: a pooled analysis of six prospective cohort studies. Lancet Neurol 13: 59-66.

78. Gross BA, Ropper AE, Du R (2012) Cerebral dural arteriovenous fistulas and aneurysms. Neurosurg Focus. 2012 May;32(5):E2.

79. Gross BA, Rosalind Lai PM, Frerichs KU, Du R (2014) Aspirin and aneurysmal subarachnoid hemorrhage. World Neurosurg 82: 1127-1130.

80. Hansson GK (2009) Atherosclerosis--an immune disease: The Anitschkov Lecture 2007. Atherosclerosis 202: 2-10.

81. Hansson GK, Jonasson L (2009) The discovery of cellular immunity in the atherosclerotic plaque. Arterioscler Thromb Vasc Biol 29: 1714-1717.

82. Hansson GK, Libby P (2006) The immune response in atherosclerosis: a double-edged sword. Nat Rev Immunol 6: 508-519.

83. Hasan D, Chalouhi N, Jabbour P, Hashimoto T (2012) Macrophage imbalance (M1 vs. M2) and upregulation of mast cells in wall of ruptured human cerebral aneurysms: preliminary results. J Neuroinflammation 9: 222-2094-9-222.

84. Hasan D, Chalouhi N, Jabbour P, Dumont AS, Kung DK, Magnotta VA, Young WL, Hashimoto T, Winn HR, Heistad D (2012) Early change in ferumoxytol-enhanced magnetic resonance imaging signal suggests unstable human cerebral aneurysm: a pilot study. Stroke 43: 3258-3265.

85. Hasan DM, Mahaney KB, Brown RD,Jr, Meissner I, Piepgras DG, Huston J, Capuano AW, Torner JC, International Study of Unruptured Intracranial Aneurysms Investigators (2011) Aspirin as a promising agent for decreasing incidence of cerebral aneurysm rupture. Stroke 42: 3156-3162.

86. He L, Gao J, Thomas AJ, Fusco MR, Ogilvy CS (2015) Disappearance of a Ruptured Distal Flow-Related Aneurysm after Arteriovenous Malformation Nidal Embolization. World Neurosurg 84: 1496. e1-1496.e6.

87. Heid HW, Moll R, Schwetlick I, Rackwitz HR, Keenan TW (1998) Adipophilin is a specific marker of lipid accumulation in diverse cell types and diseases. Cell Tissue Res 294: 309-321.

88. Hermiston ML, Xu Z, Weiss A (2003) CD45: a critical regulator of signaling thresholds in immune cells. Annu Rev Immunol 21: 107-137.

89. Hoff HH (1972) Human intracranial atherosclerosis. A histochemical and ultrastructural study of gross fatty steak lesions. Am J Pathol 69: 421-438.

90. Hoh BL, Hosaka K, Downes DP, Nowicki KW, Wilmer EN, Velat GJ, Scott EW (2014) Stromal cell-derived factor-1 promoted angiogenesis and inflammatory cell infiltration in aneurysm walls. J Neurosurg 120: 73-86.

91. Honkanen P, Frösen JK, Abo-Ramadan U, Hernesniemi JA, Niemelä MR (2014) Visualization of luminal thrombosis and mural Iron accumulation in giant aneurysms with Ex vivo 4.7T magnetic resonance imaging. Surg Neurol Int 5: 74-7806.132960.

92. Hostettler IC, Alg VS, Shahi N, Jichi F, Bonner S, Walsh D, Bulters D, Kitchen N, Brown MM, Houlden H, Grieve J, Werring DJ, Genetics and Observational Subarachnoid Haemorrhage (GOSH) Study investigators (2017) Characteristics of Unruptured Compared to Ruptured Intracranial Aneurysms: A Multicenter Case-Control Study. Neurosurgery 2017 Jul 25.

93. Huang Y, DiDonato JA, Levison BS, Schmitt D, Li L, Wu Y, Buffa J, Kim T, Gerstenecker GS, Gu X, Kadiyala CS, Wang Z, Culley MK, Hazen JE, Didonato AJ, Fu X, Berisha SZ, Peng D, Nguyen TT, Liang S, Chuang CC, Cho L, Plow EF, Fox PL, Gogonea V, Tang WH, Parks JS, Fisher EA, Smith JD, Hazen SL (2014) An abundant dysfunctional apolipoprotein A1 in human atheroma. Nat Med 20: 193-203.

94. Huttunen T, von und zu Fraunberg M, Frösen J, Lehecka M, Tromp G, Helin K, Koivisto T, Rinne J, Ronkainen A, Hernesniemi J, Jääskeläinen JE (2010) Saccular intracranial aneurysm disease: distribution of site, size, and age suggests different etiologies for aneurysm formation and rupture in 316 familial and 1454 sporadic eastern Finnish patients. Neurosurgery 66: 631-8.

95. Inagawa T (2010) Risk factors for the formation and rupture of intracranial saccular aneurysms in Shimane, Japan. World Neurosurg 73: 155-64; discussion e23.

96. Ingall T, Asplund K, Mähönen M, Bonita R (2000) A multinational comparison of subarachnoid hemorrhage epidemiology in the WHO MONICA stroke study. Stroke 31: 1054-1061.

97. International Study of Unruptured Intracranial Aneurysms Investigators (1998) Unruptured intracranial aneurysms--risk of rupture and risks of surgical intervention. N Engl J Med 339: 1725-1733.

98. Isaksen J, Egge A, Waterloo K, Romner B, Ingebrigtsen T (2002) Risk factors for aneurysmal subarachnoid haemorrhage: the Tromso study. J Neurol Neurosurg Psychiatry 73: 185-187.

99. Ishibashi R, Aoki T, Nishimura M, Hashimoto N, Miyamoto S (2010) Contribution of mast cells to cerebral aneurysm formation. Curr Neurovasc Res 7: 113-124.

100. Ishii T, Itoh K, Sato H, Bannai S (1999) Oxidative stress-inducible proteins in macrophages. Free Radic Res 31: 351-355.

101. Iwasaki A, Medzhitov R (2010) Regulation of adaptive immunity by the innate immune system. Science 327: 291-295.

102. Jalava I, Pyysalo L, Alanen M, Snicker O, Öhman J, Ronkainen A (2017) Regional differences in the incidence of aneurysmal subarachnoid haemorrhage in Finland. Acta Neurochir (Wien). 2017 Sep;159(9):1657-1662.

103. James JE (1997) Is habitual caffeine use a preventable cardiovascular risk factor? Lancet 349: 279-281.

104. Jamous MA, Nagahiro S, Kitazato KT, Tamura T, Aziz HA, Shono M, Satoh K (2007) Endothelial injury and inflammatory response induced by hemodynamic changes preceding intracranial aneurysm formation: experimental study in rats. J Neurosurg 107: 405-411.

105. Jayaraman T, Berenstein V, Li X, Mayer J, Silane M, Shin YS, Niimi Y, Kilic T, Gunel M, Berenstein A (2005) Tumor necrosis factor alpha is a key modulator of inflammation in cerebral aneurysms. Neurosurgery 57: 558-64; discussion 558-64.

106. Jessup W, Mander EL, Dean RT (1992) The intracellular storage and turnover of apolipoprotein B of oxidized LDL in macrophages. Biochim Biophys Acta 1126: 167-177.

107. Jeziorska M, Woolley DE (1999) Local neovascularization and cellular composition within vulnerable regions of atherosclerotic plaques of human carotid arteries. J Pathol 188: 189-196.

108. Johnston SC, Colford JM,Jr, Gress DR (1998) Oral contraceptives and the risk of subarachnoid hemorrhage: a meta-analysis. Neurology 51: 411-418.

109. Jonasson L, Holm J, Skalli O, Gabbiani G, Hansson GK (1985) Expression of class II transplantation antigen on vascular smooth muscle cells in human atherosclerosis. J Clin Invest 76: 125-131.

110. Juvela S, Korja M (2017) Intracranial Aneurysm Parameters for Predicting a Future Subarachnoid Hemorrhage: A Long-Term Follow-up Study. Neurosurgery. 2017 Sep 1;81(3):432-440.

111. Juvela S, Poussa K, Lehto H, Porras M (2013) Natural history of unruptured intracranial aneurysms: a long-term follow-up study. Stroke 44: 2414-2421.

112. Kaartinen M, Penttilä A, Kovanen PT (1996) Mast cells accompany microvessels in human coronary atheromas: implications for intimal neovascularization and hemorrhage. Atherosclerosis 123: 123-131.

113. Kanbe N, Kurosawa M, Miyachi Y, Kanbe M, Kempuraj D, Tachimoto H, Saito H (1998) Carnoy's fixative reduces the number of chymase-positive cells in immunocytochemical staining of cord-blood-derived human cultured mast cells. Allergy 53: 981-985.

114. Karakas M, Koenig W (2012) Myeloperoxidase production by macrophage and risk of atherosclerosis. Curr Atheroscler Rep 14: 277-283.

115. Kataoka H (2015) Molecular mechanisms of the formation and progression of intracranial aneurysms. Neurol Med Chir (Tokyo) 55: 214-229.

116. Kataoka K, Taneda M, Asai T, Kinoshita A, Ito M, Kuroda R (1999) Structural fragility and inflammatory response of ruptured cerebral aneurysms. A comparative study between ruptured and unruptured cerebral aneurysms. Stroke 30: 1396-1401.

117. Kawabori S, Denburg JA, Schwartz LB, Irani AA, Wong D, Jordana G, Evans S, Dolovich J (1992) Histochemical and immunohistochemical characteristics of mast cells in nasal polyps. Am J Respir Cell Mol Biol 6: 37-43.

118. Kleinloog R, de Mul N, Verweij BH, Post JA, Rinkel GJE, Ruigrok YM (2017) Risk Factors for Intracranial Aneurysm Rupture: A Systematic Review. Neurosurgery. 2018 Apr 1;82(4):431-440.

119. Kolb S, Vranckx R, Huisse MG, Michel JB, Meilhac O (2007) The phosphatidylserine receptor mediates phagocytosis by vascular smooth muscle cells. J Pathol 212: 249-259.

120. Kolodgie FD, Gold HK, Burke AP, Fowler DR, Kruth HS, Weber DK, Farb A, Guerrero LJ, Hayase M, Kutys R, Narula J, Finn AV, Virmani R (2003) Intraplaque hemorrhage and progression of coronary atheroma. N Engl J Med 349: 2316-2325.

121. Korja M, Kaprio J (2016) Controversies in epidemiology of intracranial aneurysms and SAH. Nat Rev Neurol 12: 50-55.

122. Korja M, Lehto H, Juvela S (2014) Lifelong rupture risk of intracranial aneurysms depends on risk factors: a prospective Finnish cohort study. Stroke 45: 1958-1963.

123. Korja M, Lehto H, Juvela S, Kaprio J (2016) Incidence of subarachnoid hemorrhage is decreasing together with decreasing smoking rates. Neurology 87: 1118-1123.

124. Korja M, Silventoinen K, McCarron P, Zdravkovic S, Skytthe A, Haapanen A, de Faire U, Pedersen NL, Christensen K, Koskenvuo M, Kaprio J, GenomEUtwin Project (2010) Genetic epidemiology of spontaneous subarachnoid hemorrhage: Nordic Twin Study. Stroke 41: 2458-2462.

125. Kosierkiewicz TA, Factor SM, Dickson DW (1994) Immunocytochemical studies of atherosclerotic lesions of cerebral berry aneurysms. J Neuropathol Exp Neurol 53: 399-406.

126. Koskinen LO, Blomstedt PC (2006) Smoking and non-smoking tobacco as risk factors in subarachnoid haemorrhage. Acta Neurol Scand 114: 33-37.

127. Kotowski M, Naggara O, Darsaut TE, Nolet S, Gevry G, Kouznetsov E, Raymond J (2013) Safety and occlusion rates of surgical treatment of unruptured intracranial aneurysms: a systematic review and meta-analysis of the literature from 1990 to 2011. J Neurol Neurosurg Psychiatry 84: 42-48.

128. Kovanen PT (2009) Mast cells in atherogenesis: actions and reactions. Curr Atheroscler Rep 11: 214-219.

129. Kovanen PT (2007) Mast cells: multipotent local effector cells in atherothrombosis. Immunol Rev 217: 105-122.

130. Kristiansen M, Graversen JH, Jacobsen C, Sonne O, Hoffman HJ, Law SK, Moestrup SK (2001) Identification of the haemoglobin scavenger receptor. Nature 409: 198-201.

131. Krystel-Whittemore M, Dileepan KN, Wood JG (2016) Mast Cell: A Multi-Functional Master Cell. Front Immunol. 2016 Jan 6;6:620.

132. Kurki MI, Häkkinen SK, Frösen J, Tulamo R, von und zu Fraunberg M, Wong G, Tromp G, Niemelä M, Hernesniemi J, Jääskeläinen JE, Ylä-Herttuala S (2011) Upregulated signaling pathways in ruptured human saccular intracranial aneurysm wall: an emerging regulative role of Toll-like receptor signaling and nuclear factor-kappaB, hypoxia-inducible factor-1A, and ETS transcription factors. Neurosurgery 68: 1667-75.

133. Laaksamo E, Tulamo R, Liiman A, Baumann M, Friedlander RM, Hernesniemi J, Kangasniemi M, Niemelä M, Laakso A, Frösen J (2013) Oxidative stress is associated with cell death, wall degradation, and increased risk of rupture of the intracranial aneurysm wall. Neurosurgery 72: 109-117.

134. Lappalainen H, Laine P, Pentikäinen MO, Sajantila A, Kovanen PT (2004) Mast cells in neovascularized human coronary plaques store and secrete basic fibroblast growth factor, a potent angiogenic mediator. Arterioscler Thromb Vasc Biol 24: 1880-1885.

135. Larigauderie G, Furman C, Jaye M, Lasselin C, Copin C, Fruchart JC, Castro G, Rouis M (2004) Adipophilin enhances lipid accumulation and prevents lipid efflux from THP-1 macrophages: potential role in atherogenesis. Arterioscler Thromb Vasc Biol 24: 504-510.

136. Lau D, Baldus S (2006) Myeloperoxidase and its contributory role in inflammatory vascular disease. Pharmacol Ther 111: 16-26.

137. Lee-Rueckert M, Kovanen PT (2011) Extracellular modifications of HDL in vivo and the emerging concept of proteolytic inactivation of prebeta-HDL. Curr Opin Lipidol 22: 394-402.

138. Lee-Rueckert M, Blanco-Vaca F, Kovanen PT, Escola-Gil JC (2013) The role of the gut in reverse cholesterol transport--focus on the enterocyte. Prog Lipid Res 52: 317-328.

139. Lehti S, Sjövall P, Käkelä R, Mäyränpää MI, Kovanen PT, Öörni K (2015) Spatial Distributions of Lipids in Atherosclerosis of Human Coronary Arteries Studied by Time-of-Flight Secondary Ion Mass Spectrometry. Am J Pathol 185: 1216-1233.

140. Levy AP, Purushothaman KR, Levy NS, Purushothaman M, Strauss M, Asleh R, Marsh S, Cohen O, Moestrup SK, Moller HJ, Zias EA, Benhayon D, Fuster V, Moreno PR (2007) Downregulation of the hemoglobin scavenger receptor in individuals with diabetes and the Hp 2-2 genotype: implications for the response to intraplaque hemorrhage and plaque vulnerability. Circ Res 101: 106-110.

141. Libby P (2012) Inflammation in atherosclerosis. Arterioscler Thromb Vasc Biol 32: 2045-2051.

142. Libby P (2002) Inflammation in atherosclerosis. Nature 420: 868-874.

143. Libby P, Lichtman AH, Hansson GK (2013) Immune effector mechanisms implicated in atherosclerosis: from mice to humans. Immunity 38: 1092-1104.

144. Libby P, Ridker PM, Hansson GK (2011) Progress and challenges in translating the biology of atherosclerosis. Nature 473: 317-325.

145. Lindbohm JV, Kaprio J, Korja M (2016) Cholesterol as a Risk Factor for Subarachnoid Hemorrhage: A Systematic Review. PLoS One 11: e0152568.

146. Lindgren AE, Koivisto T, Björkman J, von Und Zu Fraunberg M, Helin K, Jääskeläinen JE, Frösen J (2016) Irregular Shape of Intracranial Aneurysm Indicates Rupture Risk Irrespective of Size in a Population-Based Cohort. Stroke 47: 1219-1226.

147. Lindgren AE, Kurki MI, Riihinen A, Koivisto T, Ronkainen A, Rinne J, Hernesniemi J, Eriksson JG, Jääskeläinen JE, von und zu Fraunberg M (2014) Hypertension predisposes to the formation of saccular intracranial aneurysms in 467 unruptured and 1053 ruptured patients in Eastern Finland. Ann Med 46: 169-176.

148. Lindgren AE, Kurki MI, Riihinen A, Koivisto T, Ronkainen A, Rinne J, Hernesniemi J, Eriksson JG, Jääskeläinen JE, von und zu Fraunberg M (2013) Type 2 diabetes and risk of rupture of saccular intracranial aneurysm in eastern Finland. Diabetes Care 36: 2020-2026.

149. Liu A, Huang J (2015) Treatment of Intracranial Aneurysms: Clipping Versus Coiling. Curr Cardiol Rep 17: 628-015-0628-2.

150. Lougheed M, Zhang HF, Steinbrecher UP (1991) Oxidized low density lipoprotein is resistant to cathepsins and accumulates within macrophages. J Biol Chem 266: 14519-14525.

151. Lusis AJ (2000) Atherosclerosis. Nature 407: 233-241.

152. Maaninka K, Lappalainen J, Kovanen PT (2013) Human mast cells arise from a common circulating progenitor. J Allergy Clin Immunol. 2013 Aug;132(2):463-9.e3.

153. Marbacher S, Marjamaa J, Bradacova K, von Gunten M, Honkanen P, Abo-Ramadan U, Hernesniemi J, Niemelä M, Frösen J (2014) Loss of mural cells leads to wall degeneration, aneurysm growth, and eventual rupture in a rat aneurysm model. Stroke 45: 248-254.

154. Martinez-Lemus LA, Hill MA, Meininger GA (2009) The plastic nature of the vascular wall: a continuum of remodeling events contributing to control of arteriolar diameter and structure. Physiology (Bethesda) 24: 45-57.

155. Martin-Ventura JL, Madrigal-Matute J, Martinez-Pinna R, Ramos-Mozo P, Blanco-Colio LM, Moreno JA, Tarin C, Burillo E, Fernandez-Garcia CE, Egido J, Meilhac O, Michel JB (2012) Erythrocytes, leukocytes and platelets as a source of oxidative stress in chronic vascular diseases: detoxifying mechanisms and potential therapeutic options. Thromb Haemost 108: 435-442.

156. Matsushige T, Akiyama Y, Okazaki T, Shinagawa K, Ichinose N, Awai K, Kurisu K (2015) Vascular Wall Imaging of Unruptured Cerebral Aneurysms with a Hybrid of Opposite-Contrast MR Angiography. AJNR Am J Neuroradiol 36: 1507-1511.

157. Matsushige T, Chen B, Ringelstein A, Umutlu L, Forsting M, Quick HH, Sure U, Wrede KH (2016) Giant Intracranial Aneurysms at 7T MRI. AJNR Am J Neuroradiol 37: 636-641.

158. Mayadas TN, Cullere X, Lowell CA (2014) The multifaceted functions of neutrophils. Annu Rev Pathol 9: 181-218.

159. Mäyränpää MI, Resendiz JC, Heikkilä HM, Lindstedt KA, Kovanen PT (2007) Improved identification of endothelial erosion by simultaneous detection of endothelial cells (CD31/CD34) and platelets (CD42b). Endothelium 14: 81-87.

160. Mäyränpää MI, Heikkilä HM, Lindstedt KA, Walls AF, Kovanen PT (2006) Desquamation of human coronary artery endothelium by human mast cell proteases: implications for plaque erosion. Coron Artery Dis 17: 611-621.

161. Mäyränpää MI, Trosien JA, Fontaine V, Folkesson M, Kazi M, Eriksson P, Swedenborg J, Hedin U (2009) Mast cells associate with neovessels in the media and adventitia of abdominal aortic aneurysms. J Vasc Surg 50: 388-95.

162. McDowell MM, Zhao Y, Kellner CP, Barton SM, Sussman E, Claassen J, Ducruet AF, Connolly ES (2017) Demographic and clinical predictors of multiple intracranial aneurysms in patients with subarachnoid hemorrhage. J Neurosurg: 1-8.

163. McEvoy AW, Kitchen ND, Thomas DG (2000) Intracerebral haemorrhage and drug abuse in young adults. Br J Neurosurg 14: 449-454.

164. Meguro R, Asano Y, Odagiri S, Li C, Iwatsuki H, Shoumura K (2007) Nonheme-iron histochemistry for light and electron microscopy: a historical, theoretical and technical review. Arch Histol Cytol 70: 1-19.

165. Michel JB, Martin-Ventura JL, Nicoletti A, Ho-Tin-Noe B (2014) Pathology of human plaque vulnerability: mechanisms and consequences of intraplaque haemorrhages. Atherosclerosis 234: 311-319.

166. Michel JB, Virmani R, Arbustini E, Pasterkamp G (2011) Intraplaque haemorrhages as the trigger of plaque vulnerability. Eur Heart J 32: 1977-85, 1985a, 1985b, 1985c.

167. Miyata H, Koseki H, Takizawa K, Kasuya H, Nozaki K, Narumiya S, Aoki T (2017) T cell function is dispensable for intracranial aneurysm formation and progression. PLoS One 12: e0175421.

168. Molyneux A, Kerr R, Stratton I, Sandercock P, Clarke M, Shrimpton J, Holman R, International Subarachnoid Aneurysm Trial (ISAT) Collaborative Group (2002) International Subarachnoid Aneurysm Trial (ISAT) of neurosurgical clipping versus endovascular coiling in 2143 patients with ruptured intracranial aneurysms: a randomised trial. Lancet 360: 1267-1274.

169. Molyneux AJ, Birks J, Clarke A, Sneade M, Kerr RS (2015) The durability of endovascular coiling versus neurosurgical clipping of ruptured cerebral aneurysms: 18 year follow-up of the UK cohort of the International Subarachnoid Aneurysm Trial (ISAT). Lancet 385: 691-697.

170. Moreno PR, Purushothaman M, Purushothaman KR (2012) Plaque neovascularization: defense mechanisms, betrayal, or a war in progress. Ann N Y Acad Sci 1254: 7-17.

171. Morgan L, Hawe E, Palmen J, Montgomery H, Humphries SE, Kitchen N (2005) Polymorphism of the heme oxygenase-1 gene and cerebral aneurysms. Br J Neurosurg 19: 317-321.

172. Morita T (2005) Heme oxygenase and atherosclerosis. Arterioscler Thromb Vasc Biol 25: 1786-1795.

173. Murayama Y, Takao H, Ishibashi T, Saguchi T, Ebara M, Yuki I, Arakawa H, Irie K, Urashima M, Molyneux AJ (2016) Risk Analysis of Unruptured Intracranial Aneurysms: Prospective 10-Year Cohort Study. Stroke 47: 365-371.

174. Murray CD (1926) The Physiological Principle of Minimum Work: II. Oxygen Exchange in Capillaries. Proc Natl Acad Sci U S A 12: 299-304.

175. Murray PJ, Wynn TA (2011) Protective and pathogenic functions of macrophage subsets. Nat Rev Immunol 11: 723-737.

176. Mut F, Aubry R, Lohner R, Cebral JR (2010) Fast Numerical Solutions of Patient-Specific Blood Flows in 3D Arterial Systems. Int J Numer Method Biomed Eng 26: 73-85.

177. Mut F, Lohner R, Chien A, Tateshima S, Vinuela F, Putman C, Cebral J (2011) Computational Hemodynamics Framework for the Analysis of Cerebral Aneurysms. Int J Numer Method Biomed Eng 27: 822-839.

178. Navab M, Reddy ST, Van Lenten BJ, Fogelman AM (2011) HDL and cardiovascular disease: atherogenic and atheroprotective mechanisms. Nat Rev Cardiol 8: 222-232.

179. Nielsen JS, McNagny KM (2008) Novel functions of the CD34 family. J Cell Sci 121: 3683-3692.

180. Nieuwkamp DJ, Setz LE, Algra A, Linn FH, de Rooij NK, Rinkel GJ (2009) Changes in case fatality of aneurysmal subarachnoid haemorrhage over time, according to age, sex, and region: a meta-analysis. Lancet Neurol 8: 635-642.

181. O'Brien KD, Olin KL, Alpers CE, Chiu W, Ferguson M, Hudkins K, Wight TN, Chait A (1998) Comparison of apolipoprotein and proteoglycan deposits in human coronary atherosclerotic plaques: colocalization of biglycan with apolipoproteins. Circulation 98: 519-527.

182. Oettgen P (2006) Regulation of vascular inflammation and remodeling by ETS factors. Circ Res 99: 1159-1166.

183. Oksjoki R, Kovanen PT, Pentikäinen MO (2003) Role of complement activation in atherosclerosis. Curr Opin Lipidol 14: 477-482.

184. Oksjoki R, Laine P, Helske S, Vehmaan-Kreula P, Mäyränpää MI, Gasque P, Kovanen PT, Pentikäinen MO (2007) Receptors for the anaphylatoxins C3a and C5a are expressed in human atherosclerotic coronary plaques. Atherosclerosis 195: 90-99.

185. Ollikainen E, Tulamo R, Lehti S, Hernesniemi J, Niemelä M, Kovanen PT, Frösen J (2018) Myeloperoxidase Associates With Degenerative Remodeling and Rupture of the Saccular Intracranial Aneurysm Wall. J Neuropathol Exp Neurol. 2018 Jun 1;77(6):461-468.

186. Onofre G, Kolackova M, Jankovicova K, Krejsek J (2009) Scavenger receptor CD163 and its biological functions. Acta Medica (Hradec Kralove) 52: 57-61.

187. Paine A, Eiz-Vesper B, Blasczyk R, Immenschuh S (2010) Signaling to heme oxygenase-1 and its anti-inflammatory therapeutic potential. Biochem Pharmacol 80: 1895-1903.

188. Palinski W, Ylä-Herttuala S, Rosenfeld ME, Butler SW, Socher SA, Parthasarathy S, Curtiss LK, Witztum JL (1990) Antisera and monoclonal antibodies specific for epitopes generated during oxidative modification of low density lipoprotein. Arteriosclerosis 10: 325-335.

189. Park CK, Shin HS, Choi SK, Lee SH, Koh JS (2014) Clinical analysis and surgical considerations of atherosclerotic cerebral aneurysms: experience of a single center. J Cerebrovasc Endovasc Neurosurg 16: 247-253.

190. Pedrigi RM, Papadimitriou KI, Kondiboyina A, Sidhu S, Chau J, Patel MB, Baeriswyl DC, Drakakis EM, Krams R (2017) Disturbed Cyclical Stretch of Endothelial Cells Promotes Nuclear Expression of the Pro-Atherogenic Transcription Factor NF-kappaB. Ann Biomed Eng 45: 898-909.

191. Pedrigi RM, Mehta VV, Bovens SM, Mohri Z, Poulsen CB, Gsell W, Tremoleda JL, Towhidi L, de Silva R, Petretto E, Krams R (2016) Influence of shear stress magnitude and direction on atherosclerotic plaque composition. R Soc Open Sci 3: 160588.

192. Pentikäinen MO, Öörni K, Ala-Korpela M, Kovanen PT (2000) Modified LDL - trigger of atherosclerosis and inflammation in the arterial intima. J Intern Med 247: 359-370.

193. Perrone RD, Malek AM, Watnick T (2015) Vascular complications in autosomal dominant polycystic kidney disease. Nat Rev Nephrol 11: 589-598.

194. Perrotta I, Sciangula A, Concistre G, Mazzulla S, Aquila S, Agnino A (2014) Internal mammary artery atherosclerosis: an ultrastructural study of two cases. Ultrastruct Pathol 38: 199-203.

195. Pow DV, Diaz CM (2008) AMD-like lesions in the rat retina: a latent consequence of perinatal hemorrhage. Invest Ophthalmol Vis Sci 49: 2790-2798.

196. Pritz MB (2011) Cerebral aneurysm classification based on angioarchitecture. J Stroke Cerebrovasc Dis 20: 162-167.

197. Pyysalo MJ, Pyysalo LM, Pessi T, Karhunen PJ, Öhman JE (2013) The connection between ruptured cerebral aneurysms and odontogenic bacteria. J Neurol Neurosurg Psychiatry 84: 1214-1218.

198. Pyysalo MJ, Pyysalo LM, Pessi T, Karhunen PJ, Lehtimäki T, Oksala N, Öhman JE (2016) Bacterial DNA findings in ruptured and unruptured intracranial aneurysms. Acta Odontol Scand 74: 315-320.

199. Qureshi AI, Malik AA, Saeed O, Defillo A, Sherr GT, Suri MF (2016) Hormone replacement therapy and the risk of subarachnoid hemorrhage in postmenopausal women. J Neurosurg 124: 45-50.

200. Räisänen S, Frösen J, Kurki MI, Huttunen T, Huttunen J, Koivisto T, Helin K, von Und Zu Fraunberg M, Jääskeläinen JE, Lindgren AE (2018) Impact of Young Age on the Presentation of Saccular Intracranial Aneurysms: Population-Based Analysis of 4082 Patients. Neurosurgery 82(6):815-823.

201. Ramakrishna G, Rooke TW, Cooper LT (2003) Iron and peripheral arterial disease: revisiting the iron hypothesis in a different light. Vasc Med 8: 203-210.

202. Rao KN, Brown MA (2008) Mast cells: multifaceted immune cells with diverse roles in health and disease. Ann N Y Acad Sci 1143: 83-104.

203. Reis JP, Loria CM, Steffen LM, Zhou X, van Horn L, Siscovick DS, Jacobs DR,Jr, Carr JJ (2010) Coffee, decaffeinated coffee, caffeine, and tea consumption in young adulthood and atherosclerosis later in life: the CARDIA study. Arterioscler Thromb Vasc Biol 30: 2059-2066.

204. Renna NF, de Las Heras N, Miatello RM (2013) Pathophysiology of vascular remodeling in hypertension. Int J Hypertens 2013: 808353.

205. Rensen SS, Doevendans PA, van Eys GJ (2007) Regulation and characteristics of vascular smooth muscle cell phenotypic diversity. Neth Heart J 15: 100-108.

206. Ribatti D, Levi-Schaffer F, Kovanen PT (2008) Inflammatory angiogenesis in atherogenesis--a double-edged sword. Ann Med 40: 606-621.

207. Ridger V, Krams R, Carpi A, Evans PC (2008) Hemodynamic parameters regulating vascular inflammation and atherosclerosis: a brief update. Biomed Pharmacother 62: 536-540.

208. Rinkel GJ (2008) Natural history, epidemiology and screening of unruptured intracranial aneurysms. J Neuroradiol 35: 99-103.

209. Rinkel GJ, Djibuti M, Algra A, van Gijn J (1998) Prevalence and risk of rupture of intracranial aneurysms: a systematic review. Stroke 29: 251-256.

210. Rinne J, Hernesniemi J, Puranen M, Saari T (1994) Multiple intracranial aneurysms in a defined population: prospective angiographic and clinical study. Neurosurgery 35: 803-808.

211. Rosenson RS, Brewer HB,Jr, Ansell BJ, Barter P, Chapman MJ, Heinecke JW, Kontush A, Tall AR, Webb NR (2015) Dysfunctional HDL and atherosclerotic cardiovascular disease. Nat Rev Cardiol. 2016 Jan;13(1):48-60.

212. Rubio-Navarro A, Amaro Villalobos JM, Lindholt JS, Buendia I, Egido J, Blanco-Colio LM, Samaniego R, Meilhac O, Michel JB, Martin-Ventura JL, Moreno JA (2015) Hemoglobin induces monocyte recruitment and CD163-macrophage polarization in abdominal aortic aneurysm. Int J Cardiol 201: 66-78.

213. Ruigrok YM, Rinkel GJ (2008) Genetics of intracranial aneurysms. Stroke 39: 1049-1055.

214. Ruigrok YM, Rinkel GJ, Algra A, Raaymakers TW, Van Gijn J (2004) Characteristics of intracranial aneurysms in patients with familial subarachnoid hemorrhage. Neurology 62: 891-894.

215. Rumalla K, Reddy AY, Mittal MK (2016) Association of Recreational Marijuana Use with Aneurysmal Subarachnoid Hemorrhage. J Stroke Cerebrovasc Dis 25: 452-460.

216. Ryan GB, Majno G (1977) Acute inflammation. A review. Am J Pathol 86: 183-276.

217. Sakaki T, Kohmura E, Kishiguchi T, Yuguchi T, Yamashita T, Hayakawa T (1997) Loss and apoptosis of smooth muscle cells in intracranial aneurysms. Studies with in situ DNA end labeling and antibody against single-stranded DNA. Acta Neurochir (Wien) 139: 469-74.

218. Sakakura K, Nakano M, Otsuka F, Ladich E, Kolodgie FD, Virmani R (2013) Pathophysiology of atherosclerosis plaque progression. Heart Lung Circ 22: 399-411.

219. Sandow SL, Gzik DJ, Lee RM (2009) Arterial internal elastic lamina holes: relationship to function? J Anat 214: 258-266.

220. Schaer CA, Schoedon G, Imhof A, Kurrer MO, Schaer DJ (2006) Constitutive endocytosis of CD163 mediates hemoglobin-heme uptake and determines the noninflammatory and protective transcriptional response of macrophages to hemoglobin. Circ Res 99: 943-950.

221. Shaaban AM, Duerinckx AJ (2000) Wall shear stress and early atherosclerosis: a review. AJR Am J Roentgenol 174: 1657-1665.

222. Shinitzky M, Inbar M (1976) Microviscosity parameters and protein mobility in biological membranes. Biochim Biophys Acta 433: 133-149.

223. Shiraya S, Miyake T, Aoki M, Yoshikazu F, Ohgi S, Nishimura M, Ogihara T, Morishita R (2009) Inhibition of development of experimental aortic abdominal aneurysm in rat model by atorvastatin through inhibition of macrophage migration. Atherosclerosis 202: 34-40.

224. Sluimer JC, Kolodgie FD, Bijnens AP, Maxfield K, Pacheco E, Kutys B, Duimel H, Frederik PM, van Hinsbergh VW, Virmani R, Daemen MJ (2009) Thin-walled microvessels in human coronary atherosclerotic plaques show incomplete endothelial junctions relevance of compromised structural integrity for intraplaque microvascular leakage. J Am Coll Cardiol 53: 1517-1527.

225. Sneck M, Kovanen PT, Öörni K (2005) Decrease in pH strongly enhances binding of native, proteolyzed, lipolyzed, and oxidized low density lipoprotein particles to human aortic proteoglycans. J Biol Chem 280: 37449-37454.

226. Soehnlein O, Steffens S, Hidalgo A, Weber C (2017) Neutrophils as protagonists and targets in chronic inflammation. Nat Rev Immunol 17: 248-261.

227. Stancu CS, Toma L, Sima AV (2012) Dual role of lipoproteins in endothelial cell dysfunction in atherosclerosis. Cell Tissue Res 349: 433-446.

228. Starke RM, Chalouhi N, Ding D, Hasan DM (2015) Potential role of aspirin in the prevention of aneurysmal subarachnoid hemorrhage. Cerebrovasc Dis 39: 332-342.

229. Stehbens WE (1999) Relationship of cerebral aneurysms and medial raphes. Surg Neurol 52: 536-538.

230. Stehbens WE (1990) Pathology and pathogenesis of intracranial berry aneurysms. Neurol Res 12: 29-34.

231. Stehbens WE (1989) Etiology of intracranial berry aneurysms. J Neurosurg 70: 823-831.

232. Stoneman VE, Bennett MR (2009) Role of Fas/Fas-L in vascular cell apoptosis. J Cardiovasc Pharmacol 53: 100-108.

233. Sutherland GR, Auer RN (2006) Primary intracerebral hemorrhage. J Clin Neurosci 13: 511-517.

234. Swedenborg J, Mäyränpää MI, Kovanen PT (2011) Mast cells: important players in the orchestrated pathogenesis of abdominal aortic aneurysms. Arterioscler Thromb Vasc Biol 31: 734-740.

235. Sydora BC, Yuksel N, Veltri NL, Marillier J, Sydora CP, Yaskina M, Battochio L, Shandro TML, Ross S (2017) Patient characteristics, menopause symptoms, and care provided at an interdisciplinary menopause clinic: retrospective chart review. Menopause. 2018 Jan;25(1):102-105.

236. Syväranta S, Helske S, Laine M, Lappalainen J, Kupari M, Mäyränpää MI, Lindstedt KA, Kovanen PT (2010) Vascular endothelial growth factor-secreting mast cells and myofibroblasts: a novel self-perpetuating angiogenic pathway in aortic valve stenosis. Arterioscler Thromb Vasc Biol 30: 1220-1227.

237. Tabas I (2002) Consequences of cellular cholesterol accumulation: basic concepts and physiological implications. J Clin Invest 110: 905-911.

238. Tabas I, Williams KJ, Boren J (2007) Subendothelial lipoprotein retention as the initiating process in atherosclerosis: update and therapeutic implications. Circulation 116: 1832-1844.

239. Taylor CA, Hughes TJ, Zarins CK (1998) Finite element modeling of three-dimensional pulsatile flow in the abdominal aorta: relevance to atherosclerosis. Ann Biomed Eng 26: 975-987.

240. Tennant M, McGeachie JK (1990) Blood vessel structure and function: a brief update on recent advances. Aust N Z J Surg 60: 747-753.

241. Tromp G, Weinsheimer S, Ronkainen A, Kuivaniemi H (2014) Molecular basis and genetic predisposition to intracranial aneurysm. Ann Med 46: 597-606.

242. Tulamo R, Frösen J, Hernesniemi J, Niemelä M (2010) Inflammatory changes in the aneurysm wall: a review. J Neurointerv Surg 2: 120-130.

243. Tulamo R, Frösen J, Paetau A, Seitsonen S, Hernesniemi J, Niemelä M, Järvelä I, Meri S (2010) Lack of complement inhibitors in the outer intracranial artery aneurysm wall associates with complement terminal pathway activation. Am J Pathol 177: 3224-3232.

244. Tulamo R, Frösen J, Junnikkala S, Paetau A, Kangasniemi M, Pelaez J, Hernesniemi J, Niemelä M, Meri S (2010) Complement system becomes activated by the classical pathway in intracranial aneurysm walls. Lab Invest 90: 168-179.

245. Tulamo R, Frösen J, Junnikkala S, Paetau A, Pitkäniemi J, Kangasniemi M, Niemelä M, Jääskeläinen J, Jokitalo E, Karatas A, Hernesniemi J, Meri S (2006) Complement activation associates with saccular cerebral artery aneurysm wall degeneration and rupture. Neurosurgery 59: 1069-76

246. Turjman AS, Turjman F, Edelman ER (2014) Role of fluid dynamics and inflammation in intracranial aneurysm formation. Circulation 129: 373-382.

247. van Dijk RA, Rijs K, Wezel A, Hamming JF, Kolodgie FD, Virmani R, Schaapherder AF, Lindeman JH (2016) Systematic Evaluation of the Cellular Innate Immune Response During the Process of Human Atherosclerosis. J Am Heart Assoc. 2016 Jun 16;5(6).

248. van Gijn J, Kerr RS, Rinkel GJ (2007) Subarachnoid haemorrhage. Lancet 369: 306-318.

249. Vartiainen E, Laatikainen T, Peltonen M, Juolevi A, Männistö S, Sundvall J, Jousilahti P, Salomaa V, Valsta L, Puska P (2010) Thirty-five-year trends in cardiovascular risk factors in Finland. Int J Epidemiol 39: 504-518.

250. Virmani R, Kolodgie FD, Burke AP, Finn AV, Gold HK, Tulenko TN, Wrenn SP, Narula J (2005) Atherosclerotic plaque progression and vulnerability to rupture: angiogenesis as a source of intraplaque hemorrhage. Arterioscler Thromb Vasc Biol 25: 2054-2061.

251. Vlak MH, Rinkel GJ, Greebe P, Algra A (2013) Independent risk factors for intracranial aneurysms and their joint effect: a case-control study. Stroke 44: 984-987.

252. Vlak MH, Algra A, Brandenburg R, Rinkel GJ (2011) Prevalence of unruptured intracranial aneurysms, with emphasis on sex, age, comorbidity, country, and time period: a systematic review and meta-analysis. Lancet Neurol 10: 626-636.

253. Wang LD, Wagers AJ (2011) Dynamic niches in the origination and differentiation of haematopoietic stem cells. Nat Rev Mol Cell Biol 12: 643-655.

254. Watanabe A, Shimada T (2008) Vascular type of Ehlers-Danlos syndrome. J Nippon Med Sch 75: 254-261.

255. Willems S, Vink A, Bot I, Quax PH, de Borst GJ, de Vries JP, van de Weg SM, Moll FL, Kuiper J, Kovanen PT, de Kleijn DP, Hoefer IE, Pasterkamp G (2013) Mast cells in human carotid atherosclerotic plaques are associated with intraplaque microvessel density and the occurrence of future cardiovascular events. Eur Heart J. 2013 Dec;34(48):3699-706.

256. Woodfin A, Voisin MB, Nourshargh S (2007) PECAM-1: a multi-functional molecule in inflammation and vascular biology. Arterioscler Thromb Vasc Biol 27: 2514-2523.

257. Wrede KH, Matsushige T, Goericke SL, Chen B, Umutlu L, Quick HH, Ladd ME, Johst S, Forsting M, Sure U, Schlamann M (2017) Non-enhanced magnetic resonance imaging of unruptured intracranial aneurysms at 7 Tesla: Comparison with digital subtraction angiography. Eur Radiol 27: 354-364.

258. Yao XY, Jiang CQ, Jia GL, Chen G (2016) Diabetes mellitus and the risk of aneurysmal subarachnoid haemorrhage: A systematic review and meta-analysis of current evidence. J Int Med Res 44: 1141-1155.

259. Ylä-Herttuala S, Palinski W, Butler SW, Picard S, Steinberg D, Witztum JL (1994) Rabbit and human atherosclerotic lesions contain IgG that recognizes epitopes of oxidized LDL. Arterioscler Thromb 14: 32-40.

260. Yoshimura K, Nagasawa A, Kudo J, Onoda M, Morikage N, Furutani A, Aoki H, Hamano K (2015) Inhibitory effect of statins on inflammation-related pathways in human abdominal aortic aneurysm tissue. Int J Mol Sci 16: 11213-11228.

261. You SA, Wang Q (2005) Ferritin in atherosclerosis. Clin Chim Acta 357: 1-16.

262. Young SG, Witztum JL, Casal DC, Curtiss LK, Bernstein S (1986) Conservation of the low density lipoprotein receptor-binding domain of apoprotein B. Demonstration by a new monoclonal antibody, MB47. Arteriosclerosis 6: 178-188.

263. Yuan XM (1999) Apoptotic macrophage-derived foam cells of human atheromas are rich in iron and ferritin, suggesting iron-catalysed reactions to be involved in apoptosis. Free Radic Res 30: 221-231.

264. Zanaty M, Chalouhi N, Starke RM, Jabbour P, Hasan D (2016) Molecular Imaging in Neurovascular Diseases: The Use of Ferumoxytol to Assess Cerebral Aneurysms and Arteriovenous Malformations. Top Magn Reson Imaging 25: 57-61.

265. Zugibe FT, Brown KD (1961) Histochemical studies in atherogenesis. Human cerebral arteries. Circ Res 9: 897-905.